Degradation of Indigo Carmine by TiO_2 Immobilized on Natural Rubber Latex

Chaval Sriwong

A Thesis Submitted in Fulfillment of the Requirements for the Degree of

Doctor of Philosophy in Chemistry

Prince of Songkla University

2012

Thesis Title	Degradation of Indigo Carmine by TiO_2 Immobilized on Natural Rubber Latex
Author	Mr. Chaval Sriwong
Major Program	Chemistry

Major Advisor :

…….

(Assoc. Prof. Dr. Sumpun Wongnawa)

Co-Advisor :

…….

(Asst. Prof. Dr. Orasa Patarapaiboolchai)

Examining Committee :

..…...……...…….Chairperson

(Assoc. Prof. Dr. Apisit Songsasen)

……

(Assoc. Prof. Dr. Sumpun Wongnawa)

..…....……...……...

(Asst. Prof. Dr. Orasa Patarapaiboolchai)

…..……..…….....

(Asst. Prof. Dr. Pongsaton Amornpitoksuk)

The Graduate School, Prince of Songkla University, has approved this thesis as fulfillment of the requirements for the Doctor of Philosophy Degree in Chemistry

…….

(Prof. Dr. Amornrat Phongdara)

Dean of Graduate School

I hereby certify that this work has not already been accepted in substance for any degree, and is not being concurrently submitted in candidature for any degree.

_____Signature

(Mr. Chaval Sriwong)

Candidate

This is to certify that the work here submitted is the result of the candidate's own investigations. Due acknowledgement has been made of any assistance received.

_____Signature

(Assoc. Prof. Dr. Sumpun Wongnawa)

Major Advisor

_____Signature

(Mr. Chaval Sriwong)

Candidate

ชื่อวิทยานิพนธ์ การสลายสีอินดิโก้คาร์มีนโดย TiO_2 ที่ตรึงบนน้ำยางธรรมชาติ
ผู้เขียน นายชวาลย์ ศรีวงษ์
สาขาวิชา เคมี
ปีการศึกษา 2555

บทคัดย่อ

นำเสนอวิธีการแตกต่างกัน 3 วิธี ในการเตรียมแผ่นไทเทเนียมไดออกไซด์ 3 ชนิด โดยผงไทเทเนียมไดออกไซด์ได้ถูกตรึงไว้บนยาง วิธีการเหล่านี้เป็นวิธีที่ทำได้ง่าย ราคาถูก และมีประสิทธิภาพ ด้วยการใช้ผงไทเทเนียมไดออกไซด์เชิงการค้า และน้ำยางธรรมชาติ (60 %HA) เป็นสารตั้งต้น แผ่นยางที่ตรึงไทเทเนียมไดออกไซด์ทั้ง 3 ชนิดประกอบด้วย (1) แผ่นยาง TiO_2-impregnated (2) แผ่นยาง TiO_2-strewn และ (3) แผ่นยาง TiO_2-embedded ลักษณะเฉพาะของแผ่นยางที่ตรึงไทเทเนียมไดออกไซด์แต่ละชนิดสามารถศึกษาได้จากการใช้เทคนิค SEM/EDS และ XRD ผลที่ได้พบว่า แผ่นยางที่ตรึงไทเทเนียมไดออกไซด์แต่ละชนิดมีพื้นผิวขรุขระแตกต่างกันโดยขึ้นอยู่กับวิธีการเตรียม การศึกษาสมบัติการเป็นโฟโตคะตะลิสต์ของแผ่นยางที่ตรึงไทเทเนียมไดออกไซด์แต่ละชนิดจะใช้สีย้อมอินดิโก้คาร์มีน (indigo carmine) เป็นต้นแบบของสีย้อมอินทรีย์สารซึ่งเป็นมลพิษ (organic dye pollutant) ในน้ำ ผลปรากฏว่าแผ่นยางที่ตรึงไทเทเนียมไดออกไซด์ทั้งหมดสามารถสลายสารละลายสีย้อมอินดิโก้คาร์มีนได้ภายใต้การฉายแสงยูวี นอกจากนี้ยังได้ศึกษาผลของ ค่าพี-เอส ความเข้มข้นเริ่มต้นของสารละลายสีย้อมอินดิโก้คาร์มีน และความเข้มของแสงยูวีที่ใช้ต่อกระบวนการโฟโตคะตะลิสต์ การเกิดปฏิกิริยาโฟโตคะตะลิสต์ของแผ่นยางที่ตรึงไทเทเนียมไดออกไซด์ทั้งหมดเป็นปฏิกิริยาอันดับที่ 1 ที่สำคัญแผ่นยางที่ตรึงไทเทเนียมไดออกไซด์ทั้งหมดสามารถนำกลับคืนมาใช้ซ้ำใหม่ได้ โดยประสิทธิภาพการเป็นโฟโตคะตะลิสต์ไม่ลดลงเมื่อใช้เป็นเวลานาน

Thesis Title Degradation of Indigo Carmine by TiO_2 Immobilized on Natural Rubber Latex
Author Mr. Chaval Sriwong
Major Program Chemistry
Academic Year 2012

ABSTRACT

Three different methods for the preparation of three types of immobilized TiO_2 powder on the rubber sheet are presented. These methods - simple, low cost, and more effective - are based on the use of commercial TiO_2 powder and natural rubber latex (60% HA) as starting materials. The three types of immobilized TiO_2 sheets include (1) TiO_2-impregnated sheets, (2) TiO_2-strewn sheets, and (3) TiO_2-embedded sheets. The characteristics of each type of TiO_2 sheets were studied by using scanning electron microscopy/energy dispersive X-ray spectrometer (SEM/EDS), and X-ray diffractometer (XRD) techniques. The studies revealed that the surface roughness of each sheet had different surface which depended on the preparation method. The photocatalytic properties of each type of TiO_2 sheets were evaluated using indigo carmine (IC) dye as a model of organic dye pollutant in water. The results showed that all types of immobilized TiO_2 sheets could degrade IC dye solution under UV light irradiation. Moreover, the effects of pH, initial concentration of IC dye solution, and the intensity of UV light on the photodegradation were also investigated. Kinetics of all types of immobilized TiO_2 sheets were of the first-order reaction. Importantly, all types of TiO_2 sheets can be recovered and reused. From our studies they could be reused with no decline in the photodegradation efficiency over the long-term usage.

ACKNOWLEDGEMENTS

I would like to express my sincere thanks to my advisor, Associate Professor Dr. Sumpun Wongnawa, who suggested this research problem, for his numerous suggestion, encouragement and criticism without which I would have been unable to complete this work.

I am very grateful to thank my co-advisor, Assistant Professor Dr. Orasa Patarapaiboolchai for the valuable comments on my thesis, and thanks are also extended to the examination committee members of this thesis for their valuable time.

I am deeply indebted to the Royal Golden Jubilee Ph.D. Program (RGJ) of the Thailand Research Fund (TRF) for scholarship (Grant No.PHD/0003/2550), the Center for Innovation in Chemistry (PERCH-CIC), and the Graduate School, Prince of Songkla University, for the partial supports of the research fund.

I would like to thank the Department of Chemistry, Faculty of Science, Prince of Songkla University, for all necessary laboratory facilities used throughout this research.

I also would like to thank my family, my friends, and all of my collaborators who helped creating an enjoyable atmosphere to be working in and for their helpful in many countless ways throughout the years.

Chaval Sriwong

THE RELEVANCE OF THE RESEARCH WORK TO THAILAND

Synthetic dyes are the major industrial source of wastewater contaminants. The release of this colored wastewater into the eco-system is mainly the environmental problem. Owing to its high photocatalytic activity and stability, TiO_2 is generally used as a photocatalyst for environmental applications. However, the application of powder TiO_2 in wastewater treatment is limited due to (i) difficulty and high cost in the separation and recovery of the catalyst from suspension, (ii) non-reusable of the catalyst, (iii) easy aggregation of the suspended particles, (iv) difficulty in application to continuous flow systems, and (v) possibility to cause adverse human health problems by the loose powder. The purpose of this thesis is to find the method to prepare the immobilized TiO_2 sheet and use it as photocatalytic tool to solve the problem of wastewater. In this work, three types of immobilized TiO_2 sheets were prepared by three different methods, using commercial TiO_2 powder (Degussa P25) and rubber latex (60% HA) as starting materials. The photocatalyst of these immobilized TiO_2 sheets could be used to degrade indigo carmine (IC), a model organic dye compound, in wastewater. The recyclability of the immobilized TiO_2 sheets should be attractive to the water treatment industry as it helps keep the operation cost low. We deem that this work could be used in Thailand as a method for the destruction of synthetic dye pollutants in the factories before releasing wastewater into the natural water system. Furthermore, since rubber latex is used to make the sheets, this should be another way of utilizing the rubber latex which Thailand is the number one producer in the world.

CONTENTS

CONTENTS (CONTINUED)

CONTENTS (CONTINUED)

CONTENTS (CONTINUED)

LIST OF FIGURES

LIST OF FIGURES (CONTINUED)

LIST OF FIGURES (CONTINUED)

LIST OF FIGURES (CONTINUED)

LIST OF SCHEME

CHAPTER 1
INTRODUCTION

1.1 Introduction

Water contamination is caused by various sources such as industrial effluents, chemical spills, domestic consumes, and agricultural runoff. These effluents released into the rivers are highly contaminated and pose a potential environmental pollution (Qamar, et al., 2005). Color is usually the first contaminant to be recognized in wastewater which generated by using synthetic dyes in the industrials. Considering both discharged volumes and effluent composition, the wastewater generated by the textile industry is rated as one of the most polluting among all industry sectors. With the great variety of fibers, dyes, process aids and finishing products in use, the textile industry generated wastewater of great chemical complexity, diversity and volume (Bizani, et al., 2006). Synthetic dyes are extensively used in the textile industries because of their simple dyeing procedure and good stability during washing process. Over 10,000 dyes with an annual production over 7×10^5 metric ton worldwide are commercially available and it is estimated that approximately 15% of the dyestuffs are lost in the industrial effluents during manufacturing and processing operations. Synthetic dyes, classified by their chromophores, have different and stable chemical structures to meet various coloring requirements (Toor, et al., 2006). When, the release of this colored wastewater in the eco-system is a dramatic source of aesthetic pollution, eutrophication, and perturbation in aquatic life. Therefore, the removal of colored wastewater is a necessary before being released into the environment (Senthikumaar, et al., 2005).

Traditional techniques used for color removal are filtration, adsorption by activated carbon (charcoal), and coagulation. Each method has few advantages and disadvantages. For example, the use of charcoal is technically easy but has high waste disposal cost. Coagulation using alums, ferric salts or limes is a low cost process, but all these methods have a major disadvantage of simply transferring the pollutants from one phase to another phase rather than destroying them and sometime the by-products may

be more toxic than the dye itself. Biological treatment is a proven method and cost effective. However, it has been reported that majority of dyes are adsorbed on the sludge and very long degraded times, due to the bio-recalcitrant nature of these dyes molecules. This leads to a search for highly effective method to degrade the dye into environmentally compatible products (Toor, et al., 2006).

During the last two decades, heterogeneous photocatalysis has attracted considerable attention for the complete destruction of undesirable organic pollutants both in aqueous and gaseous phases with the help of solar or artificial light (Ao, et al., 2008; Wu, et al., 2008; Qamar, et al., 2010). This technique is based on the use of UV irradiated semiconductors, generally titanium dioxide (TiO_2) as one of the most promising photocatalysts due to its chemical stability, non-toxicity, inexpensiveness, and high efficiency in the photocatalysis process (Nagaveni, et al., 2004; Parida, et al., 2008). Among different commercially available titanium dioxide powders Degussa P25 shows the highest activity and it is commonly used in many kinds of photocatalytic reactions (Kirchnerova, et al., 2005; Byrne, et al., 2009; Qin, et al., 2009; Ohtani, et al., 2010). However, many disadvantages of the use of TiO_2 in powder form have been noted: (i) difficulty and high cost in the separation and recovery of the catalyst from suspension, (ii) non-reusable of the catalyst, (iii) easy aggregation of the suspended particles, (iv) difficulty in application to continuous flow systems, (v) possibility to cause adverse human health problems by the loose powder (Yuan, et al., 2005; Habibi, et al., 2007; Shi, et al., 2008; Guo, et al., 2010). To avoid the use of photocatalyst in powder form, several efforts have been made to coat TiO_2 as films on various substrates such as glass (Losito, et al., 2005), ITO glass (Sankapal, et al., 2005), stainless steel (Yu, et al., 2006), plastics (Kwon, et al., 2004), and polymers (Yang, et al., 2006), as well as employing several techniques such as flame synthesis (Partsinis, et al., 1996), chemical vapor deposition (CVD) (Ding, et al., 2001), spray pyrolysis deposition (Weng, et al., 2005), and sol-gel dip/spin coating (Sen, et al., 2005; Yogi, et al., 2008). These methods, however, have some disadvantages for industrial applications, for instance, the chemical vapor deposition, spray pyrolysis deposition, and flame synthesis methods require special and rather expensive apparatus and complex procedures for the deposition of TiO_2 film while the sol-gel dip/spin coating method needs repeated coating in order to get a thick film and requires high annealing temperature for

crystallization. In addition, the heating process precludes the fabrication of TiO_2 film on substrates with low thermal stability such as plastics and hydrocarbon polymers (Yang, et al., 2006). Therefore, a simple, less expensive, and more effective method for the preparation of immobilized TiO_2 powder is still an interesting topic under investigation in many laboratories including us.

In this work, we focused on the preparation of immobilized TiO_2 powder on the rubber sheet substrate by three different methods, using commercial TiO_2 powder (Degussa P25) and rubber latex (60% HA) as starting materials. The three types of immobilized TiO_2 sheets include (1) TiO_2-impregnated sheets, (2) TiO_2-strewn sheets, and (3) TiO_2-embedded sheets. The rubber strikes our interest because of its versatility in daily life, available locally, and to the best of our knowledge has never been used as a substrate for TiO_2 coating (except in our group). The effects of pH, initial concentration of indigo carmine (IC) dye solution, and UV light intensity were studied on the photocatalytic activity of each immobilized TiO_2 sheets. Furthermore, the reaction kinetic and recycling uses of the immobilized TiO_2 sheets on the photodegradation for IC dye solution were also presented. The recyclability of the immobilized TiO_2 sheets should be attractive to the water treatment industry as it helps keep the operation cost low. The relatively low cost of the materials (photocatalyst powder and rubber latex) is a onetime investment and will last over a long period of uses. We hope this should have potential applications in environmental business.

1.2 Review of literatures

1.2.1 Background of titanium dioxide (TiO_2)

Titanium dioxide (TiO_2) or titania is a polymorphic compound, having three polymorphous structures: anatase, brookite, and rutile. These polymorphic forms of titanium dioxide are shown in Figure 1. Both anatase and rutile are tetragonal, whereas brookite is orthorhombic. In all three oxide modifications, each titanium atom is coordinated to six almost equidistant oxygen atoms, and each oxygen atom to three titanium atoms (Clark, et al., 1968). In the case of anatase, the TiO_6 octahedron is slightly distorted, with two Ti-O bonds slightly greater than the other four, and

with some of the O-Ti-O bond angles deviating from 90°. The distortion is greater in anatase than rutile. The structures of anatase and rutile crystals have been described frequently in terms of chains of TiO_6 octahedral having common edges. Two or four edges are shared in rutile and anatase, respectively. The third form of titanium dioxide; brookite, the inter-atomic distances and the O-Ti-O bond angles are similar to those of rutile and anatase. The essential difference is that there are six different Ti-O bonds ranging from 1.87 to 2.04 Å. Accordingly, there are 12 different O-Ti-O bond angles ranging from 77° to 105°. Brookite is formed by joining together the distorted TiO_6 octahedral sharing three edges. All three oxide modifications are birefringent; anatase is uniaxial negative, brookite is biaxial positive and rutile is uniaxial positive.

(a) Anatase

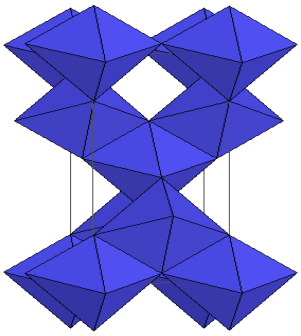

(b) Rutile

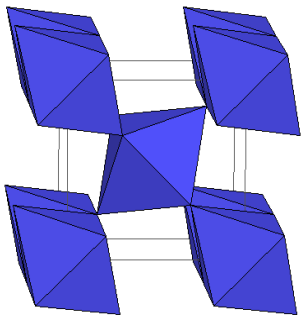

(c) Brookite

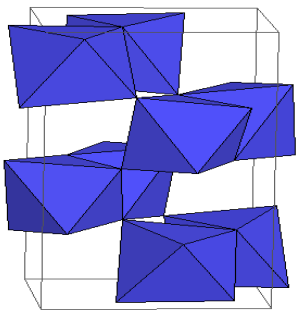

Figure 1 Crystal structures of TiO_2; (a) Anatase, (b) Rutile, and (c) Brookite (http://ruby.colorado.edu).

Titanium dioxide occurs primarily in three different forms: anatase, rutile, and brookite. The most common are anatase and rutile, since brookite is rather unstable. The brookite type cannot be used in industries because of its instability at room temperature. The anatase type has high photocatalytic due to appropriate energy gap, heat resistant, and photo-stability. It also has advantage for purification environmental applications such as air purification, deodorization, soil proof, sterilization, and water purification. The rutile type used as a white pigments and outdoor applicability because of its good light resistance, high refractive index, and can be applied to surfaces by the use of adsorption technology without advanced skills or sophisticated equipment.

In industry, it is well known that TiO_2 pigments are produced by the older sulfate or newer chloride processes. The economics of the two processes are very much dependent upon the raw material available. The starting materials for TiO_2 production are ilmenite and titaniferous slag in the case of the sulfate process (Figure 2) and leucoxene, rutile, synthetic rutile, and in the future possibly also anatase, for the chloride process (Figure 3) (Büchner, et al., 1989).

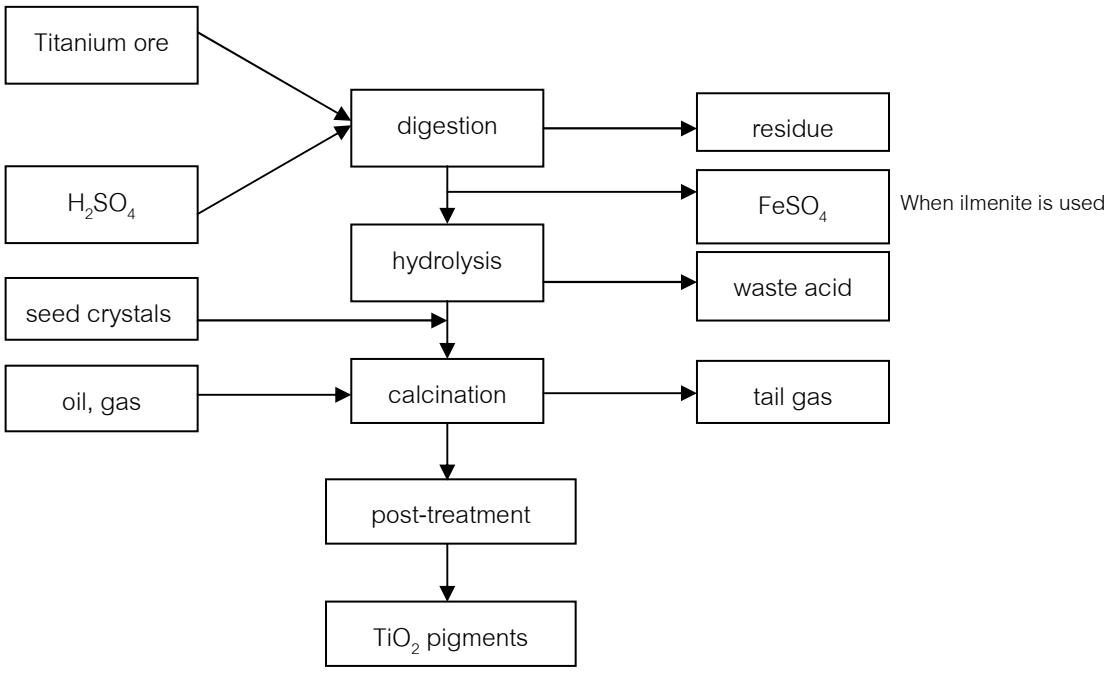

Figure 2 TiO_2 pigment manufactured by the sulfate process (Büchner, et al.,1989).

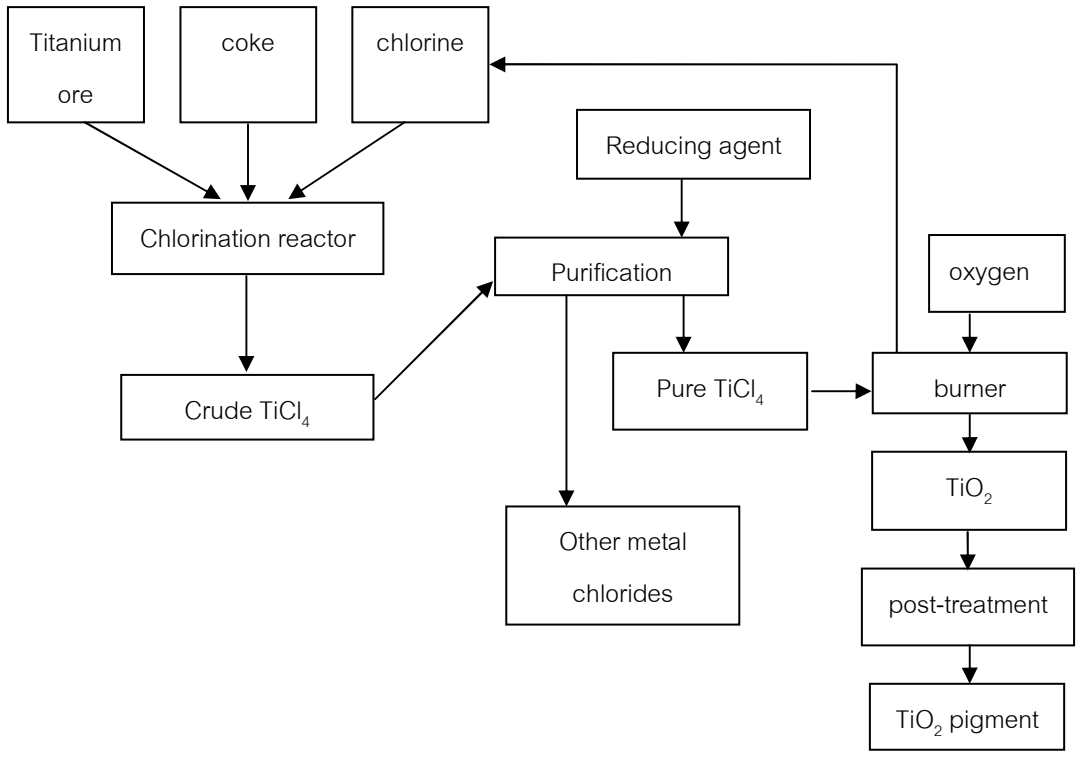

Figure 3 TiO_2 pigment manufactured by the chloride process (Büchner, et al., 1989).

The sulfate process was the first commercial scale technology used to convert ilmenite to TiO_2. The process started from digestion the finely ground raw materials in an exothermic reaction with concentrated sulfuric acid, the digested cake dissolved in cold water and the residue separated off. To prevent their precipitation during the subsequent hydrolysis the Fe (III) ions are reduced to Fe (II) by adding a Ti (III) solution. Upon evaporation of the solution, the large quantities of Fe (II) sulfate heptahydrate are produced, when ilmenite is used, and crystallizes out. The titanium oxysulfate is then hydrolyzed to titanium oxyhydrate by heating the clear solution with

steam at 95-110^{o}C. TiO_2 seed crystals are added or formed before hydrolysis to ensure yields of 93-96 % TiO_2 and to obtain a hydrolysis product which yields the optimum particle size of ca. 0.2 μm upon firing. Diluted sulfuric acid remains as "waste acid". The hydrolysis product is washed, treated with a Ti (III) solution to remove adsorbed heavy metal ions (Fe, Cr, Mn, V) and calcined at temperature between 800-1,000^{o}C. Anatase or rutile pigments can be produced in the calcination process depending upon the choice of additives, which determine the characteristics of the product. TiO_2 obtained in this way usually has the structure of anatase since the sulfate ions stabilize this modification which could not be removed during the process of washing, and it would benefit to the formation of anatase and the transformation temperature must take place at high temperature (about 1,000^{o}C) to obtain rutile TiO_2 (Yang, et al., 2002).

The newer chloride process offers tighter product control, less labors intensive, avoids the iron sulfate waste problem and, at larger scales, is cheaper to operate. Currently about 60% of 4 million ton of pigment produced worldwide is produced by this process. This process required the ilmenite to be processed to the rutile form (i.e. removal of the iron component to yield crude titanium dioxide (synthetic rutile)). The chloride process started from the reaction of chlorine with synthetic rutile to form raw titanium tetrachloride which is then mixed with reducing agent to convert impurities such as vanadium oxychloride, iron chloride to lower oxidation state compounds. It is then distilled yielding titanium tetrachloride in almost any required purity. Finally, it is combusted with pure oxygen to TiO_2 and chlorine, which is reused in the chlorination. Usually, TiO_2 prepared from this process has the mixture structure of anatase and rutile with the average diameter about 20 nm. For instance, the typical commercial formed TiO_2 (anatase) made by Degussa, contains about 20-30 % rutile.

Titanium dioxide is extensively used as a white permanent pigment with good covering power in paint, paper, printing ink, plastic, polymer and cosmetic products. Paints made with titanium dioxide are excellent reflectors of infrared radiation and are used in exterior paints. It is also used as strengthening filler in paper and cement. Recently, there has been increasing interest in application of nanocrystalline materials for catalyst, supports, ceramics, inorganic membranes, gas sensing, water purification, and solar energy conversion. Furthermore, photocatalysis of nanocrystalline titanium dioxide has a great many advantage on waste water treatment

such as high catalysis efficiency, energy saving, no pollution, etc. and can degrade all kinds of organic pollutants from water effectively. These entire merits make photocatalysis of water treatment and it is supposed to be used widely in the future (Baolong, et al., 2003).

Coloration is a key factor in the commercial success of textile products, particularly those with high fashion content, especially garments, furnishings and upholstery. The business generated by the dye industry over the last two years was approximately US$ 22 billion, and constituted a total employment of about 1.45 million people. Excluding fluorescent brighteners, the dye consumption per capita is approximately 150 g per year, serving an average consumption of textile fiber of about 14 kg per year per inhabitant. Despite, the high economic importance of the textile industry in the world, this industry is responsible for over 7×10^5 metric ton of about 10,000 different types of dyes on pigments produced each year. During dye use among the several industries responsible for pollution of the aquatic ecosystems, the textile dyeing and printing industries are major players, around a half of a ton of these dyestuffs are lost per day to the environment. Approximately 200 L of water is required, for every kilogram of finished cotton fabric. The reactions necessary to fix these dyes to the fibers are not very efficient. Therefore, residual dyes, several types of chemicals and salts are dumped into the water and are discharged in the wastewater system. At least 15% of those not used dyes might enter the environment through effluents from wastewater treatment plants (Carneiro, et al., 2004). Removal of color in wastewater generated by the textile industries is an issue of discussion and regulation all over the world. Among the relative dyes, the textile azo dyes with synthetic intermediates as contaminant and its degradation products have undoubtedly attracted the most attention with regard to high environmental impact, because of their widespread use, their potentiality to form toxic aromatic products (carcinogenicity and mutagenic-city properties) and their low removal rate during primary and secondary treatment. They represent about 50% of the worldwide production and correspond to an important source of contamination considering that a significant part of the synthetic textile dyes are lost in waste streams during manufacturing or processing operations. Therefore, it is important to develop effective wastewater remediation technologies for these compounds.

Various chemical and physical treatment processes are currently proposed for these dyes. These largely fall into the categories of direct precipitation or elimination by adsorption, flocculation, membrane separation, coagulation and chlorination. These methods have been largely incomplete and ineffective because the problem is not completely resolved, being required further treatment. A number of biological processes, such as sequenced anaerobic/aerobic digestion, have been proposed in the treatment of textile wastewater, but they are limited due to the fact that many of the dyes are xenobiotic and non-biodegradable. Alternative methods based on advanced oxidation processes combining ultraviolet irradiation and oxidative agents for dye treatment have been also investigated, but the presence of intermediates arising from the photodegradation reaction could be more harmful than the pollutant itself.

In recent years attention has been focused on heterogeneous photocatalysis for the treatment of recalcitrant chemical present in the wastewater. Among these heterogeneous photocatalysis in the presence of irradiated semiconductors (TiO_2, WO_3, SnO_2, ZnO, CdS, and others), TiO_2 has been successfully used to decolorize and mineralize many organic pollutants including several dyes and their intermediates present in aqueous systems using both artificial light and under sunlight using solar technology (Muruganandham, et al., 2005). TiO_2 is the most widely used photocatalyst because of its good activity, chemical stability, commercial availability and inexpensiveness. It is generally used as a photocatalyst for environmental applications such as air purification, water disinfection, hazardous waste remediation and water purification (Nagaveni, et al., 2004). The efficiency of advanced oxidation processes for degradation of recalcitrant compounds has been extensively documented. Photochemical processes are used to degrade toxic organic compounds to CO_2 and H_2O without the use of additional chemical oxidants, because the degradation is assisted by high concentrations of hydroxyl radicals ($OH^{\bullet}$) generated in the process. In this case, the photoexcitation of TiO_2 particles promotes an electron from the valence band to the conduction band, generating an electron (e_{CB}^-)/hole (h_{VB}^+) pair. Both reductive and oxidative processes can occur at or near the surface of the photoexcited TiO_2 particle. In general, oxygen is used to scavenge the conduction band electron, producing a superoxide anion radical ($O_2^{\bullet -}$), effectively preventing electron (e_{CB}^-)/hole (h_{VB}^+) recombination, and prolonging the lifetime of the hole. The photogenerated hole has the

potential to oxidize several substrates by electron transfer. In aqueous solutions, oxidation of water to hydroxyl radical ($OH^{\bullet}$) by the photogenerated hole appears to be the predominant pathway. Hydroxyl radicals ($OH^{\bullet}$) and, to a lesser extent, superoxide anion can act as oxidants, ultimately leading to the mineralization of organic compounds (Gomes de Moraes, et al., 2000).

The mineralization of most of the organic pollutants could be degraded following the usually proposed mechanism (Eqs.1-9); for the heterogeneous photocatalytic oxidation processes as shown in Figure 4.

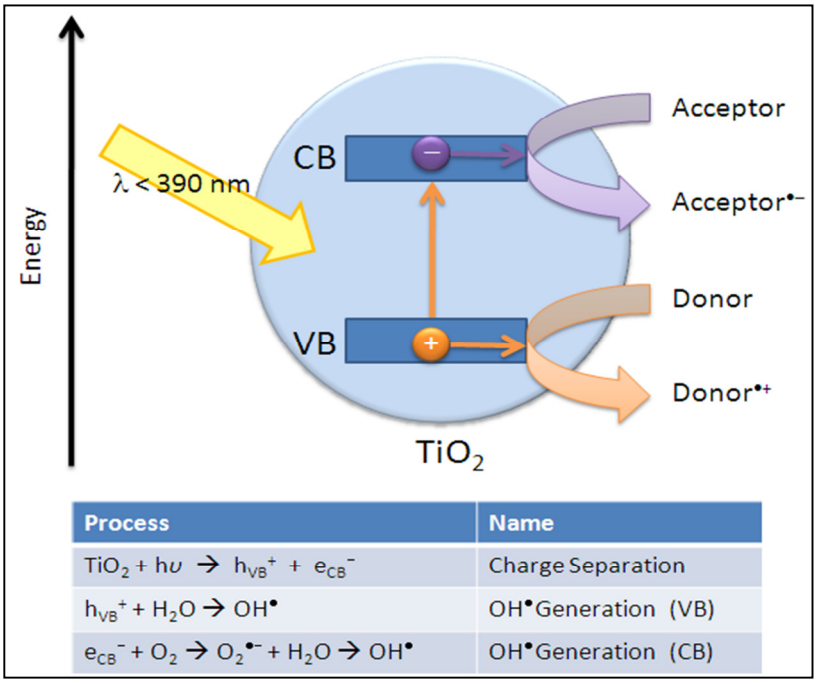

Process	Name
$TiO_2 + h\upsilon \rightarrow h_{VB}^+ + e_{CB}^-$	Charge Separation
$h_{VB}^+ + H_2O \rightarrow OH^{\bullet}$	$OH^{\bullet}$ Generation (VB)
$e_{CB}^- + O_2 \rightarrow O_2^{\bullet-} + H_2O \rightarrow OH^{\bullet}$	$OH^{\bullet}$ Generation (CB)

Figure 4 The heterogeneous photocatalytic oxidation processes of titanium dioxide photocatalyst (http://photochemistryportal.net).

1. Absorption of efficient photons ($h\nu > E_g = 3.2$ eV) by titanium dioxide

$$TiO_2 + h\nu \rightarrow e_{CB}^- + h_{VB}^+ \quad .....(1)$$

2. Oxygen ionosorption (first step of oxygen reduction; oxidation state of oxygen changes from 0 to -1/2)

$$(O_2)_{ads} + e_{CB}^- \rightarrow O_2^{\bullet-} \quad .....(2)$$

3. Neutralization of OH^- groups by photoholes which produces $OH^{\bullet}$ radicals

$$(H_2O \leftrightarrow H^+ + OH^-)_{ads} + h_{VB}^+ \rightarrow H^+ + OH^\bullet \quad .....(3)$$

4. Neutralization of $O_2^{\bullet-}$ by protons

$$O_2^{\bullet-} + H^+ \rightarrow HO_2^\bullet \quad .....(4)$$

5. Transient hydrogen peroxide formation and dismutation of oxygen

$$2\,HO_2^\bullet \rightarrow H_2O_2 + O_2 \quad .....(5)$$

6. Decomposition of H_2O_2 and second reduction of oxygen

$$H_2O_2 + e^- \rightarrow OH^\bullet + OH^- \quad .....(6)$$

7. Oxidation of the organic reactant via successive attacks by $OH^\bullet$ radicals

$$R + OH^\bullet \rightarrow R^\bullet + H_2O \quad .....(7)$$

8. Direct oxidation by reaction with holes

$$R + h^+ \rightarrow R^{+\bullet} \rightarrow \text{degradation products} \quad .....(8)$$

As an example of the last process, holes can react directly with carboxylic acid generating CO_2:

$$RCOO^- + h^+ \rightarrow R^\bullet + CO_2 \quad .....(9)$$

In the field of TiO_2 photocatalytic reactions, the commercial TiO_2 powder called “Degussa P25” has been used as a standard material (Ohno, et al., 2001). Because the P25 powder shows better activity for many kinds of photocatalytic reactions, it has been used in many studies. The better photocatalytic activity of Degussa P25 could be explained on the basis of the fact that P25 being consists of small nano-crystallite of rutile disperses within an anatase phases TiO_2 matrix. Each of these matrix surface and interface factors increases the possibility of a chemical reaction by the photo-generated holes and electrons. The principal hypothesis to justify the enhanced activity of mixed phases, relative to pure phases, suggests the transfer of photo-generated electrons from anatase (3.2 eV) to a lower energy rutile (3.0 eV) electron trapping site. This electron transfer reduces the recombination rate of anatase by increasing the separation between the electron and hole, resulting in greater catalytic reactivity of TiO_2 Degussa P25 (Deanna, et al., 2003; Hurum, et al., 2006; Luis, et al 2011). The possible process of electron transfer in the photocatalytic reaction of Degussa P25 is shown in Figure 5. In this research work, the commercial TiO_2 Degussa P25 power (Degussa P25; 80% anatase and 20% rutile; specific surface area 50 m^2/g;

and mean particle sizes of 30 nm) was obtained from Degussa AG, Frankfurt, Germany (Toor, et al., 2006; Yu, et al., 2008).

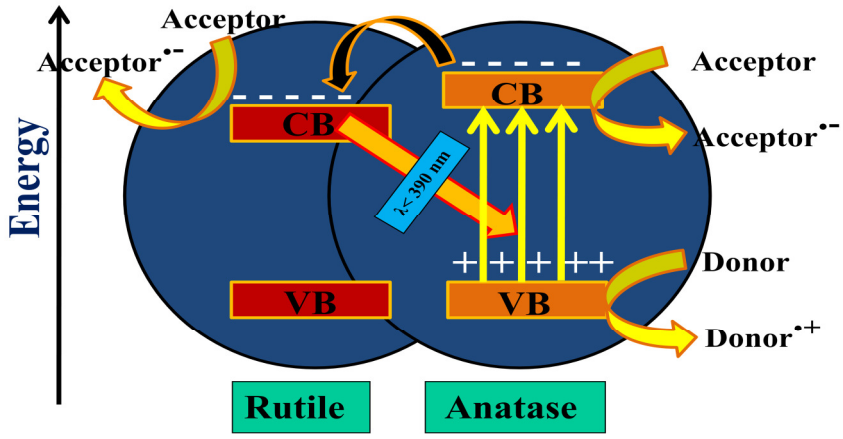

Figure 5 Possible process of electron transfer in the photocatalytic reaction of Degussa P25(Deanna, et al., 2003; Hurum, et al., 2006; Luis, et al 2011)**.**

There are many studies on photocatalytic degradation of organic dye pollutants by Degussa P25 and other TiO_2 powder catalysts. Ding, et al., (2000) prepared a series of TiO_2 samples with different anatase-to-rutile ratios, and studied the roles of the two crystallite phase of TiO_2 on the photocatalytic activity in oxidation of phenol in aqueous solution. It was shown that samples with higher anatase-to-rutile ratios had higher activities for phenol degradation. Houas, et al., (2001) investigated the TiO_2/UV photocatalytic degradation of MB in aqueous solution. They showed that photocatalysis could decontaminate colored used-waters by converting organic pollutants to CO_2 and water without heating nor using high pressure of oxygen nor requiring chemical reactants or additives. These results suggested that TiO_2/UV photocatalysis might be envisaged as a method for treatment of diluted wastewater in textile industries. Chiang, et al., (2002) synthesized Cu (II) oxide loaded onto the surface of Degussa P25 TiO_2 particles by photodecomposition. It was found that the rate of photooxidation of cyanide assisted with the doped catalyst was improved slightly at 0.10 wt% of Cu. Any further increase of the copper dopant concentration decreased the oxidation rate remarkably. The decrease in the activity was explained in terms of the

competition reaction of Cu (II) cyanide complex ions for surface hydroxyl radical. In all cases cyanide was being oxidized to cyanate, the end product of cyanide photooxidation. Tsuji, et al., (2003) reported that the modification of rutile TiO_2 by Ag negative-ion implantation found Ag nanoparticles formed in the surface layer of rutile. The photocatalytic efficiencies for Ag-implanted titania were evaluated by means of decolorization of methylene blue solution under fluorescent light. Ag-implanted rutile after annealing at 500 ^oC showed the better photocatalytic efficiency 2.2 times higher than that of unimplanted rutile titania. In the evaluation under fluorescent light through UV-cut filters, the Ag-implanted rutile showed 6.7 times better efficiency. Nagaveni, et al., (2004) investigated the solar photocatalytic degradation of various dyes such as methylene blue (MB), remazol brill blue R (RBBR) and orange G (OG) over combustion synthesized nano TiO_2 and the activity was compared with that of commercial Degussa P-25 TiO_2 under similar conditions. The effect of catalyst loading, initial concentration of the dye and the deactivation studies of the catalysts were also investigated. The initial degradation rates with combustion synthesized nano TiO_2 was 20 times higher for RBBR, 4 times higher for MB and 1.6 times higher for OG, compared to Degussa P-25 TiO_2. The enhanced photocatalytic of combustion synthesized catalyst is attributed to the crystallinity, nano-size, large amount of surface hydroxyl species and reduced band-gap. Wu, et al., (2004) synthesized vanadium doped TiO_2 catalysts by sol-gel method. The results showed that the increase of vanadium doping promoted the particle growth, and enhanced red-shift in the UV-Vis absorption spectra. The photocatalytic activity was evaluated by the degradation of crystal violet (CV) and methylene blue (MB) under visible light irradiation. The degradation rate of CV and MB on V-doped TiO_2 were higher than those of pure TiO_2. Faisal, et al., (2005) investigated the photocatalytic degradation of two selected dyes, such as Acridine Orange (1) and Ethidium Bromide (2) in aqueous suspension of titanium dioxide (TiO_2) under a variety of conditions, which is essential for application point of view. The photocatalyst, Degussa P25, was found to be more efficient for the photocatalytic degradation of dye derivative (1) and (2). The dye derivative (1) was degraded faster as compared to the dye derivative (2). Muruganandham, et al., (2005) investigated the photocatalytic decolorization and degradation of an azo dye Reactive Yellow 14 (RY14) in aqueous solution with TiO_2-P25 (Degussa) as photocatalyst in slurry using solar light.

The study on the effect of various photocatalysts on the decolorization and degradation reveals the following order of reactivity: ZnO > TiO_2-P25 > TiO_2 (anatase). CdS, Fe_2O_3 and SnO_2 have negligible activity on RY14 decolourization and degradation. Qamar, et al., (2005) investigated the photocatalytic degradation of two selected dye derivatives, chromotrope 2B (1) and amido black 10B (2) in aqueous suspension of titanium dioxide under a variety of conditions which is essential from an application point of view. The photocatalyst Degussa P25 was found to be more efficient as compared with other catalysts. The dye derivative (1) was found to be degraded faster than the dye derivative (2). Sameiro, et al., (2005) investigated the photocatalytic degradation of the commercial azo dye C.I. Reactive Orange 4 in its reactive and hydrolysed, using commercial samples of TiO_2 as a photocatalyst. With UV light, aqueous solutions containing only dye and no dye-bath additives are decolorized slightly more rapidly with Riedel-de-Haen TiO_2 than with Degussa P-25 TiO_2. Senthilkumaar, et al., (2005) prepared nanocrystalline pure anatase titania by sol-gel process at room temperature followed by ultra-sonication (Ti-US). The photocatalytic activity of Ti-US has evaluated by the degradation of textile dye, Methylene Blue in the presence and absence of common inorganic salts (NO_3^-, $C_2O_4^{2-}$, SO_4^{2-}, and citrate). It was observed that, in the presence of anions, the degradation of the dye increase significantly. The photocatalytic rate of methylene blue increased in the presence of hydrogen peroxide (H_2O_2). Senthilkumaar, et al., (2005) prepared nanostructured TiO_2 ultrafine powder (Ti-SG) 100% anatase phase by sol-gel method was used as a photocatalyst in the decomposition reaction of a basic dye, Crystal Violet (CV) in water under UV light irradiation. From the experimental results, sol-gel derived TiO_2 (Ti-SG) showed higher photocatalytic activity than commercially available TiO_2 (Degussa P-25) for the degradation of CV. Bizani, et al., (2006) investigated the photocatalytic degradation of two commercial azo dyes in the presence of TiO_2 suspensions as photocatalyst. The photodegradation of the dyes follows pseudo-first order kinetics according to Langmuir-Hinshelwood model. Silva, et al., (2006) investigated the degradation of three commercially available textile azo dyes, Solophenyl Green BLE 155% (SG), Erionyl Red B (ER) and Chromotrope 2R (C2R) by using photochemical and photocatalytic process under UV irradiation. The photocatalytic process, using either slurry of Degussa P-25 TiO_2 or a biphasic mixture of TiO_2 and activated carbon (AC), more effectively bleaches heavier colored solutions.

Toor, et al., (2006) investigated the adsorption and photocatalytic degradation of diazo Direct Yellow 12 (Chrysophenine G), commonly used as a cotton, paper and leather in aqueous suspension of semiconductor oxide TiO_2 as photocatalyst in a non-concentrating shallow pond slurry type reactor under UV light. The photodegradation of dye on the semiconductor showed dependence effects of initial concentration of dye, catalyst loading, pH and addition of oxidant. The disappearance of the organic molecule followed approximately a pseudo-first kinetic order according to the Langmuir-Hinshelwood model. Faisal, et al., (2007) investigated the photocatalytic degradation of two selected dyes, Acridine (1), and Ethidium (2) using TiO_2 under a variety of condition, which is essential from application point of view. It can be found that the photocatalyst, Degussa P25, has high efficient for the photocatalytic degradation of dye derivatives (1) and (2). The dye derivative (1) was found to degrade faster as compared to the dye derivative (2). Tian, et al., (2007) prepared Au/TiO_2 photocatalyst by water washing (W) and rotary evaporation (E), then study their photodegradation of methyl orange (MO). The results showed that the photocatalytic activity of Au/TiO_2 photocatalyst is related to the preparation process, with a similar gold loading, the photocatalyst prepared by water washing showed higher photocatalytic activity compared to the catalyst prepared by rotary evaporation. Baran, et al., (2008) studied the correlation between the adsorption of the various cationic and anionic dye solution exposed UV irradiation and their photocatalytic degradation in solution. It can be seen that only cationic dyes can adsorbed on the surface of photocatalyst; simultaneously, their photocatalytic degradation is faster than the degradation of anionic dyes. Ishibai, et al., (2008) prepared nano-sized TiO_2 photocatalysts by hydrolysis of $TiCl_4$ followed by calcination at different temperatures. It can be observed that the photocatalytic activity of TiO_2 powder clearly decreased with increasing calcination temperature. Parida, et al., (2008) prepared hydrated titania by a sol-gel method and then promoted with different weight percentages of sulfate by an incipient wetness impregnation method. It was found that at 2.5 wt% sulfate loading, the average percentage of photodegradation of methyl orange was nearly two times than that of the neat TiO_2. The photocatalytic degradation followed first-order kinetics. Li, et al., (2009) prepared nano-anatase TiO_2 of high crystallinity by a novel simple route at a temperature of 100 °C under mild condition. The photocatalytic activity of the prepared photocatalyst was evaluated by

the photodegradation of formaldehyde in aqueous solution and compared with the commercial photocatalyst, namely, Degussa P25. The result showed that the sample prepared at low temperature showed photocatalytic activity. The activity of the sample prepared at 120 °C was high and close to the sample calcined at 300 °C for 2 h. The degradation of formaldehyde by the highest active sample (calcined at 400 °C for 1 h) could almost achieve 100% within 80 min, which exhibited much higher photocatalytic activity than Degussa P25. Wang, et al., (2009) synthesized nano-sized multi-walled carbon nanotubes (MWCNTs)/TiO_2 composite and neat TiO_2 photocatalysts by sol–gel technique using tetrabutyl titanate as a precursor. The samples were evaluated for their photocatalytic activity towards the degradation of 2,4-dinitrophenol (DNP) under solar irradiation. The results indicated that the addition of an appropriate amount of MWCNTs could remarkably improve the photocatalytic activity of TiO_2. The optimal MWCNTs: TiO_2 ratio of 0.05% (w/w) was found to achieve the maximum rate of DNP degradation. Ohtani, et al., (2010) isolated anatase and rutile crystallites TiO_2 from Degussa P25 (Evonic) by selective solution with a hydrogen peroxide-ammonia mixture and diluted hydrofluoric acid, respectively. In comparison, the photocatalytic activity of original Degussa P25 and restructured P25 with those of isolated anatase and rutile particles suggested a less-probably synergetic effect of the co-presence of anatase and rutile. Kanna, et al., (2010) investigated the decolorization of dye solutions, crystal violet (CV) and congo red (CR) using the synthesized amorphous titanium dioxide and compared with commercial titanium dioxides; Degussa P25 and anatase. The result showed that amorphous TiO_2 had good adsorptivity that could decolorize the dye polluted water effectively mainly by adsorption. Decolorization by photocatalytic property was also detected but was very low. Saepurahman, et al., (2010) synthesized tungsten-loaded TiO_2 photocatalyst. From the photocatalytic studies showed that tungsten-loaded TiO_2 was superior to unmodified TiO_2 with 2-fold increase in degradation rate of methylene blue, and equally effective for degradation of different class of dyes such as methyl violet and methyl orange at 1 mol% tungsten loading. Yang, et al., (2010) prepared fluorine–sulfur (F–S) co-doped TiO_2 materials using low temperature solvo-thermal method, and tested for catalytic activity by the visible light photocatalytic degradation of the methylene blue. The results showed that F–S co-doped TiO_2 has a higher photocatalytic activity than that of mono-doped F- and S-doped

samples under visible light irradiation. It is believed that the co-doping gives rise to a localized state in the band gap of the oxide and creates active surface oxygen vacancies, both which are responsible for visible light absorption and the promotion of electrons from the localized states to the conduction band. Chen, et al., (2011) synthesized the phosphorous-modified TiO_2 (P-TiO_2) by a hydrothermal method. The as-prepared P-TiO_2 was evaluated for the degradation of methylene blue and the dechlorination of 4-chlorophenol. In all these experiments, P-TiO_2 showed superior activity compared with pure TiO_2 and even better activity than the commercially available P25 in most cases. Li, et al., (2011) prepared mixed amorphous and crystalline MgA_2O_4 nano-powders with visible light-induced photocatalytic activity via a simple solution combustion method using glycine and urea as fuel mixtures. The photocatalytic results for degradation of methylene blue (MB) indicated that the combustion-synthesized samples had photocatalytic activity, whereas the annealed well crystalline MgA_2O_4 nano-powders had none. The MgA_2O_4 sample containing about 45.6% crystalline and 55.4% amorphous materials showed the highest photocatalytic activity, with a 99.5% MB removal in 100 min under visible light irradiation. Luis, et al., (2011) prepared nanocrystalline titanium dioxide (TiO_2) powders with different crystal phase composition were obtained by controlled hydrolysis and post-thermal treatments. The influence of the TiO_2 phase composition on its photocatalytic activity, concerning the methylene blue photodegradation was studied. It was found that higher TiO_2 photocatalytic activity is related with the co-existence of the three TiO_2 polymorphs: anatase, brookite, and rutile. Oliveira, et al., (2011) investigated the photodegradation of dyes under visible light irradiation represents an important step in the study of advanced oxidation processes (AOP). The sensitization of dyes and surface modification of titanium dioxide with adsorption of dyes promote the electron transfer from excited dyes to the conduction band of semiconductor, optimizing and accelerating the dye degradation. Putta, et al., (2011) synthesized tungsten doping and hydrothermal TiO_2 photocatalyst by the sol-gel method. It was observed that TiO_2 doped with a 0.5%W: Ti mole ratio and treated with 4 h of hydrothermal curing showed photoactivity under blue light irradiation equal to 74% of the commercial Degussa P25 under UV irradiation, i.e., 0.01 mM 2-chlorophenol was completely removed in 120 and 90 min, respectively.

However, many disadvantages of the use of TiO_2 in powder form have been noted: (i) difficulty and high cost in the separation and recovery of the catalyst from suspension, (ii) non-reusable of the catalyst, (iii) easy aggregation of the suspended particles, (iv) difficulty in application to continuous flow systems, (v) possibility to cause adverse human health problems by the loose powder To avoid the use of photocatalyst in powder form, several efforts have been made to coat TiO_2 as films on various substrates such as glass, ITO glass, stainless steel, plastics, and polymers, as well as employing several techniques such as flame synthesis, chemical vapor deposition (CVD), spray pyrolysis deposition, and sol-gel dip/spin coating.

There are many studies on the photocatalytic degradation of organic dyes pollutants by using Degussa P25 and other TiO_2 films and thin films. Wang, et al., (1998) presented the results of the photocatalytic experiment involving a series of semiconductor oxide thin films mixed with TiO_2 and WO_3, immobilized on glass plates by reactive sputtering method. It can be seen that the TiO_2 thin film showed that the TiO_2 thin film has better destruction effect than the Degussa P25 powder, due to its unique microstructure. This kind of immobilized photocatalyst achieves good experimental results in treating Rhodamine B dyeing wastewater. Byun, et al., (2000) prepared TiO_2 thin films on window glass substrates by chemical vapor deposition (CVD). It is clear that the thin film TiO_2 should be controlled to exhibit the preferred orientation for optimum photocatalytic reaction rate. CVD method is an alternative for the deposition of the photocatalytic TiO_2. Dumitriu, et al., (2000) prepared TiO_2 thin films by direct current (DC) reactive sputtering, using various kinds of supports such as glass, silicon, alumina and glass coated with indium tin oxide. The photocatalytic properties of the samples were tested on the degradation of phenol. The best efficiency with respect to phenol mineralization was obtained for simple preparation using an Ar-H_2O mixture as the reactive gas. Ding, et al., (2001) investigated coating TiO_2 onto three difference activated carbon (AC), ϒ- alumina (Al_2O_3) and silica gel (SiO_2) by chemical vapor deposition (CVD) method. It can be observed that among the three types of material supports, silica gel was the best for coating anatase TiO_2 by CVD and TiO_2/SiO_2 showed the highest activity in the photocatalytic degradation of phenol in water due to higher surface hydroxyl groups and macropore surface area. Michael, et al., (2002) prepared TiO_2 thin film photo-semiconductor electrodes by chemical vapor

deposition (CVD) and compared for the photocatalytic (PC) and photo-electrocatalytic (PEC) degradation of 4-chlorophenol (4-CP) in aqueous solution. The efficiency of PC degradation of 4-CP were low, but were found to be improved significantly by PEC with an applied potential. Arabarzis, et al., (2003) investigated nanocrystalline titania thin film photocatalysts by gold deposition via electron beam evaporation, with an attempt to study decomposition reaction rate of industrial water pollutants. It can be found that higher surface loading result in an efficiency decrease and this can be understood in terms of an optimum gold particle size and surface characteristics as well as the semiconductor availability for light absorption and pollutant adsorption. Kwon, et al., (2004) prepared titanium dioxide nano-crystalline thin films on glass, polycarbonate and aluminum via a sol-gel process using different alkoxide precursors. Surface morphology and thereby photocatalytic reactivity of the TiO_2 thin films can be tailored by proper heat treatment. The maximum photocatalytic decomposition of methylene blue solution was a heat treatment at 400°C, which was ascribed to the enlarged surface area upon morphological change of the surface. Wang, et al., (2005) prepared muti-walled carbon nanotubes (MWNT) and TiO_2 composite catalysts by a modified sol-gel method. The photocatalytic degradation of phenol was performed under visible light irradiation on these catalysts. An optimum of synergetic effect on photocatalytic activity was observed for a weight ratio MWNT/TiO_2 equal to 20% with an increase in the first order rate constant by factor of 4.1. The synergetic effect, induced by a strong interphase between MWNT and TiO_2, was discussed in terms of different role played by MWNT in the composite catalysts. Yuan, et al., (2005) investigated the photocatalytic degradation of methylene blue (MB) in aqueous solution by using TiO_2 immobilized on activated carbon fibers (ACFs). After six cycles, the amount of MB removal for the TiO_2/ACF composite was slightly higher than that for fresh P25 TiO_2 in suspension. Zainal, et al., (2005) investigated the photodegradation of various dyes in aqueous solution by using glass coated titanium dioxide thin film as photocatalyst. The dyes removal efficiency was studies and compared using UV-vis spectrophotometer analysis. The result showed that the total removal of each dye was: methylene blue (90.3%), methyl orange (98.5%), indigo camine (92.4%), Chicago sky blue 6B (60.3%) and mixed dyes (70.1%), respectively. Ge, et al., (2006) prepared anatase TiO_2 thin films on glass slide substrates via a sol-gel method from refluxed sol (RS) containing anatase

TiO_2 crystals at low temperature of 100°C. The degradation of methyl orange of RS-6 thin films reached 99% after being irradiated for 120 min, the results suggested that the TiO_2 thin films prepared from RS sol exhibited high photoactivities. Yang, et al., (2006) developed dip-coating process for TiO_2 thin film on polymer substrates (acrylonitrile-butadiene-styrene polymer: ABS, polystyrene: PS). It can be found that the photocatalytic degradation of methylene blue (MB) on the TiO_2 thin films showed complete decomposition after 180 min under UV light irradiation. Yu, et al., (2006) prepared Fe-doped TiO_2 thin films in situ on stainless steel substrates by liquid phase deposition, followed by calcinations at various temperatures. It was found that at 400°C, the film became photoactive due to the formation of anatase phase. At 500°C, the film showed the highest photocatalytic activity due to an optimal Fe^{3+} ion concentration in the film. Habibi, et al., (2007) investigated the photocatalytic degradation of a non-biodegradable azo dye called (C.I. Direct 80, Red Sulphonyl 3BL) using TiO_2 thin films in aqueous solution under UV light irradiation. Results show that the employment of efficient photocatalyst and the selection of optimal operational parameters lead to complete decolorization. The best conditions for maximum photocatalytic degradation were found to be pH 1 at 5 ppm concentration of dye over TiO_2 thin films deposited on glass substrate coated with indium-tin oxide having 350 nm thicknesses annealed at 550 °C. Paola, et al., (2007) prepared pure brookite films obtained by peptizing a mixture brookite-rutile by thermolysis of $TiCl_4$ in a HCl solution. The result showed that the brookite films efficiency degraded 2-propanol under UV light illumination. Yuan, et al., (2007) synthesized anatase TiO_2 films by a modified sol-gel method. It can be found that the hydrophilicity and photocatalytic activity of the films were remarkably by doping transition metal ion Fe^{3+}. Ao, et al., (2008) prepared the different titania films by a sol-gel spin coating technique. The photocatalytic property of the prepared porous film was evaluated by degrading X-3B under UV irradiation. Results showed that photocatalytic performance of as-prepared porous film was much higher than that of smooth titania and P25 films. Ao, et al., (2008) prepared anatase titania-activated carbon composite film by a simple method at low temperature (75 °C at most). The photocatalytic property of the prepared porous film was determined by degradation of 4-cholophenol (4-CP) under UV irradiation. It can be exhibited that the photocatalytic activity of composite film enhanced a lot. Yogi, et al., (2008) studied photodegradation

and demethylation reactions of methylene blue (MB) by a TiO_2 photocatalytic film. It can be found that MB was less demethylated by reaction with an Au particles-TiO_2 composite film than the TiO_2 photocatalytic film. Ren, et al., (2009) prepared porous TiO_2 sheets by aqueous tape casting were modified with Ag deposition. The results showed that Ag-deposited TiO_2 sheets had better photocatalytic activity than the pure TiO_2 sheets, the optimum deposition time was found to be 2 min and the corresponding Ag loading was 1.48 mg/cm^2 TiO_2 sheet. Suwanchawalit, et al., (2009) prepared higher-ordered 3D macroporous TiO_2-functionalized chitosan scaffolds by ice segregation induced self-assembly. The result showed that the hybrid scaffolds could reuse substrates for the photocatalytic degradation of methylene blue and orange II dye molecules. Guo, et al., (2010) synthesized through-porous steel fiber matrix with high specific surface area and self-support strength as the support of TiO_2 film photocatalyst. The photodegradation of methyl orange was used for evaluating the photocatalytic properties. The results show that compared with TiO_2 films deposited on flat Si wafers, TiO_2 films on the porous support display higher photocatalytic activities, owing to their higher specific surface areas. Tehrani, et al., (2011) prepared thin films of titanium dioxide with high surface area by sol-gel dip-coating technique. The photocatalytic activities of titanium dioxide thin films were measured in the presence of methylene blue. The thin films prepared by using nitric acid as a stabilizer, revealed higher photocatalytic activity, surface area and sol stability and these data were more than those prepared with acetic acid. Seabra, et al., (2011) prepared active TiO_2 layers immobilized, on aluminium sheets by a common and cheap deposition technique: jet spray. The result indicated that a better performance was attained for layers having a 1:1 weight ratio of TiO_2 and polyester ink and a thickness of 60 μm (100 g/m^2).

These methods, however, have some disadvantages for industrial applications, for instance, the chemical vapor deposition, spray pyrolysis deposition, and flame synthesis methods require special and rather expensive apparatus and complex procedures for the deposition of TiO_2 film while the sol-gel dip/spin coating method needs repeated coating in order to get a thick film and requires high annealing temperature for crystallization. In addition, the heating process precludes the fabrication of TiO_2 film on substrates with low thermal stability such as plastics and hydrocarbon polymers (Yang, et al., 2006). Therefore, a simple, less expensive and more effective

method for the preparation of immobilized TiO_2 powder is still an interesting topic under investigation in many laboratories including ours.

In this work the author presents, simple, less expensive, and effective method for the preparation of immobilized TiO_2 powder on the rubber sheet substrate by three different methods, using commercial TiO_2 powder (Degussa P25) and rubber latex (60% HA) as starting materials. The rubber latex strikes our interest because of its versatility in daily life, available locally, and -to the best of our knowledge -has never been used as a substrate for TiO_2 coating (except in our group).

1.2.2 Natural rubber (NR) latex

Natural rubber (NR) latex, obtained from the *Hevea brasiliensis* tree, is a dispersion of *cis*-polyisoprene latex particles and nonrubber particles in an aqueous serum phase (Ho, et al., 1996; Kang, et al., 2000; Yeang, et al., 2002). The photograph of fresh latex and *cis*-1-4-polyisoprene monomer of natural rubber latex are shown in Figure 6. Rubber latex from field collection contains many natural substances including nonrubber, 30-35% polyisoprene rubber polymer, and 60-65% water. Generally, ammonia is usually added to the latex as a preservative to increase the alkalinity (pH) and retard microbial growth. The additional benefit from adding ammonia is the increase in stability of the NR due to the increase in negative surface charge of the rubber particles (Perrella, et al., 2002). Apart from the rubber latex hydrocarbon, a large number of nonrubber constituents (mainly carbohydrate, phospholipids, and proteins) are also present in relatively small amounts in the aqueous phase. Some are associated with the rubber particles themselves (Ho, et al., 1996).

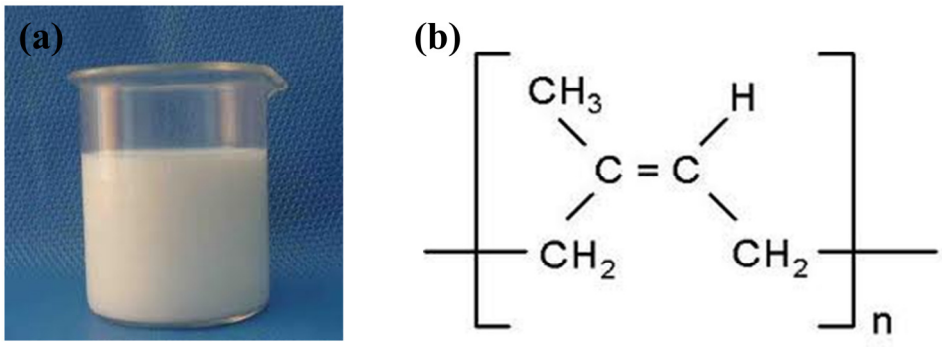

Figure 6 (a) fresh latex and (b) *cis*-1-4-polyisoprene monomer of natural rubber (NR) latex.

The NR particles of the fresh field latex are stabilized by adsorbed proteins and phospholipids. The NR particle surface was surrounded by a layer made up of mixed domains of proteins and phospholipids (Fig. 7B), in contrast to the previously perceived structure of a double-layer (Fig. 7A). Here, the NR molecule linked with proteins and phospholipids at respectively the ω- and α-terminal ends was believed to orientate them, so that these hydrophilic ends were located on the particle surface as a thin layer. The polyisoprene molecules should then form the hydrophobic core, in essence giving rise to a core-shell-like particle (Nawamawat, et al., 2011).

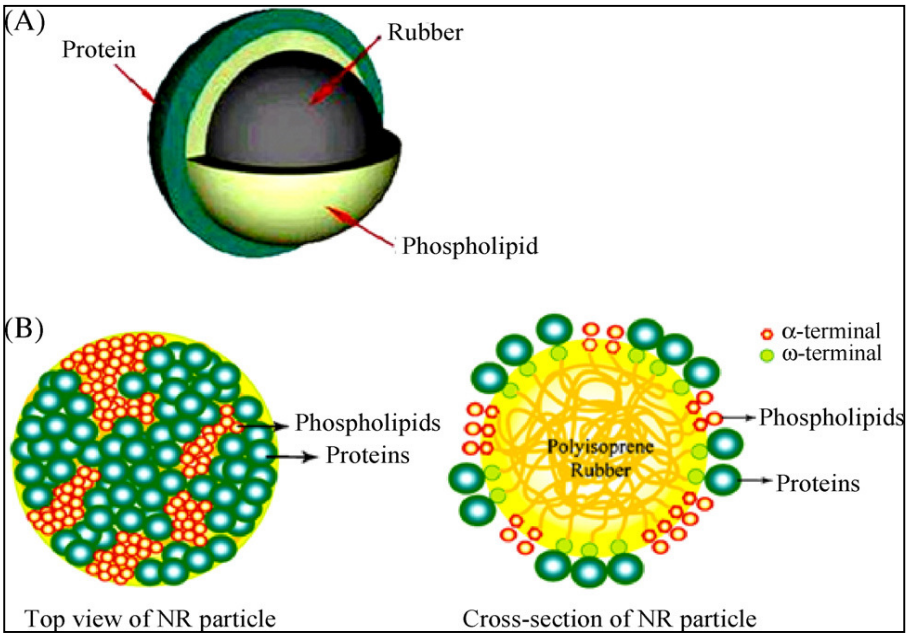

Figure 7 Two possible models for the structure of the rubber latex particle surfaces. (A) a current model of an NR latex particle surrounded by a double-layer of proteins and phospholipids and (B) the proposed new model consisting of a mixed layer of proteins and phospholipids around the latex particle (Nawamawat, et al., 2011).

Commercial high-ammonia (HA) latex concentrate is produced by centrifugation which removes about two-three of the water soluble nonrubber and smaller latex particles of the field latex (Sansatsadeekul, et al., 2011). Hydrolysis of the

phospholipids results in changes of the chemical composition of the rubber/water interface with time in latex concentrates well after production. Thus, the latex particles in HA latex concentrate are stabilized mainly by adsorbed long-chain fatty acid soaps, hydrolysis products of phospholipids. The role of adsorbed proteins on latex stabilization is less important in latex concentrate (Ho, et al., 1996).

The colloidal stability of the latex is extremely sensitive to pH as well as to the ionic environment of the dispersing medium. The negative charge on the particle surface is derived mainly from carboxylic groups of long chain fatty acid soap (Nawamawat, et al., 2011). Due to having high carboxylic groups of the rubber latex particles, it can be bonded to the other molecules. Therefore, in this work, we expect that the TiO_2 particles may react with the carboxylic groups on the rubber latex particle, resulting to the stability of TiO_2-rubber latex composite through the strong bonded -COO-TiO_2 in the further solid sheet form. The possible bonding of TiO_2 particle and natural rubber (NR) latex particles is shown in Figure 8.

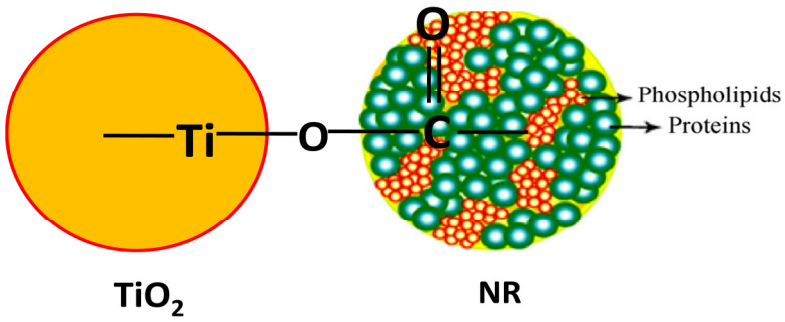

Figure 8 Possible bonding of TiO_2 particle and natural rubber latex (NR) particle (modified from Nawamawat, et al., 2011).

Interestingly, natural rubber (NR) latex is a renewable material produced at a very low cost and used in large and growing amounts, in the making of tires, carpet lining, diving gear, and adhesives (Ripple, et al., 2004). It has been widely used in the form of thin film in many applications such as tubing, balloon, and glove owing to its excellent elasticity, flexibility, tack, adhesiveness, and high surface friction (Sanguansap, et al., 2005; Sruanganurak, et al, 2006). From these properties, in this work, we are interested in using the rubber latex (HA) as a substrate and adhesive material for the preparation of immobilized TiO_2 powder on the rubber sheet surface.

1.2.3 Organic dye pollutant: indigo carmine (IC)

Organic dyes constitute one of the larger groups of pollutants in wastewater released from textile and other industries. The discharge of highly coloured wastewater into the ecosystem involves environmental problems like aesthetic pollution (even a small amount of dye is clearly apparent), and perturbation of aquatic life. Among the most useful dyes, there is indigo carmine (3,3'-dioxo-2,2'-bis-indolyden-5,5'-disulfonic acid disodium salt) or acid blue 74 which is one of the oldest dyes and still one of the most important used. Its major industrial application is the dyeing of clothes (blue jeans) and other blue denim (Othman, et al., 2006; 2007). Apart from its use as textile colouring agent and additive in pharmaceutical tablets and capsules as well as in confectionery items, indigo carmine is also used for medical diagnostic purposes. In conjunction with acetic acid, the dye facilitates diagnosis of Barrett's esophagus. It can also help to target biopsies, since in homogeneously stained or unstained areas seem to correlate with intraepithelial neoplasia (Mittal, et al., 2006). However, indigo carmine is not readily metabolized but is rather freely filterable by the kidneys. Giving intravenous injection of indigo carmine for intra-operative cystoscopy is a safe technique that can detect otherwise undetected intra-operative compromise of the urinary tract. It also contributes to intra-vital staining for contrasting and accentuating changed mucosal processes. The indigo carmine is considered as highly toxic indigoid class of dye. Contact with it can cause skin and eye irritations. It can also cause permanent injury to cornea and conjunctiva. The consumption of the dye can also prove fatal, as it is carcinogenic and can lead to reproductive, developmental, neuron and acute toxicity. It has also been established that the dye leads to tumors at the site of application. When administered intravenously to determine potency of the urinary collecting system, it is also known to cause mild to severe hypertension, cardiovascular and respiratory effects in patients. It may also cause gastrointestinal irritations with nausea, vomiting and diarrhea. The toxicity tests of the dye revealed long-term toxicity

in mice and short-term toxicity in the pig (Barka, et al., 2008). Thus, keeping the toxicity of this dye in view, and various attempts have been made for the removal of indigo carmine from water and wastewater before releasing to the environment.

There are many studies for removal of indigo carmine (IC) dye pollutant in water by various materials includes TiO_2 photocatalysts. Vautier, et al., (2001) investigated TiO_2/UV photocatalytic degradations of indigo and indigo carmine dye in aqueous heterogeneous suspensions and in the solid state. These results suggest that TiO_2/UV photocatalysis might be envisaged as a method for treatment of diluted wastewaters in textile industries. They determined and presented the degradation pathway of indigo carmine (IC) dye using Degussa P25-TiO_2 as photocatalyst under UV irradiation as shown in Figure 9. In the present case, the OH radicals can break the various C–N and C–C bonds of the chromophore group, thus accounting for the various metabolites identified. The aromatic intermediates found (anthranilic acid, nitrobenzaldehyde, nitrobenzoic acid, and nitrobenzene) undergo successive attacks by OH radicals, giving hydroxylations and/or substitutions generally leading to hydroxy-hydroquinone known as the last aromatic molecule found before the aromatic ring opening. The total degradation leads to the conversion of organic carbon into gaseous CO_2, whereas nitrogen and sulfur heteroatoms are converted into inorganic ions, such as nitrate and ammonium, and sulfate ions, respectively. Mittal, et al., (2006) prepared an inexpensive adsorption method for the removal of indigo carmine (IC), a highly toxic indigoid class of dye from wastewater. Waste materials-bottom ash, a powder plant waste and de-oiled soya, an agricultural waste have been used as adsorbents. Attempts have been made through batch and bulk removal of the dye and both the adsorbents have been found to exhibit good efficiency to adsorb indigo carmine. Othman, et al., (2006) studied the discoloration (adsorption) and mineralization (in the presence of UV irradiation) of indigo carmine (IC) dye by hydrothermally synthesized ZSM-5 zeolite modified by manganese (Mn/ZSM-5) or lanthanum (La/ZSM-5) or mixture of both (Mn–La/ZSM-5) using impregnation techniques. The results indicated that MnO_x incorporated ZSM-5 that showed the highest lattice volume and pore radius between all samples presented the highest photocatalytic activity, comparatively. Othman, et al., (2007) investigated on the discoloration (adsorption) and mineralization (in the presence of UV irradiation) of indigo carmine (IC) dye over four photocatalysts TiO_2-D (from

Degussa), TiO_2-SG (prepared with a sol–gel method), Mn/TiO_2-imp (prepared with an impregnation method) and Mn/TiO_2-SG (prepared with a sol–gel method) is presented. The experimental results show that Mn/TiO_2-imp gives the highest photocatalytic activity.

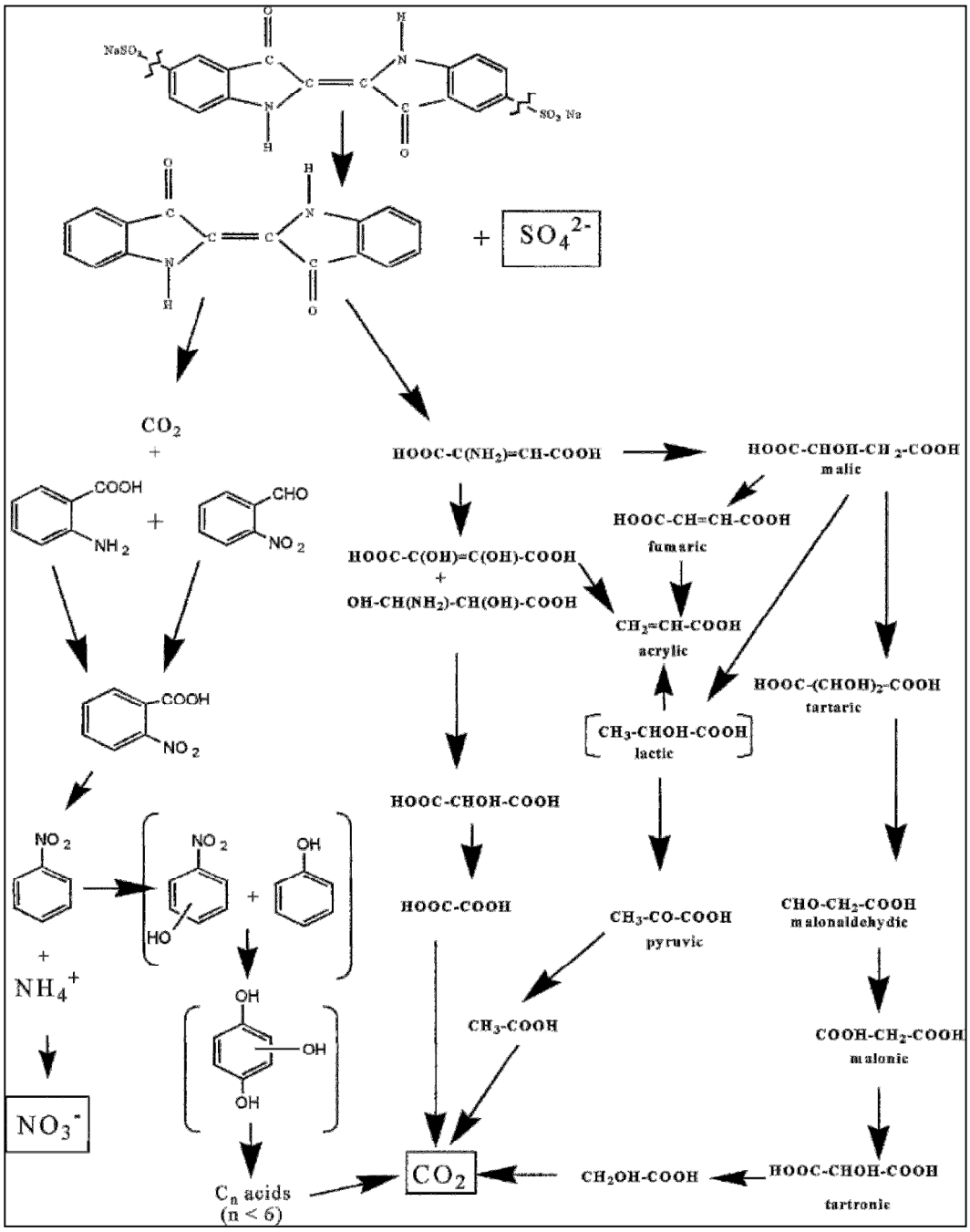

Figure 9 Photocatalytic degradation pathway of indigo carmine (IC) dye (Vautier, et al., 2001).

Barka, et al., (2008) investigated the photocatalytic degradation of indigo carmine (IC) in aqueous solutions using TiO_2 coated non-woven fibres as photocatalyst. The experimental results show that adsorption is an important parameter controlling the apparent kinetic constant of the degradation. The photocatalytic degradation rate was favoured by a high concentration of solution in respect to Langmuir–Hinshelwood model. The degradation rate was pH and temperature dependent with a high degradation rate at high temperature. Prado, et al., (2008) investigated the application of Nb_2O_5 catalyst for the photodegradation of contaminant. This catalyst was applied to degrade indigo carmine dye (IC), which was compared with degradation catalyzed by TiO_2 and ZnO. It can be found that almost 100% of dye degradation occurred at 20, 45, and 90 min for TiO_2, ZnO, and Nb_2O_5, respectively. Almost 100% of dye degradation occurred at 20, 45, and 90 min for TiO_2, ZnO, and Nb_2O_5, respectively.

In this study, the photocatalytic activities of all immobilized TiO_2 sheets were evaluated using indigo carmine (IC) as a model of organic dye pollutant. Indigo carmine is a brightly colored blue anionic dye, with λ_{max} values at 610 nm. The molecular structure and absorption spectrum of IC dye are illustrated in Figure 10. And the percentage of photodegradation of IC dye was calculated by Eq. (10):

$$\text{Degradation of IC (\%)} = \frac{C_0 - C_t}{C_0} \times 100 \qquad (10)$$

where C_0 is the initial concentration of IC dye and C_t is the concentration at a specific time interval of the collected sample.

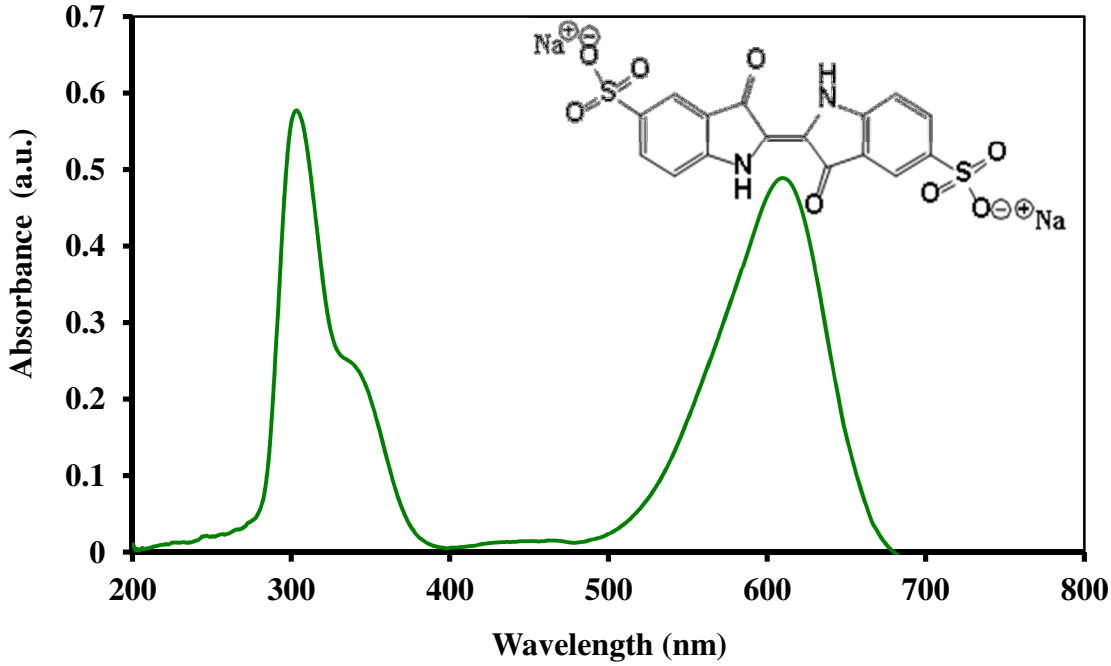

Figure 10 Molecular structure and absorption spectrum of indigo carmine (IC) dye.

1.3 Objectives

The objectives of this research concentrate on using locally available material to enhance the use of TiO_2 photocatalysts. Besides the efficiency, the recyclability of products is also of prime importance. The material in this case is rubber latex. The searches for the most possible combined uses of rubber latex and TiO_2 photocatalysts are as follows.

1.3.1 Preparation of immobilized TiO_2 (Im-TiO_2) sheets

(1) To prepare Im-TiO_2 sheets by directly mixing commercials TiO_2 powder (Anatase and Degussa P25) with rubber latex (HA) and distilled water.

(2) To characterize the properties of Im-TiO_2 sheets using SEM/EDS and XRD techniques.

(3) To evaluate the photocatalytic activities of Im-TiO_2 sheets on the degradation of indigo carmine (IC) dye.

(4) To study the effect of pH, initial concentration of IC, and the intensity of UV light on the photocatalytic degradation of Im-TiO_2 sheets and their recyclability.

1.3.2 Preparation of TiO_2-strewn sheets

(1) To prepare TiO_2-strewn sheets by strewing TiO_2 (Degussa P25) onto the sheet of rubber latex (60% HA).

(2) To characterize the properties of TiO_2-strewn sheets using SEM/EDS and XRD techniques.

(3) To evaluate the photocatalytic activities of TiO_2-strewn sheets on the degradation of indigo carmine (IC) dye.

(4) To study the effect of pH, initial concentration of IC, and the intensity of UV light on the photocatalytic degradation of TiO_2-strewn sheets and their recyclability.

1.3.3 Preparation of TiO_2-embedded (ET) sheets

(1) To prepare TiO_2-embeded sheets by water-mixed rubber latex and TiO_2 (Degussa P25) powder suspended in ammonia solution.

(2) To characterize the properties of TiO_2-embeded sheets using SEM/EDS and XRD techniques.

(3) To evaluate the photocatalytic activities of TiO_2-embeded sheets on the degradation of indigo carmine (IC) dye.

(4) To study the effect of pH, initial concentration of IC, and their recyclability.

CHAPTER 2
EXPERIMENTAL

2.1 Chemicals

1. Titanium dioxide, Degussa P25 (Anatase and Rutile (80:20)), code no. D-60287, Degussa AG, Frankfurt, Germany
2. Titanium dioxide, Anatase, code no. 488257, Carlo Erba, Milano, Italy
3. Natural rubber latex, 60% HA, Chana Latex Co. Ltd, Songkhla, Thailand
4. Indigo carmine (IC), $C_{16}H_8N_2Na_2O_8S_2$, code no. 57000, Fluka, U.S.A.
5. Ammonium hydroxide (Ammonia solution, 28.0-30.0%), NH_4OH, A.R., code no. 9721-03, J.T. Baker, U.S.A.
6. Hydrochloric acid, HCl, A.R., code no. 9535-03, J.T. Baker, U.S.A.
7. Sodium hydroxide, NaOH, A.R., BDH, England

2.2 Instruments

1. X-ray diffractometer, XRD, PHILIPS X'Pert MPD, the Netherlands
2. Scanning electron microscope, SEM, JEOL JSM-5800LV, Japan, attached with energy dispersive X-ray spectroscopy, EDS, Oxford ISIS, England
3. UV-Visible spectrophotometer, SPECORD S100, Analytik Jena GmbH, Germany
4. Photoreactor compartment (0.9m × 0.9m × 0.9m) with five tubes of 20 watts Blacklight, F20T12-BLB, G.E., U.S.A.
5. Analytical balances, AE 200S, SNR M10802, Mettler Toledo A.G., Switzerland
6. Centrifuge, EBA 20, Hettich, Germany
7. Magnetic stirrer, Jenway 1000, JENWAY, England
8. pH meter, Hanna instruments, 8519, U.S.A.
9. pH meter, pHTestr 10, Eutech/Oakton instruments, U.S.A.
10. Petri dish, 3.5 inch and 4.0 inch diameter, Pyrex, Germany
11. Steel sieve, 60-mesh sieve, 12.0 inch diameter, 250 micrometer pore size
12. Sintered glass, 150 mL, F4-4.5 ASM, U.S.A.

2.3 Methods

2.3.1.1 Preparation of TiO_2-impregnated rubber sheets

The preparation of both impregnated anatase sheet (Im-Anatase) and impregnated Degussa P25 sheet (Im-P25) has already been described elsewhere (Sriwong, et al., 2008). The Im-TiO_2 sheets were prepared by mixing 0.1 g of each TiO_2 powder in 3 mL distilled water (anatase) and in 5 mL distilled water (Degussa P25), then stirred for 3 min after which 5 mL of natural rubber latex (60% HA) was added and stirred for another 5 min. The mixtures were poured into Petri dish (3.5 inch diameter) and dried at room temperature for 15 h. After which the Im-TiO_2 sheets were taken out from Petri dish, reversed, and dried at room temperature about 2 h. The preparation process for preparing TiO_2-impregnated rubber sheet is shown in Figure 11.

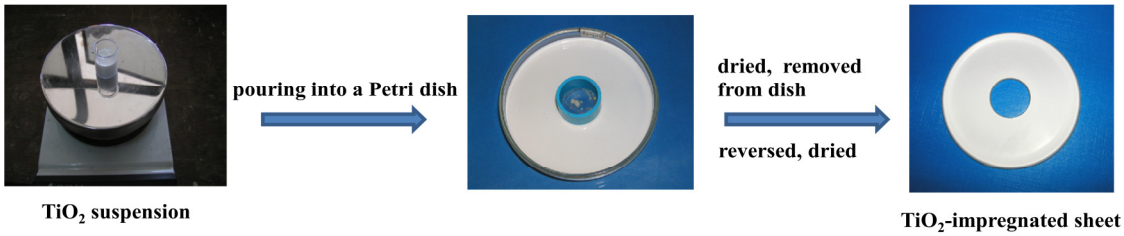

Figure 11 The preparation process for preparing TiO_2-impregnated rubber sheet.

2.3.1.2 Characterization of TiO_2-impregnated rubber sheets

2.3.1.2.1 X-ray powder diffraction (XRD)

The XRD technique was used for crystalline phase identification and to confirm structure of the TiO_2 anatase powder (Carlo Erba., Italy), TiO_2 Degussa P25 powder (Degussa AG., Germany), Im-Anatase sheet, and Im-P25 sheet. All data were acquired at the Scientific Equipment Center, Prince of Songkla University, Hat-Yai, Songkhla, Thailand, by using X-ray diffractometer, XRD: PHILIPS X'Pert MPD, Cu K_α irradiation and equipped with a Ni filter in the range 5-90° at 2θ. In the sample preparation, TiO_2 sheets were cut to an appropriate size and placed into to the sample holder for the XRD determination.

2.3.1.2.2 Scanning electron microscopy (SEM)

The surface morphology of all sheet samples were observed on a SEM: JEOL JSM-5800LV, scanning electron microscopy (SEM) using high vacuum mode with secondary electron image conditions and electron micrograph technique. All data were acquired by the Scientific Equipment Center, Prince of Songkla University, Hat Yai, Songkhla, Thailand. In the sample preparation, TiO_2 sheets were cut to 1cm × 1cm size to fit in the specimen chamber and mounted rigidly on a specimen holder (called a specimen stub). For conventional imaging in the SEM, all samples must be made electrically conductive by being sputtering-coated with gold prior to requiring image under an SEM apparatus to study the surface morphology of TiO_2 sheet.

2.3.1.2.3 Energy dispersive X-ray spectroscopy (EDS)

The EDS analysis was carried out to confirm the presence of elements in the TiO_2-impregnated sheets**.** All data were acquired at the Scientific

Equipment Center, Prince of Songkhla University, Hat Yai, Songkla, Thailand. The TiO_2 sheet samples were also prepared using the same method as the samples prepared for the SEM technique but without sputtering-coated with gold. Then the samples were measured by using energy dispersive X-ray spectroscopy (EDS), Oxford ISIS 300 attached to the scanning electron microscopy (SEM) apparatus as elemental analyzer.

2.3.1.3 Photocatalytic tests

2.3.1.3.1 Construction of calibration graph of indigo carmine (IC)

In this work, the concentration of standard IC solutions were in the range 1.0×10^{-5} M to 5.0×10^{-5} M. In order to construct reliable standard calibration graph of indigo carmine, the working concentrations were divided into five points: 1.0×10^{-5} M, 2.0×10^{-5} M, 3.0×10^{-5} M, 4.0×10^{-5} M, and 5.0×10^{-5} M. The calibration curve graph of IC dye solution is shown in Figure 12.

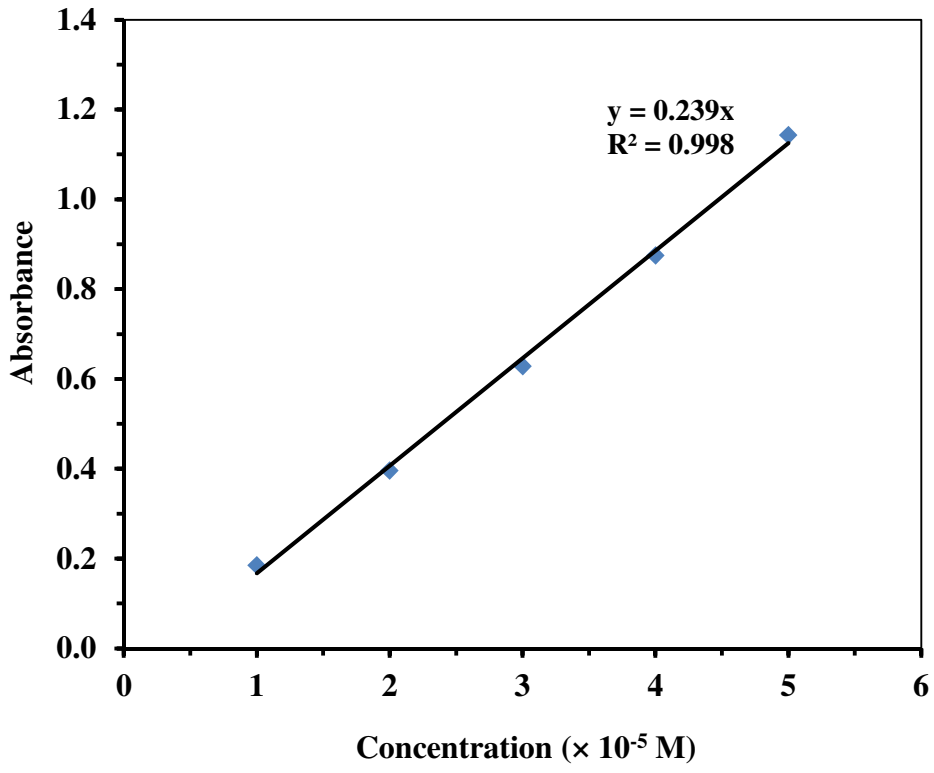

Figure 12 The standard calibration curve of IC dye solution in the range of 1.0×10^{-5} M to 5.0×10^{-5} M.

2.3.1.3.2 Photocatalytic studies

In the photocatalytic studies, the TiO_2-impregnated sheet was settled into a Petri dish (4 inch diameter) containing 60 mL of IC aqueous solution (2.5×10^{-5} M). The solution was then stirred for 30 min in the dark to reach the adsorption equilibrium in tightly closed photoreactor compartment (0.9m × 0.9m × 0.9m) to avoid interference from ambient light. Then the irradiation began under UV-light (5 tubes of blacklight, 20 watts each, F20T12-BLB, GE, U.S.A.) and magnetically stirred at 400 rpm. The blacklight tubes were attached at fixed positions inside with one tube at the top wall and one each at four side walls of the compartment. At given irradiation time intervals (every 1 h), 4 mL of IC solution samples were collected. The degradation of IC solutions was analyzed from the changes in absorbance of the absorption maximum at 610 nm using UV-Vis spectrophotometer Specord S100, Analytik Jena., Germany. The concentration of IC dye solution was determined quantitatively through the calibration graph constructed as previously mentioned.

The effect of various initial IC dye concentrations were investigated with concentrations 1.0×10^{-5} M, 2.0×10^{-5} M, and 3.0×10^{-5} M. The pH of IC dye solutions were studied in the range of 3 to 8 by adding dilute aqueous solution of HCl and NaOH. The effect of intensity of UV light was studied by varying the number of blacklight tubes. These blacklight tubes were turned on 1, 3, or 5 tubes at the time to provide, respectively, low, medium, or high intensity of UV light. In addition, the recyclability tests of Im-Anatase sheet were also studied.

2.3.2.1 Preparation of TiO_2-strewn rubber sheets

The TiO_2-strewn sheet was prepared from Degussa P25 TiO_2 powder and rubber latex (60% HA). In a typical preparation, rubber latex (10 mL) was poured into a Petri dish mould (3.5-inch diameter) and was left at room temperature for about 2 h for gelation to form. Then, 0.03 g of P25 TiO_2 was strewn onto the surface of the rubber sheet by using a 60-mesh sieve and allowed to dry at room temperature for 6 h. Afterwards, the strewn rubber sheet was taken out from the mould and dried at 100 °C for 1 h. After cooling to room temperature, the sheet surface was lightly sprayed with distilled water to wash out some of the P25 TiO_2 particles that were left unbound until the strewn surface was free of loose particles. The sheet then was again dried at 100°C

for 10 min and ready for use in the next step. The variation of parameters such as the time at strewing (0 h, 1 h, 2 h, and 3 h), the time for drying at 100 °C (0 h, 1 h, 2 h, and 3 h), and the amount of Degussa P25 TiO_2 powder (0.03 g, 0.05 g, 0.07 g, and 0.10 g) were studied to optimize the preparation of TiO_2-strewn rubber sheet for maximum photocatalytic degradation of IC dye in aqueous solution under UV light irradiation.

2.3.2.2 Characterization of TiO_2-strewn rubber sheets

The prepared TiO_2-strewn rubber sheets were characterized by XRD, SEM, and EDS techniques in the same way as described in 2.3.1.2.

2.3.2.3 Photocatalytic tests

In the photocatalytic studies, the TiO_2-strewn sheet was settled into a Petri dish (4 inch diameter) containing 60 mL of IC aqueous solution (2.5×10^{-5}M). The solution was then stirred for 15 min in the dark to reach the adsorption equilibrium in tightly closed photoreactor compartment (0.9m × 0.9m × 0.9m) to avoid interference from ambient light. Then the irradiation began under UV-light (5 tubes of blacklight, 20 watts each, F20T12-BLB, GE, U.S.A.) and magnetically stirred at 400 rpm. At given irradiation time intervals (every 1 h), 3 mL of IC solution samples were collected. The degradation of IC dye solutions was analyzed from the changes in absorbance of the absorption maximum at 610 nm using UV-Vis spectrophotometer Specord S100, Analytik Jena, Germany. The concentration of IC dye solution was determined quantitatively through the calibration graph.

The effect of various initial IC dye concentrations were investigated with concentrations 2.5×10^{-5} M, 5.0×10^{-5} M, and 7.5×10^{-5} M. The pH of IC dye solutions were studied in the range of 3 to 8 by adding dilute aqueous solution of HCl and NaOH. The effect of intensity of UV light was studied by varying the number of blacklight tubes. These blacklight tubes were turned on 1, 3, or 5 tubes at the time to provide, respectively, low, medium, or high intensity of UV light. In addition, the recyclability tests of TiO_2-strewn sheet were also studied.

2.3.3.1 Preparation of TiO_2-embedded rubber (ET) sheets

The ET sheet was prepared from water-mixed rubber latex and TiO_2 powder suspended in ammonia solution. In a typical procedure to prepare the 5 %wt FT sheet, 0. 84 mL of natural rubber latex (60% HA) was mixed with 9.16 mL of distilled water to make the total volume of 10 mL and was stirred for 15 min. The ammoniacal TiO_2 was prepared by mixing 0.5 g of TiO_2 powder (Degussa P25) with 5 mL ammonia solution and vigorously stirred for 15 min. The prepared 10 mL of water-mixed rubber latex was added to the TiO_2 suspension and then vigorously stirred for 15 min until the homogenized mixture formed. Subsequently, the mixture was subjected to vacuum suction through a sintered glass (150 mL, 4-5.5 ASM) and dried in the oven at 60 $^{\circ}$C about 3 h to remove trace of water and ammonia gas. After drying, ET sheet was carefully taken out from the sintered glass and left to dryness at room temperature overnight after which a 5 %wt ET sheet was obtained. The 10 %wt and 15 %wt ET sheets were prepared likewise using appropriate amount of natural rubber latex, 1.68 mL and 2.52 mL, respectively. (The 5 %wt means 5 unit weight of latex in 100 unit weight of all ingredients to make a sheet. When less than 5 %wt of latex was used, the sheet was too thin and not sufficiently strong enough to withstand the vacuum suction resulting in a cracked sheet).

2.3.3.2 Characterization of TiO_2-embedded rubber (ET) sheets

The prepared TiO_2-embedded (ET) rubber sheets were characterized by XRD, SEM, and EDS techniques in the same way as described in 2.3.1.2.

2.3.3.3 Photocatalytic tests

In the photocatalytic studies, the TiO_2-embedded (ET) sheet was settled into a Petri dish (4 inch diameter) containing 60 mL of indigo carmine dye aqueous solution (2.5×10^{-5}M). The solution was then stirred for 15 min in the dark to reach the adsorption equilibrium in tightly closed photoreactor compartment (0.9m × 0.9m × 0.9m) to avoid interference from ambient light. Then the irradiation began under UV-light (5 tubes of blacklight, 20 watts each, F20T12-BLB, GE, U.S.A.) and magnetically stirred at 400 rpm. At given irradiation time intervals (every 1 h), 3 mL of IC solution samples were collected. The degradation of IC dye solutions was analyzed from the changes in absorbance of the absorption maximum at 610 nm using UV-Vis

spectrophotometer (Specord S100, Analytik Jena, Germany). The concentration of IC dye solution was determined quantitatively through the calibration graph.

The effect of various initial IC dye concentrations were investigated with concentrations 2.5×10^{-5} M, 5.0×10^{-5} M, and 7.5×10^{-5} M. The pH of IC dye solutions were also studied in the range of 3 to 8 by adding dilute aqueous solution of HCl and NaOH. In addition, the recyclability tests of TiO_2-embedded (ET) sheet were also studied.

CHAPTER 3
RESULTS AND DISCUSSION

To avoid the use of TiO_2 photocatalysts in the powder form, the immobilized TiO_2 sheets have been designed and prepared. The aims of this research focus on using locally available material (natural rubber latex) as substrate to enhance the use of TiO_2 photocatalysts. The rubber latex is interesting because of its versatility in daily life and available locally. Besides the photocatalytic efficiencies, the recyclabilities of all TiO_2 sheet products are also of prime importance. The searches for the most possible combined uses of rubber latex and TiO_2 photocatalysts are as follows.

3.1 Preparation and characterization of TiO_2-impregnated rubber sheets

3.1.1 Preparation of TiO_2-impregnated rubber sheets

In this work, the preparation of both impregnated anatase sheet (Im-Anatase) and impregnated Degussa P25 sheet (Im-P25)

have been described previously (Sriwong, et al., 2008). The impregnated rubber sheet was prepared by mixing TiO_2 powder with latex and certain amount of distilled water. Then, the mixture was poured into the Petri dish mold. When the latex sheet solidified, it was taken out of the mold and flipped upside down before being used so that the bottom surface would face upward and contact with the dye solution. The photograph images of pristine-rubber sheet and both TiO_2-impregnated sheets are shown in Figure 13.

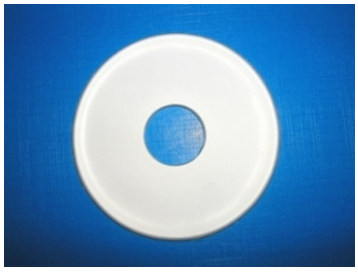

Figure 13 The photographs images of pristine-rubber sheet (left), Im-Anatase sheet (middle), and Im-P25 sheet (right).

3.1.2 Characterization of TiO_2-impregnated rubber sheets

3.1.2.1 X-ray powder diffraction (XRD)

The X-ray diffraction patterns of TiO_2 in powder form and in the impregnated rubber sheets are illustrated in Figure 14. The anatase and rutile titanium dioxide phases are marked with ‘A’ and ‘R’, respectively. From the Figure 14, a well crystallized anatase form was observed in the Im-Anatase sheet indicating successful impregnation of anatase powder into the rubber sheet (compare Figures. 14a and 14c). The same result was obtained for Im-P25 sheet as shown in Figure 14d (compare with 14b). In addition, the X-ray of pristine rubber sheet have a large broad scattering peak near $2\theta = 19°$ due to the fact that the rubber matrix is composed of low atomic number (low Z-value) element (Leyden, 1984). This broad scattering peak also shows up in the patterns of both impregnated sheets but with smaller intensity due to inclusion of TiO_2 particles in the impregnated sheets. The surface of Im-Anatase sheet has a higher content of TiO_2 particles than that of Im-P25 sheet causing the average Z-value of matrix in the former to increase. These results in lower X-ray scattering in the case of Im-Anatase sheet (Sriwong, et al., 2008).

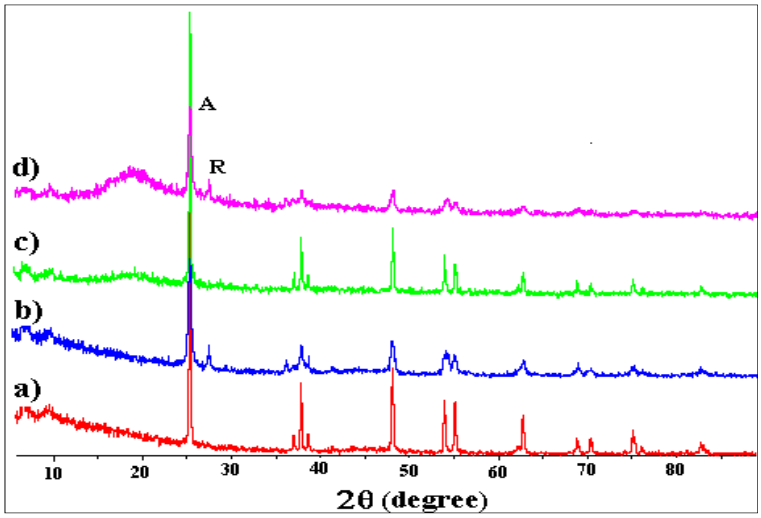

Figure 14 XRD patterns of (a) commercial anatase powder, (b) Degussa P25 powder, (c) Im-Anatase sheet, and (d) Im-P25 sheet.

3.1.2.2 Scanning electron microscopy (SEM)

The SEM images of the surface (left) and crossection (right) of Im-Anatase and Im-P25 sheets are shown in Figure 15. The surface morphology of Im-Anatase sheet showed evenly and well spread of anatase powder with higher surface roughness than the Im-P25 sheet. This results from the physical difference of anatase and P25 TiO_2 powders. The former has higher agglomeration and denser than P25, which exists as a light and fluffy-like particulates. When added to the latex, the anatase particles sank to the bottom faster and accumulated close to the bottom surface. The P25 particles, however, sank to the bottom slower so the numbers of particles to reach and accumulate at the bottom surface are smaller than in the case of anatase. This is clearly shown in Figure 15a (right) where a distinct layer of anatase particles can be seen at the surface of the sheet while that of P25 is less visible (Figure 15b, right). The rough surface of Im-Anatase sheet (Figure 15a, left) resembles the cracks running through a sun-dried mud surface. With this cracks, the anatase powders that gather near the surface will have more change to contact the dye molecules than those of the Im-P25 which are buried deep under the smoother surface of the rubber. This surface difference is responsible for a better performance of Im-Anatase sheet over Im-P25 sheet in the subsequent dye degradation studies.

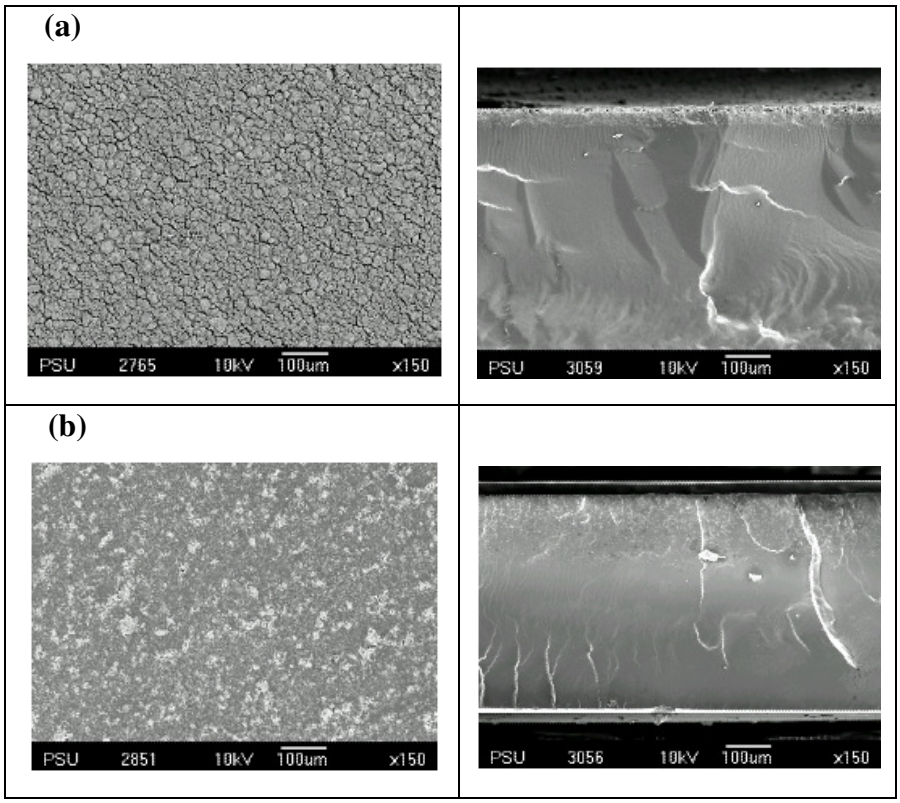

Figure 15 SEM images of the surface (left) and cross-section (right) of (a) Im-Anatase sheet and (b) Im-P25 sheet.

3.1.2.3 Energy dispersive X-ray spectroscopy (EDS)

The EDS analysis was carried out to confirm the presence of elements in the TiO_2-impregnated rubber sheets. The EDS spectra and mapping of Im-Anatase and Im-P25 sheets are shown in Figure 16 and Figure 17, respectively, which show that only three elements are present in the sheets (carbon, oxygen, and titanium). The Im-Anatase sheet (Figure 16a) clearly shows strong Ti peaks than that of Im-P25 sheet in Figure 17a corresponding to more distribution of Ti (TiO_2 particles) atoms on this sheet surface. This finding is further supported by EDS elemental mapping in Figure 16b and Figure 17b, respectively. The Im-P25 sheet (Figure 17a), however, exhibits very strong carbon peak due to high concentration of rubber latex matrix on the sheet surface. Natural rubber latex consists mostly of *cis*-1,4 polyisoprene with a repeating hydrocarbon unit, ($-CH_2CH_3C=CHCH_2-$), which is the main source of carbon signal. This observation supports the conclusion from SEM results in Figures 15a and 15b that there is high concentration of rubber latex on the surface and very small amount of TiO_2 particles (very low Ti peak) on the surface of the Im-P25 sheet.

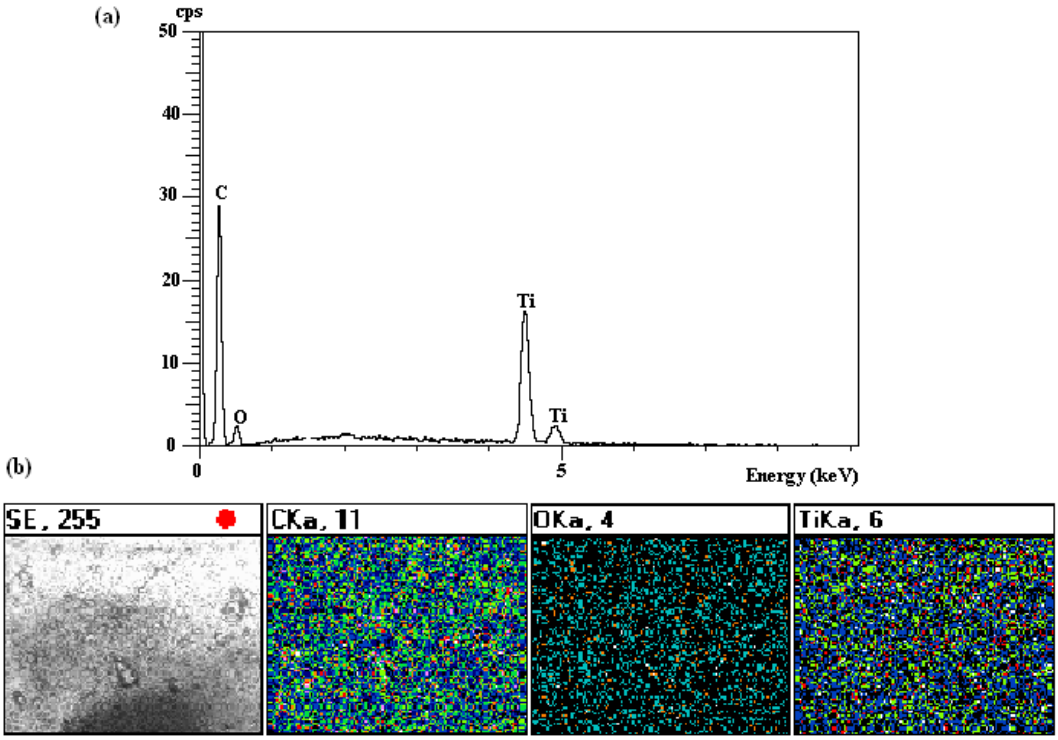

Figure 16 EDS spectra (a) and mapping images (b) of Im-Anatase sheet.

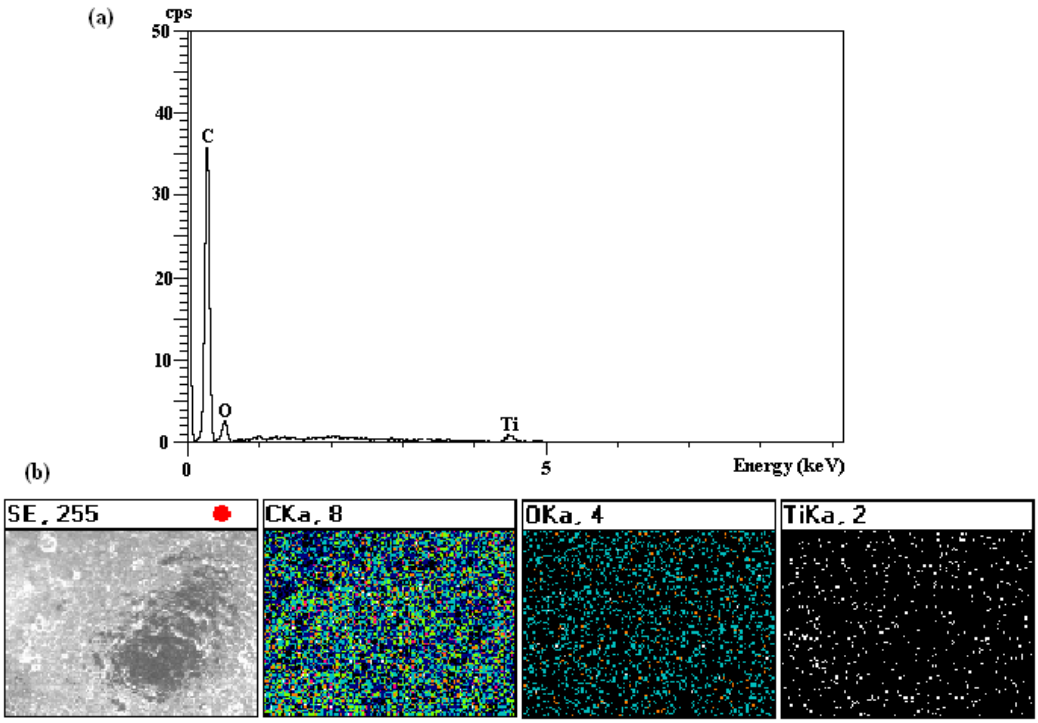

Figure 17 EDS spectra (a) and mapping images (b) of Im-P25 sheet.

3.1.3 Photocatalytic activity of TiO_2-impregnated rubber sheets

3.1.3.1 Photocatalytic degradation of indigo carmine (IC) dye by TiO_2-impregnated rubber sheets

The photocatalytic mechanism of TiO_2 has been well established and is summarized in Scheme 1. The reaction begins with TiO_2 particles being excited with UV light resulting in the formation of electron-hole pair, Eq. (11). The electron in the conduction band, e_{cb}^-, and the hole in the valence band, h_{vb}^+, may recombine and nullify further reactions. The $e_{cb}^- - h_{vb}^+$ pair, if they survive from recombination process, will eventually diffuse to the bulk surface and react with other molecules nearby. The e_{cb}^- can react with molecular O_2 adsorbed at the bulk surface and after few more steps will lead to the formation of $OH^\bullet$ radical, Eqs. (12-15), plays a major role in photocatalytic reaction. The h_{vb}^+ can react with H_2O at the bulk surface leading to formation of $OH^\bullet$ radical as well, Eq. (16). The very reactive $OH^\bullet$ radical can go on by attacking the dye molecules to completely mineralize them, Eq. (17). In addition, the h_{vb}^+ itself can also attack and mineralize dye molecules, Eq. (18) (Houas, et al., 2001; Anpo, et al., 2003).

$$TiO_2 + hv \rightarrow e_{cb}^- + h_{vb}^+ \quad (11)$$

$$O_{2ads} + e_{cb}^- \rightarrow O_2^{\bullet-} \quad (12)$$

$$O_2^{\bullet-} + H^+ \rightarrow {}^\bullet OOH \quad (13)$$

$$2\,{}^\bullet OOH \rightarrow H_2O_2 + O_2 \quad (14)$$

$$H_2O_2 + e_{cb}^- \rightarrow OH^\bullet + OH^- \quad (15)$$

$$H_2O_{ads} + h_{vb}^+ \rightarrow H^+ + OH^\bullet \quad (16)$$

$$Dye + OH^\bullet \rightarrow \text{degradation products} \quad (17)$$

$$Dye + h_{vb}^+ \rightarrow \text{degradation products} \quad (18)$$

Scheme 1 Mechanism of TiO_2 photocatalyst

The photodegradation efficiencies of IC by Im-Anatase sheet and Im-P25 sheet under UV light irradiation are shown in Figure 18. The Im-Anatase sheet has higher surface morphology and surface roughness than the Im-P25 sheet as shown in Figure 15. The cracked surface of Im-Anatase sheet has grooves running through all over the surface. These grooves give the sheet at least two advantages: (i) the dye

molecules when fall in the groove cannot easily escape from the surface, and(ii) along the groove surface the oxygen atoms have a better chance to protrude from the latex texture and their negative charges can attract or repel with charges at the dye molecular fragment (Figure 19a). The smoother surface of the Im-P25 (Figure 19b) with TiO_2 particles embedded deeper from the surface will have weaker electrostatic forces to interact with the dye molecules. Therefore, the higher surface roughness can help gather more dye molecules onto the sheet surface and the more the photocatalytic reaction can take place. This is reflected by the slightly better performance of the Im-Anatase sheet over Im-P25 sheet as shown in Figure 18.

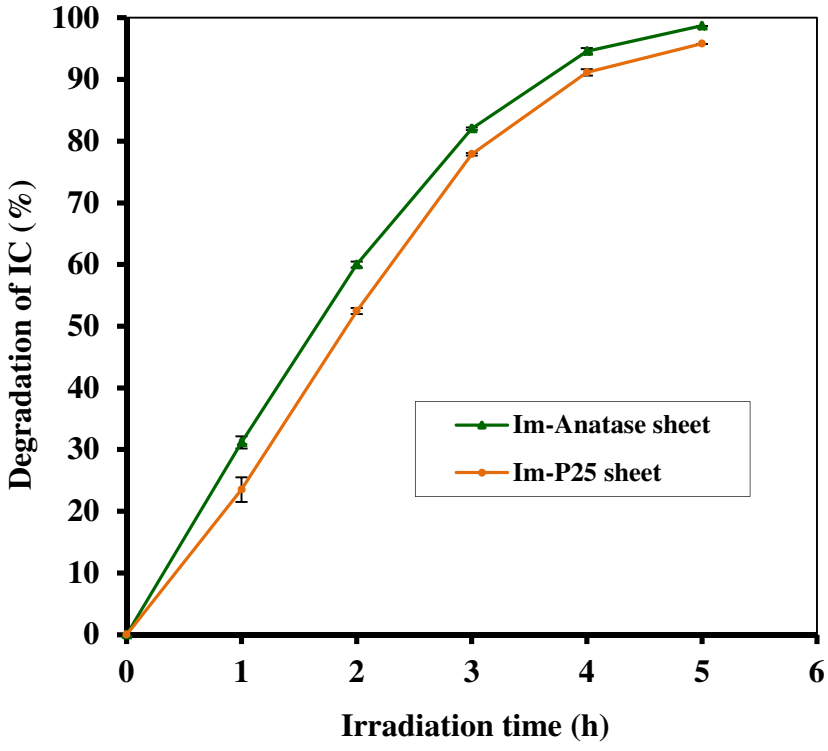

Figure 18 The efficiencies of photocatalytic degradation of IC dye by impregnated rubber sheets under UV irradiation; ▲ Im-Anatase sheet and ● Im-P25 sheet (n = 3).

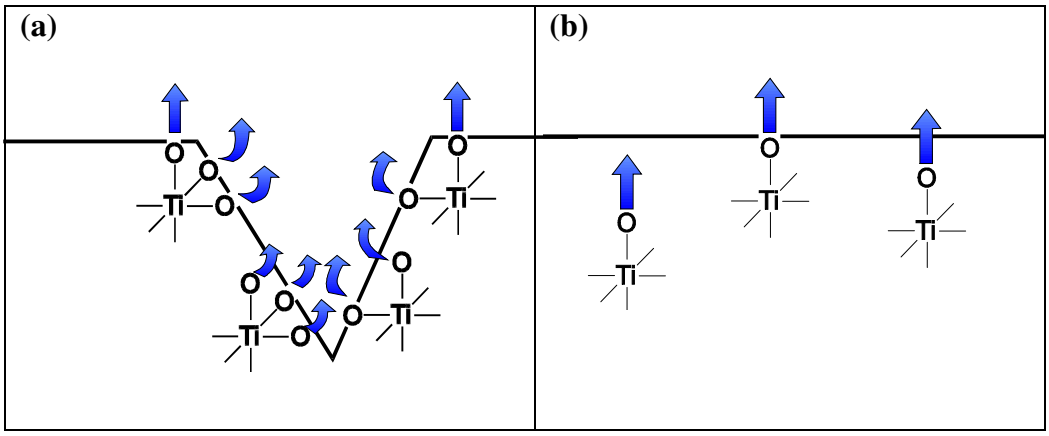

Figure 19 The effects of rough and smooth surfaces: (a) surface of Im-Anatase and (b) surface of Im-P25 sheets.

The kinetics of the degradation was studied and the data were tested with the first-order kinetic expression, Eq. (19) (Silva, et al., 2006; Baiju, et al., 2007; Ao, et al., 2008),

$$\ln\left(\frac{C_0}{C}\right) = k_{\text{app}} \times t, \qquad (19)$$

where (C_0) is the initial concentration of dye, (C) is the concentration at time "t", and k_{app} is the apparent rate constant (h^{-1}). The straight lines obtained confirm the first-order kinetics reaction of IC dye degradation, as shown in Figure 20. The rate constant, i.e., the slope of the line, of the Im-Anatase sheet is 0.717 h^{-1} and 0.595 h^{-1} for the Im-P25 sheet for IC dye degradation.

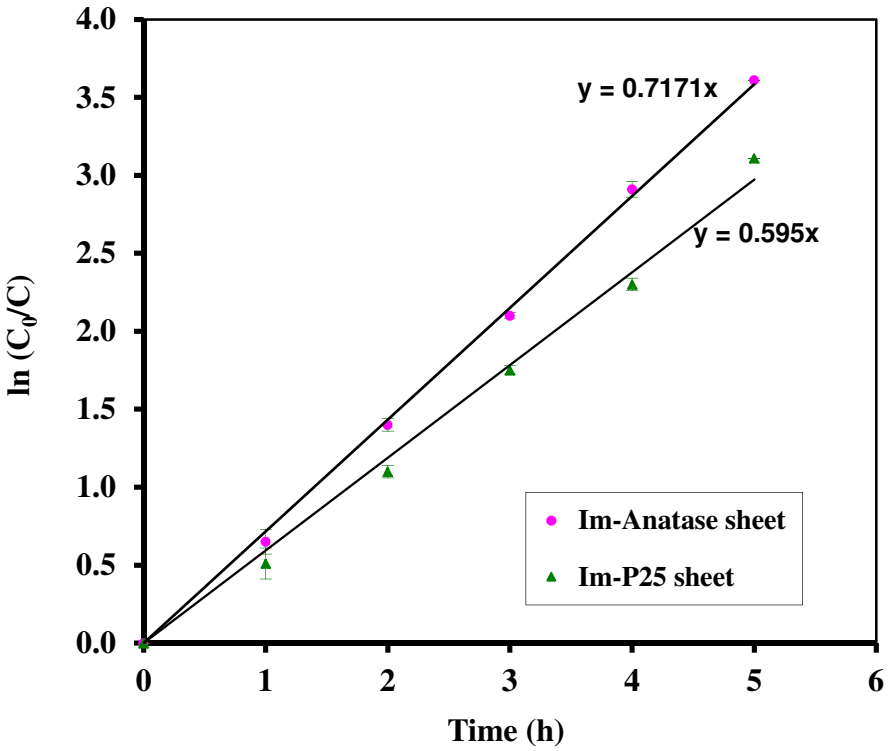

Figure 20 The kinetic plots rate of Im-Anatase and Im-P25 sheets (n = 3).

3.1.3.2 Effect of pH on the photocatalytic degradation of indigo carmine (IC) by TiO_2-impregnated rubber sheets

All of the experiments were carried out at the natural pH of IC dye solution which is 6.4. However, in real life situations the effluences from factories may cover wide range of pHs. To assess the efficiencies of degradation by the TiO_2-impregnated rubber sheet, several solutions of varying pH values were investigated. The IC dye aqueous solution was adjusted to other pH by adding either diluted HCl or NaOH solution accordingly. These pH values were: 3, 5, 6.4, and 8. The effect of pH on the photocatalytic degradation of IC in the presence of Im-Anatase sheet and Im-P25 sheet are shown in Figure 21 and Figure 22, respectively. It can be seen that both Im-Anatase and Im-P25 sheets showed parallel behavior with the efficiencies decreasing as the pH values increased in the order: (pH) 3 > 5 > 6.4 > 8.

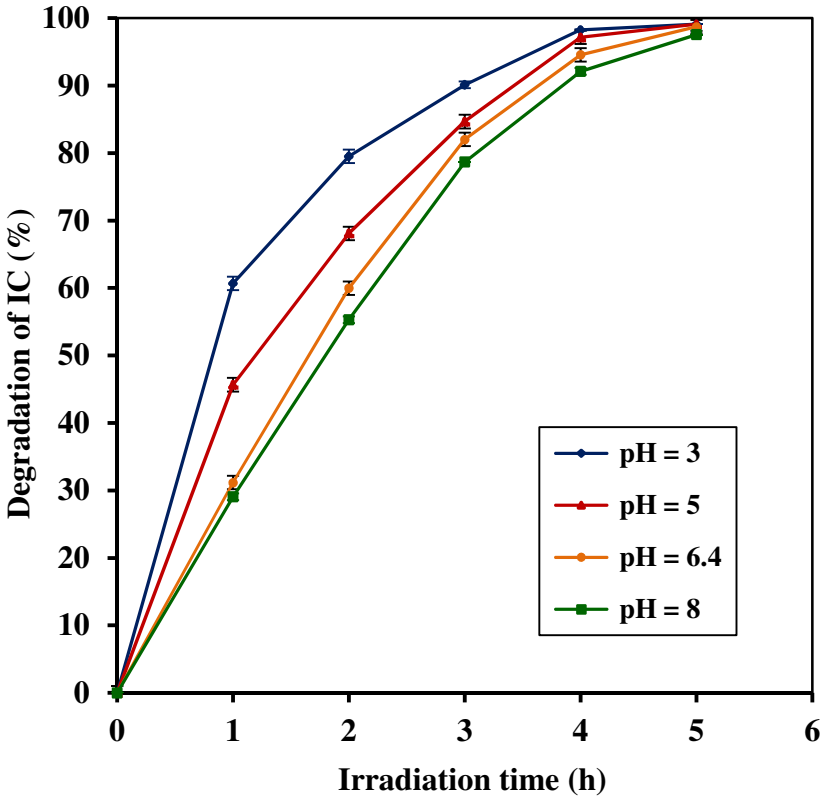

Figure 21 The effects of pH on the photodegradation efficiency of IC dye by Im-Anatase sheet (n = 3).

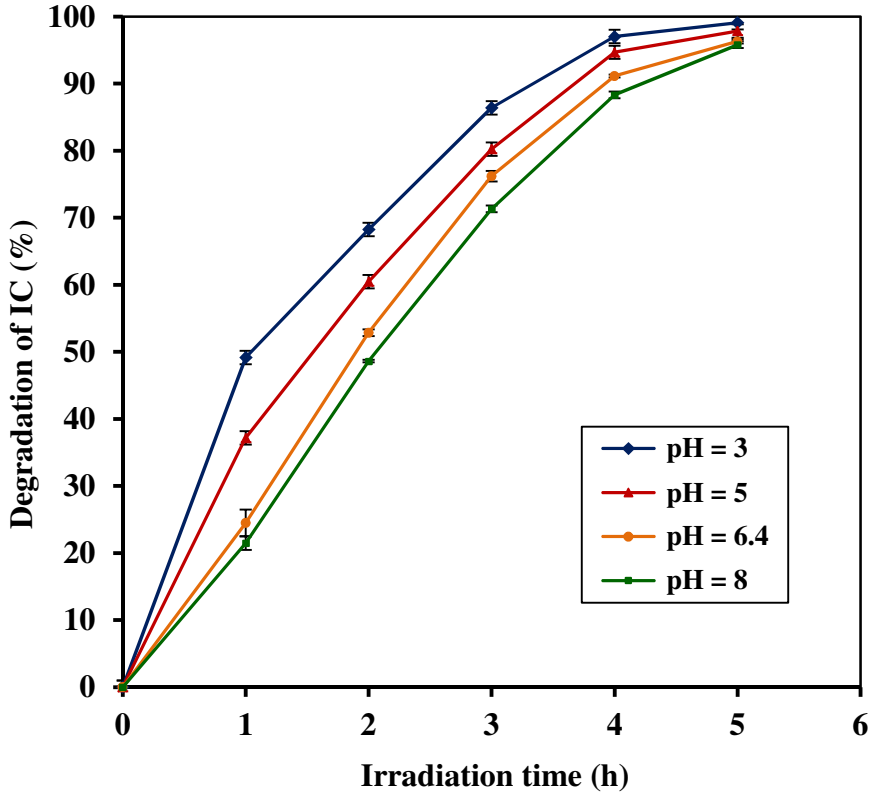

Figure 22 The Effects of pH on the photodegradation efficiency of IC dye by Im-P25 sheet (n = 3).

Generally, for charged surface of TiO_2 particles, a significant dependency of the photocatalytic efficiency on the pH value was observed, since the overall surface charge and hence the adsorptive properties of TiO_2 particles depend strongly on the solution pHs. It is known that the metal oxide particles in water exhibits amphoteric behavior and readily reacts with dye which can be described by the following chemical equilibrium equations (Kiriakidou, et al., 1999;Toor, et al., 2006):

$$\text{pH} < \text{pzc:} \qquad \text{Ti-OH} + H^+ \rightarrow \text{TiOH}_2^+ \qquad (20)$$

$$\text{pH} > \text{pzc:} \qquad \text{Ti-OH} + OH^- \rightarrow \text{TiO}^- + H_2O \qquad (21)$$

With respect to the point of zero charge (pzc), the surface charge property of TiO_2 changes with the change of solution pHs. The pH_{pzc} for TiO_2 has been reported in the range 6.25-6.90. Thus, the TiO_2 surface is positively charged in acidic media ($pH < pH_{pzc}$), whereas it is negatively charged under alkaline conditions ($pH > pH_{pzc}$) (Sun, et al., 2008). This argument, has its origin from the powder form in contact with solution,

should also be applicable when the powder is impregnated in the rubber sheet. The effect, however, should be less pronounced for the impregnated sheet than in the powder form. In this case with the impregnated sheet, the TiO_2 particles locate close to the surface may have part of oxygen atoms protrude from the rubber surface (Figure 14). (This assertion is evidenced from the fact that the photocatalytic reaction did indeed take place but with less efficiency than in the loose powder form.) Therefore, it is expected that at pH below pH_{pzc}, the surface of impregnated sheet acquires a positive charge, Eq. (20), and hence attracts with the negatively charged IC dye skeleton resulting in large number of molecules of dye are attracted (or adsorbed) onto the sheet surface. As the dye concentration at the surface increases the photodegradation activities also increases, as observed at the pH 3. On the other hand, at pH above pH_{pzc}, electrostatic repulsion between the negative charge at the surface of impregnated sheet, Eq. (21), and anionic dye skeleton retards the accumulation of dye molecules at the surface resulting in decrease of the photodegradation activity.

3.1.3.3 Effect of IC dye initial concentration on the photocatalytic degradation by TiO_2-impregnated rubber sheet

The effects of initial concentration of IC dye aqueous solution on the photocatalytic efficiency was investigated with concentrations 1.0×10^{-5} M, 2.0×10^{-5} M, and 3.0×10^{-5} M. The results are shown in Figure 23. It is found that on increasing the dye concentration the degradation efficiencies of dye decreases. Hence, the photo-oxidation process will work faster at low concentration of pollutants. These results are in agreement with many reports (Senthilkumaar, et al., 2005; Toor, et al., 2006; Liu, et al., 2006) that photodegradation of textile dye Reactive Red 2, C.I. Acid Yellow 17, and Direct Yellow 12 decreased with increasing concentrations. At high concentration of dye, the deeper colored solution would be less transparent to the UV light together with the dye molecules may absorb a significant amount of UV light causing less light reaching the catalyst, thereby reducing the $OH^{\bullet}$ radical formation. Since $OH^{\bullet}$ radical is of prime importance in the attack of the dye molecules, lowering the $OH^{\bullet}$ radical would then cause the photodegradation efficiency to decrease (Konstantinou, et al., 2004).

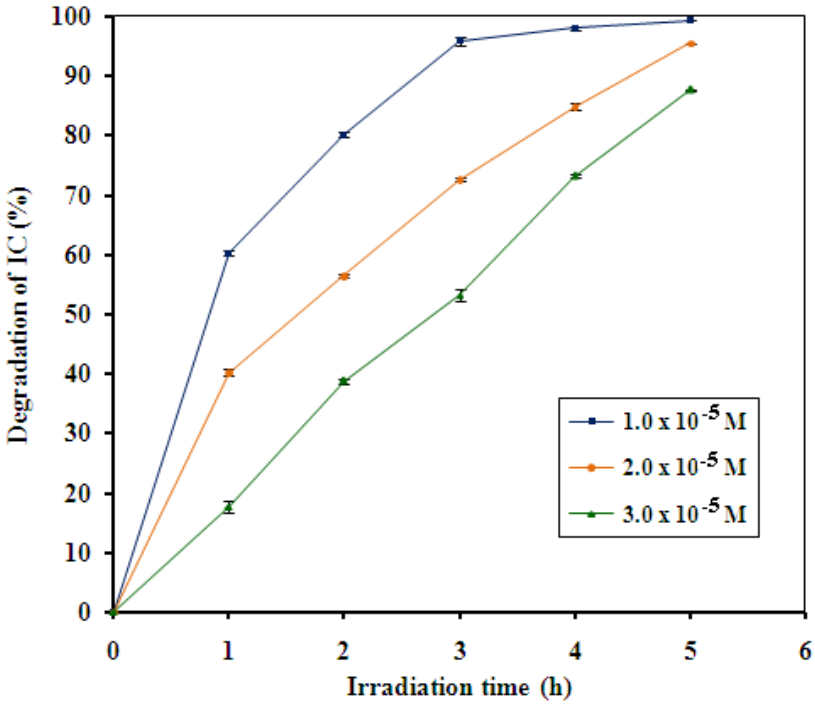

Figure 23 The effects of IC dye initial concentration on the photocatalytic efficiency of Im-Anatase sheet (n = 3).

3.1.3.4 Effect of UV light intensity on the photocatalytic degradation of IC by TiO_2-impregnated rubber sheet

The effect of UV light intensity on the photocatalytic degradation of IC dye was investigated by varying UV light intensity: Low, Medium, and High. From the Figure 24, it can be observed that on increasing intensity of UV light the degradation efficiency of dye increases. It has been reported that the photocatalytic reaction rate depends largely on the irradiation absorption of the photocatalyst leading to an increase in the degradation rate with increasing in light intensity during photocatalytic degradation (Liu, et al., 2006; Toor, et al., 2006; Jun, et al., 2007). The high UV light intensity increases photon influx entering the dye solution and consequently excites the TiO_2 particles in the sheet resulting in more $OH^{\bullet}$ radicals being formed at the surface of film. As the reactive number of $OH^{\bullet}$ radicals attacking the dye molecules increase, the photodegradation efficiency also increases. The order of activity is directly proportional to the intensity of UV light as: High > Medium > Low.

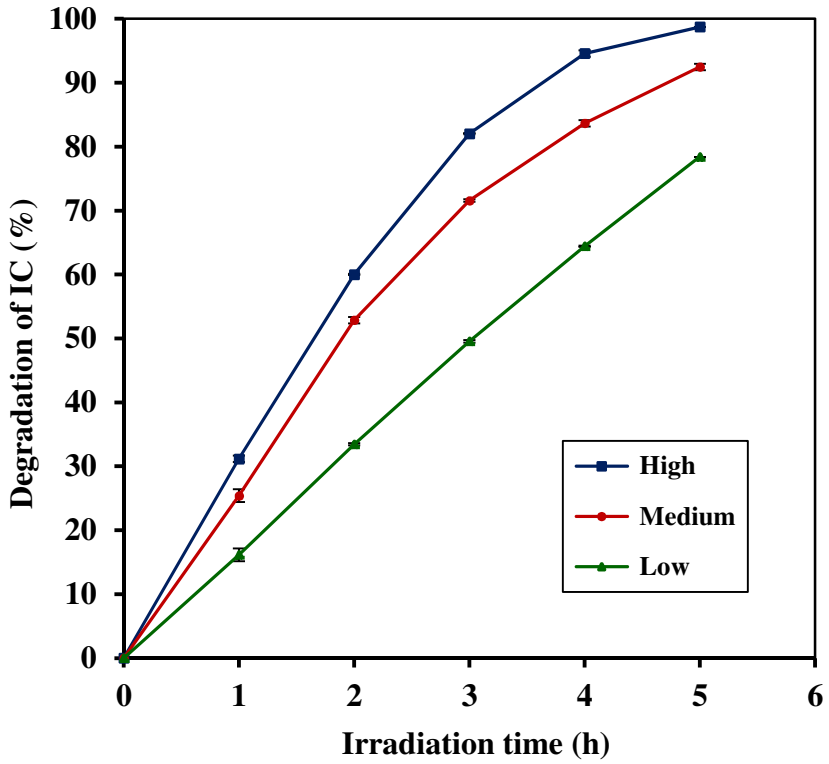

Figure 24 The effects of UV light intensity on the photocatalytic efficiency of IC dye by Im-Anatase sheet (n = 3).

3.1.3.5 Recyclability of the TiO_2-impregnated rubber sheets on the photocatalytic degradation of IC dye

Both types of impregnated sheet were tested for their recyclability up to ten times without showing any sign of deterioration of the sheets nor the decrease of performance. We thus anticipate the sheet life to go much longer than ten times of uses. One striking result was that the sheet surface remained rather clean after being used. As a result, the sheet surface need no cleaning between uses, i.e. after finishing one cycle it can be used immediately in the next cycle. The photographs of both Im-Anatase and Im-P25 sheets in Figures. 25a and 25b, respectively, clearly showed no accumulation of IC dye molecules after many repeated uses (without cleaning). The reason for this can be traced back to the repulsive force between the negative charge on the skeleton of the dye fragment and the oxygen atoms on the catalyst surface. With this repulsion accumulation of dye fragments (negative charge) on the sheet surface diminishes drastically.

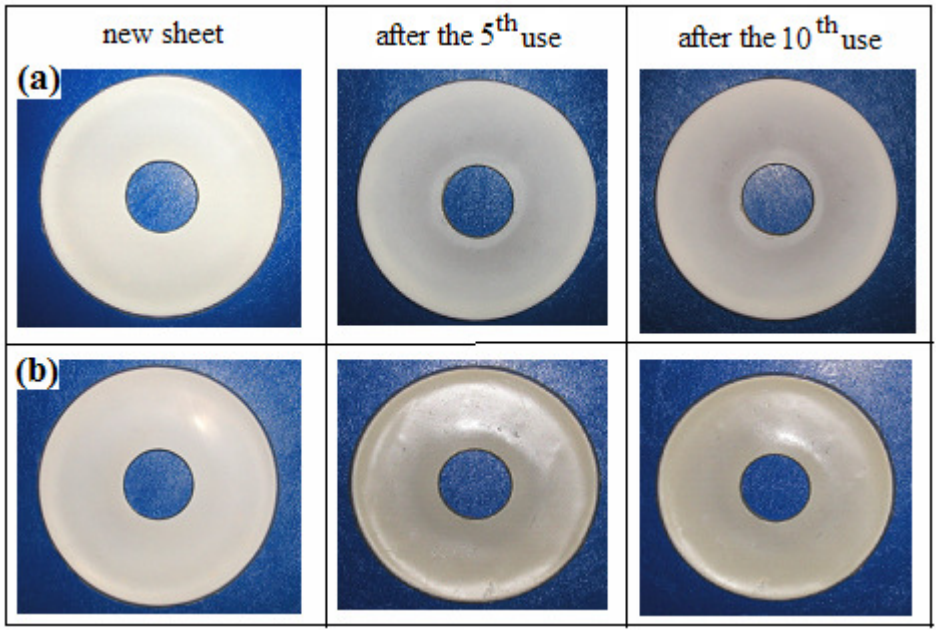

Figure 25 Photographs of (a) Im-Anatase sheet and (b) Im-P25 sheet: fresh sheets and after several uses in IC dye degradation.

The first few uses did not show the highest performance until after the third use and remained at that high efficiency until the tenth use (Figure 26). This trend can be expected to continue even after the tenth use. The lower results of the first few uses may result from the fact that the rubber surface was covered with trace of impurities during the preparation and was destroyed during the first and the second uses by the photodegradation reaction along with IC dye molecules in the solution. After the first and second uses, therefore, the sheet surface appeared to be cleaner with higher number of TiO_2 particles in contact with the dye solution and showed higher activity in the third use onward. As a result, we can see the steady increase in performance from the first to the third uses after which it remains almost constant.

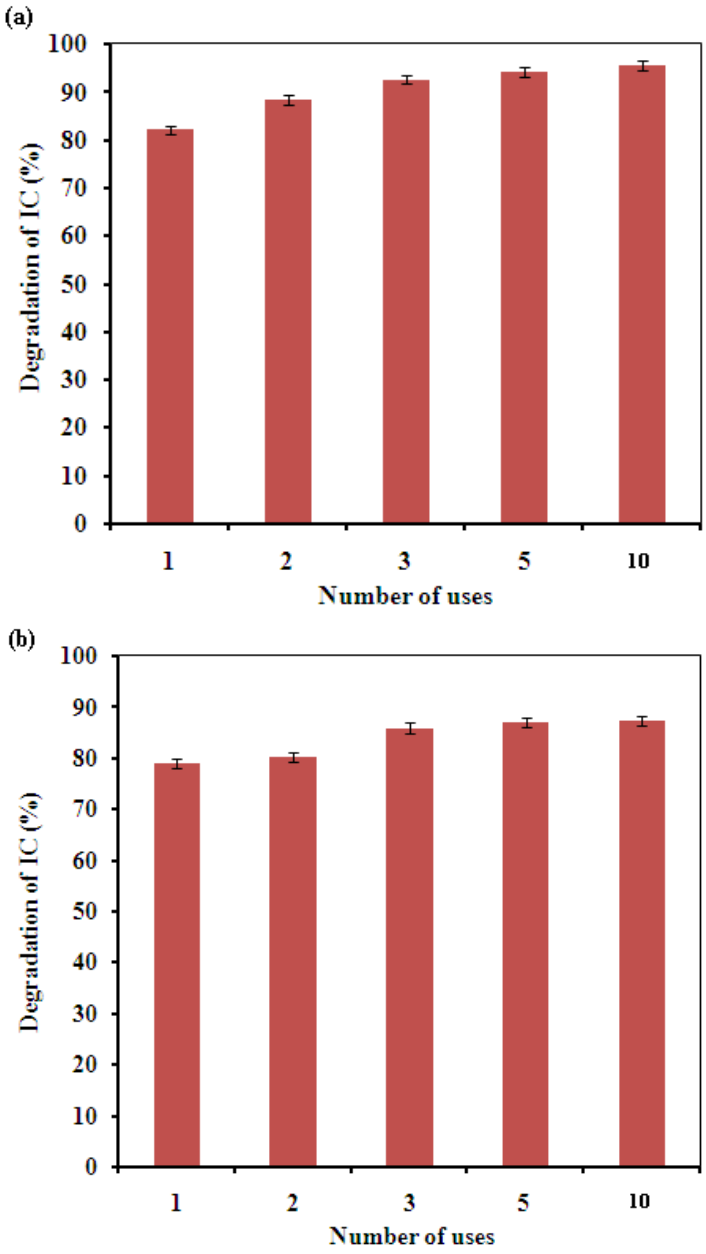

Figure 26 The efficiencies of IC dye degradation by (a) Im-Anatase sheet and (b) Im-P25 sheet on the repeating uses under UV light irradiation for 1-3 h (n = 3).

3.1.3.6 Comparison between MB and IC degradation by TiO_2-impregnated rubber sheets

Having studied both MB and IC dyes, it is worthwhile to compare the results from IC degradation in this thesis with that of MB degradation reported previously (Sriwong, et al., 2008). Since its publication, some additional studies with MB have been added. Of these, the rate constants of MB degradation were measured:

1.086 h^{-1} for Im-Anatase and 0.764 h^{-1} for Im-P25 sheets. These figures indicate that the rubber sheets exhibit higher photocatalytic activities toward MB than IC dye. Our results here agree with works from other groups where in one report, it was shown that MB degradation efficiency was higher than other dyes containing the $–SO_3^-$ group. And in the other two reports, one on MB and the other on IC dyes, the data showed that, under similar conditions, the rate of degradation of MB was faster than IC (Houas, et al., 2001; Vautier, et al., 2001; Lachheb, et al., 2002). When the rubber sheet was used with MB, significant amount of dye molecules adhered to the sheet surface rendering the sheet to appear as "dirty" after being used. The dirty surface, however, could be cleaned with relatively ease (Sriwong, et al., 2008), and could be brought back for reuse. The number of reuse for MB dye, however, appears to be shorter than with the IC dye (in this work) and, in the latter case, the surfaces need no cleaning going into the next round of uses. The trend on pH for MB was the opposite of the IC behavior, i.e., the efficiency for MB degradation increased with increasing pH. These differences can be described based on the charge type on the dye fragment. MB is cationic dye while IC is anionic dye. The positive charge of the MB fragment attracts with the negatively charged oxygen atom of TiO_2 impregnated in the rubber surface promoting accumulation of dye molecules onto the surface. As more molecules flock together on the catalyst surface the higher rate of degradation should result. On the contrary, in the IC case, the negative charge on the dye skeleton repels with the impregnated TiO_2 in the rubber surface discouraging accumulation of dye molecules on the sheet surface. As a result, on the good side, the surface remains clean, but on the bad side, the degradation rate was slower when compared with the MB case.

In addition, although the TiO_2 impregnated sheets in this part could be successfully prepared, used, and reused, however, these sheets have a few disadvantages in the photocatalyst applications, for example, less activity than the loose powder of the same catalyst and may be unstable over a long-term usage due to its thin rubber sheet substrate. Therefore to solve these problems, a new type of TiO_2 impregnated sheets with higher photocatalytic activity and more stable sheets were prepared and presented in the next section.

3.2 Preparation and characterization of TiO_2-strewn rubber sheets

3.2.1 Preparation of TiO_2-strewn rubber sheets

The TiO_2-strewn rubber sheet was easily prepared by strewing TiO_2 powder (Degussa P25) onto the sheet of rubber latex (60% HA) in a gelation to form through a steel sieve. In this work, the 60-mesh sieve was used as a strewing instrument due to it is an appropriate pore size for TiO_2 powder particles throughout to the rubber latex. The solidified rubber sheet served as substrate upon which TiO_2 powder was deposited. In the preparation, drying at 100 °C for 1 h, removes moisture from the rubber sheet to some extent. The heat drying process softened the sheet and caused subtle melting at the surface which helped increase the binding of TiO_2 particles to the sheet. On a close inspection with the naked eye one can see a colorless thin film covering the TiO_2 particles. The photograph image of TiO_2-strewn rubber sheet is shown in Figure 27.

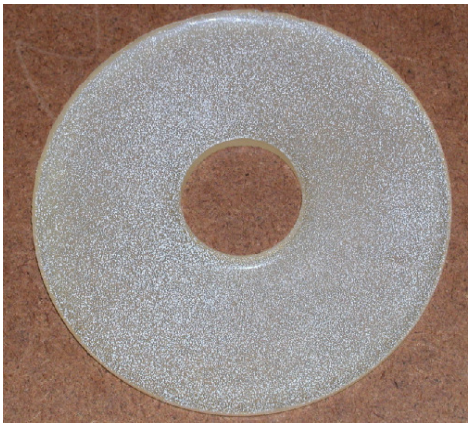

Figure 27 Photograph of TiO_2-strewn rubber sheet.

In the present study, the effect of various parameters such as the time before strewing – the gelation period (0 h, 1 h, 2 h, and 3 h), the time for drying at 100 °C (0 h, 1 h, 2 h, and 3 h), and the amount of Degussa P25 TiO_2 powder (0.03 g, 0.05 g, 0.07 g, and 0.10 g) were studied to optimize the preparation of TiO_2-strewn rubber sheet for maximum photocatalytic degradation of IC dye in aqueous solution under UV light irradiation.

3.2.2 Characterization of TiO_2-strewn rubber sheets

3.2.2.1 Scanning electron microscopy (SEM)

Scanning electron microscopy is a technique used to investigate the surface morphology of all TiO_2-strewn rubber sheets. The SEM micrographs of TiO_2-strewn rubber sheets prepared by varying the time at strewing, the time for drying at 100 °C, and the amount of Degussa P25 TiO_2 powder are shown in Figure 28, Figure 29, and Figure 30, respectively. It can be seen from Figure 28 that the surface morphology of TiO_2-strewn rubber sheet sample prepared by instantly strewing after the rubber latex was poured into Petri dish (in Figure (28(A1), 28(A2))) – has different surface morphology from each other. The TiO_2 particles can be spread evenly over the sheet surface with lower agglomeration and deeper deposited into the rubber surface than the other sheets. This result can be explained as due to the fresh rubber latex has high water in the rubber suspension. When TiO_2 particles are strewing into the rubber latex surface, it can be contacted and dispersed in water because of the super-hydrophilic property of TiO_2 resulting in some of TiO_2 particles has dispersed with low aggregation and well-spread in the rubber sheet surface which can be seen clearly in the Figure 28(A2). Due to the highest water of these, TiO_2 particles readily sink through the latex body and are buried rather deep under the sheet surface than the other sheets resulting in having less TiO_2 particles on the surface of this sheet. In contrast, when the time before strewing was extended to after 1 h, 2 h, 3 h, the above mentioned result was not observed as shown in the Figs. 28(B), 28(C), 28(D), respectively. When the time before strewing was prolonged (gelation) – 1 h, 2 h, and 3 h – like drying at RT, the water molecules evaporated from the rubber latex suspension resulting in less water to be bonded with the TiO_2 particles allowing high concentration of TiO_2 particles at the sheet surface. The TiO_2 particles deposited on the sheet surface increased with increasing strewing time (see in Figures. 28(B), 28(C)). However, if longer time before strewing was used (see in Figures 28(D)), some of TiO_2 particles could not effectively adhere to sheet surface and easily lost from the sheet surface when the sheet was lightly sprayed with distilled water to wash out some of the P25 TiO_2 particles that were left unbound until the strewn surface was free of loose particles. Figure 29 shows the SEM micrographs of TiO_2-strewn rubber sheets prepared by varying the time for drying at 100 °C; (A) 0 h, (B) 1 h, (C) 2 h, and (D) 3 h. In comparison, the surface morphology of

the TiO_2-strewn sheet prepared by using the time for drying at 100 °C as 0 h (Figure 29(A)) – no drying – has some loosely bound TiO_2 particles that could be lost from the sheet surface when the sheet surface was lightly sprayed with distilled water, whereas, the opposite result was observed in the case of the longer time for drying at 100 °C (Figure. 29(B), 29(C), and 29(D). This result indicated that the heat drying process softened the sheet and caused subtle melting at the rubber sheet surface which helped increase the binding of TiO_2 particles to the sheet surface giving high stability of the sheet samples, therefore, it cannot be lost from the sheet surface. However, the longer time for drying at 100 °C (1 h, 2 h, and 3 h) showed similar surface morphology which had no effect to the surface of each sheet as shown in Figures 29(B), 29(C), and 29(D), respectively. Figure 30 shows the SEM micrographs of TiO_2-strewn rubber sheets prepared by varying the amount of Degussa P25 powder; (A) 0,03 g, (B) 0.05 g, (C) 0.07 g, and (D) 0.10 g. It can be seen that the surface morphology and roughness of the rubber sheet samples increased with increasing amount of TiO_2 powder. When the larger amount of TiO_2 powder was used, the higher TiO_2 particles on the surface of sheets could be observed. However, in the case of 0.10 g TiO_2 powder was used (Figure 30(D)), the surface morphology of this sheet was not significantly different from the surface of sheet prepared by using 0.07 g of TiO_2 powder (Figure 30 (C)). Owning to the great amount of unbounded TiO_2 powder washed out from the surface, this sheet has similar surface to the last sheet in Finger 30(D).

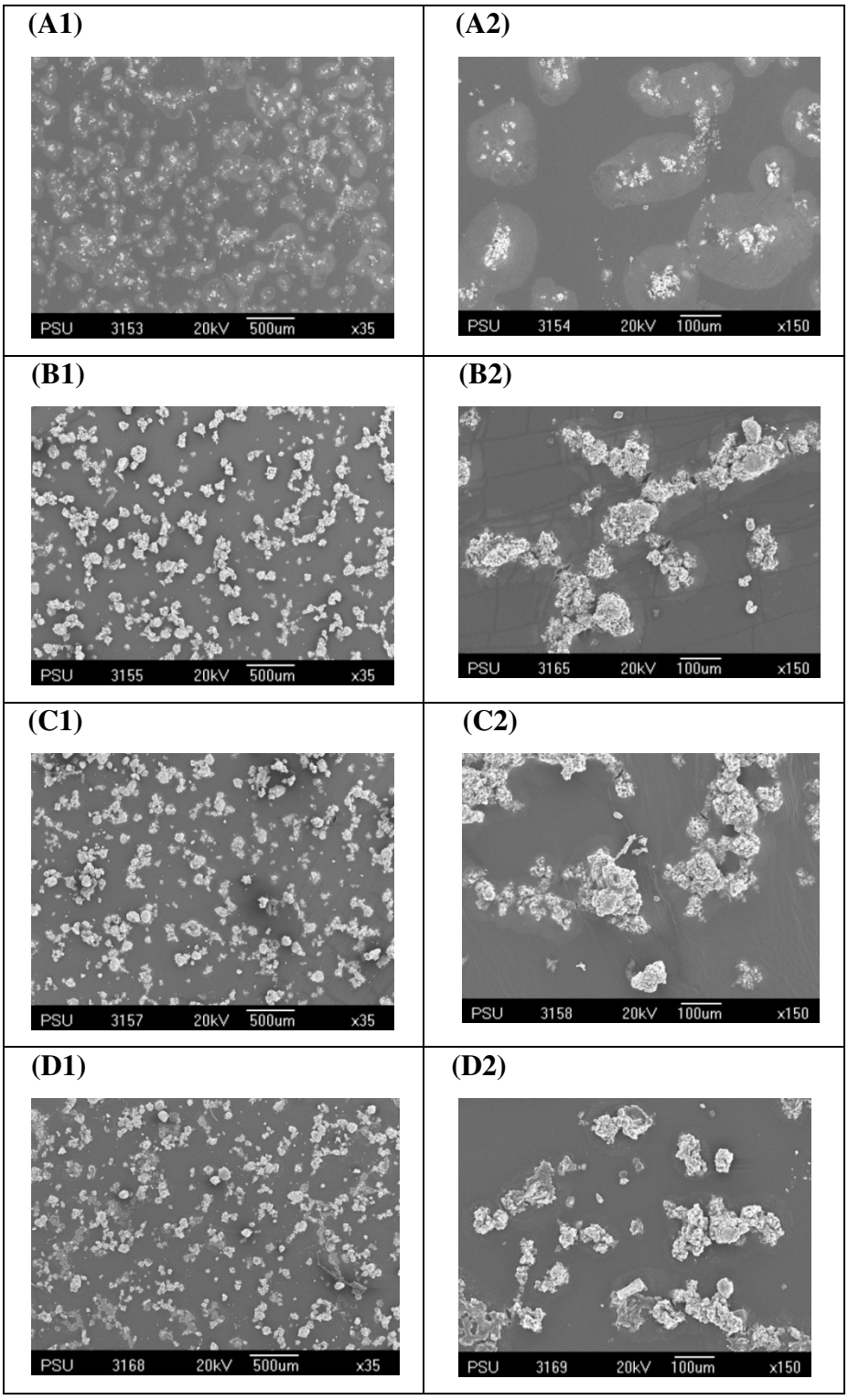

Figure 28 SEM images of TiO_2-strewn rubber sheets prepared by varying the time before strewing: (A) 0 h, (B) 1 h, (C) 2 h, and (D) 3 h (10 mL latex, 0.07g TiO_2, and 1 h drying at 100 °C). Left: low magnification_35×, and right: high magnification_150×.

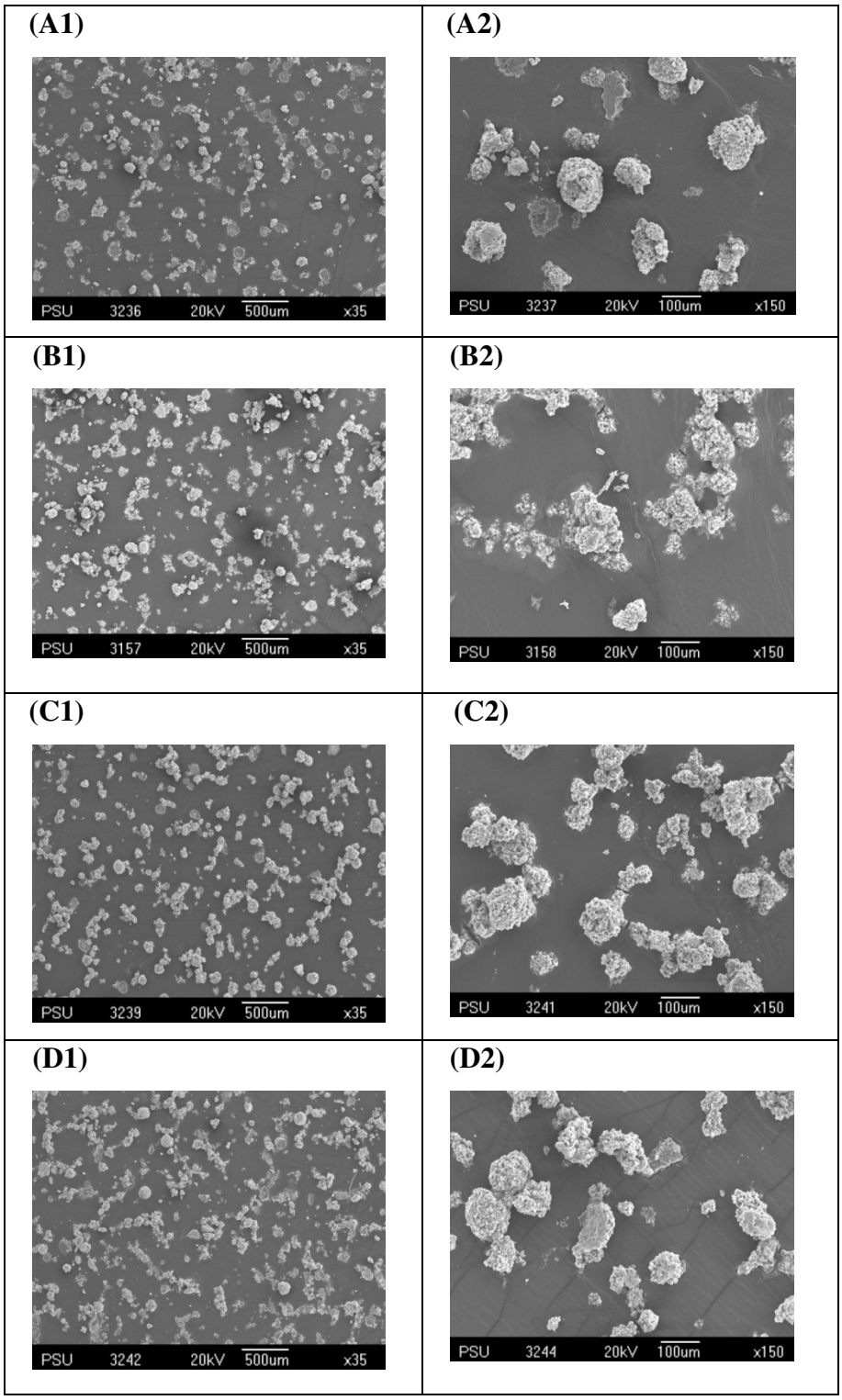

Figure 29 SEM images of TiO_2-strewn rubber sheets prepared by varying the time for-drying at 100 °C: (A) 0 h, (B) 1 h, (C) 2 h, and (D) 3 h (10 mL latex, 0.07g TiO_2, and 2 h before strewing (gelation)). Left: low magnification_35×, and right: high magnification_150×.

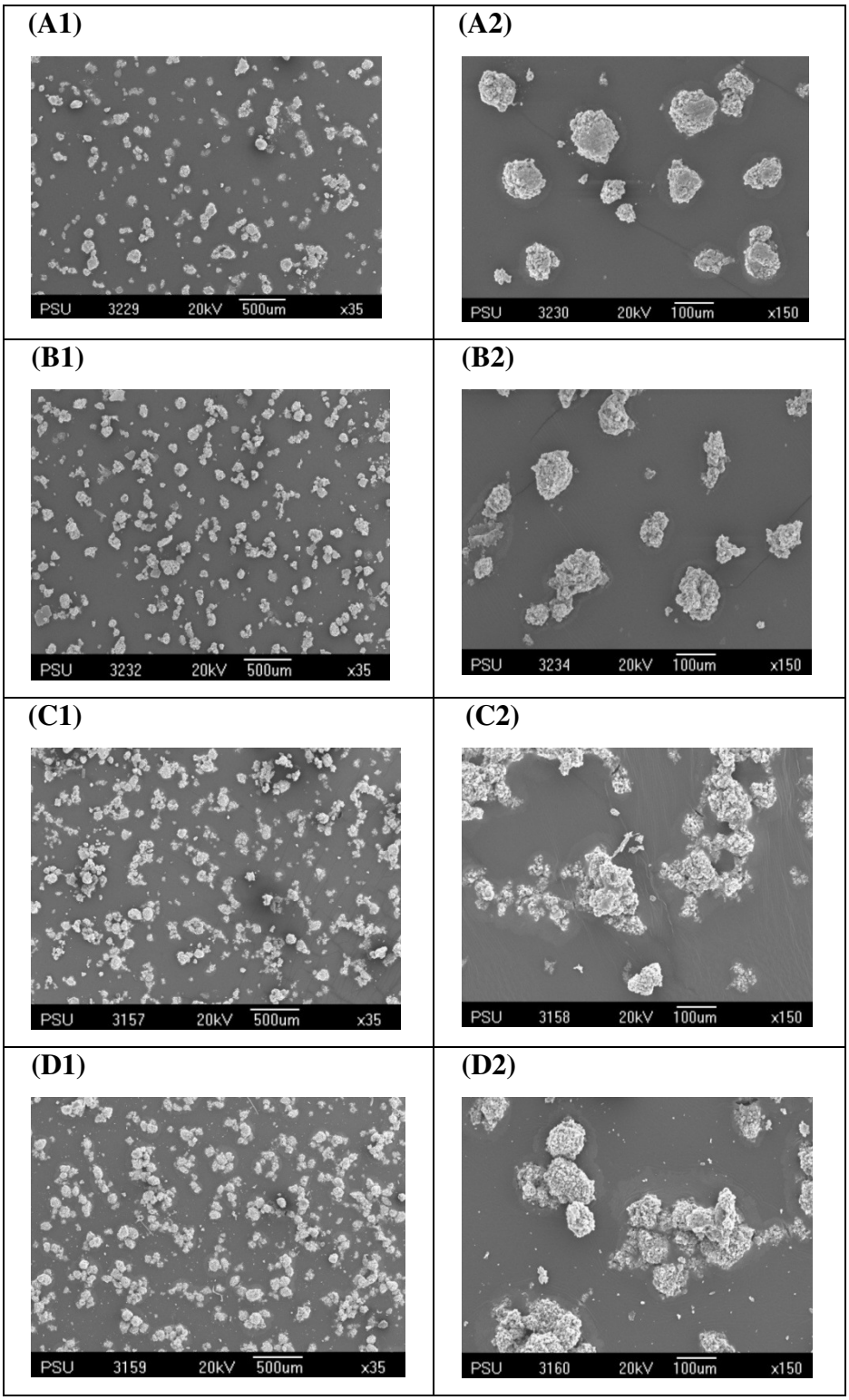

Figure 30 SEM images of TiO_2-strewn rubber sheets prepared by varying the amount of Degussa P25 TiO_2 powder: (A) 0.03 g, (B) 0.05 g, (C) 0.07 g, and (D) 0.10 g (10 mL latex, 2 h before strewing (gelation), and 1 h for drying at 100 C°,). Left: low magnification_35×, and right: high magnification_150×.

3.2.2.2 Energy dispersive X-ray spectroscopy (EDS)

The EDS analysis was carried out to determine the presence of elements in the TiO_2-strewn sheet. The EDS spectrum in Figure 31(a) shows that only three elements were present in the sheet, i.e. carbon, oxygen, and titanium, as evidenced from their corresponding K lines. Figure 31(b1) shows a SEM micrograph of an island of TiO_2 nanoparticles submerged in rubber. This is supported by Figure 31(b2) which shows distribution of carbon atoms on the sheet surface surrounding the TiO_2 island (the island is seen as a black area in this figure). Oxygen and titanium atoms are seen in the area occupied by the TiO_2 island, Figures 31(b3) and 31(b4), respectively. Titanium atoms are distributed over a narrower area within the TiO_2 island than the oxygen atoms distribution. In summary, the EDS data tell us that TiO_2 particles are located on the rubber surface with parts of the TiO_2 islands protruding from the surface (area of lighter color in Fig. 31(b4)).

(a)

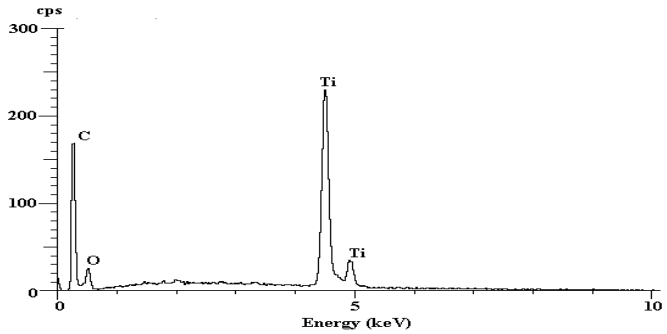

(b)

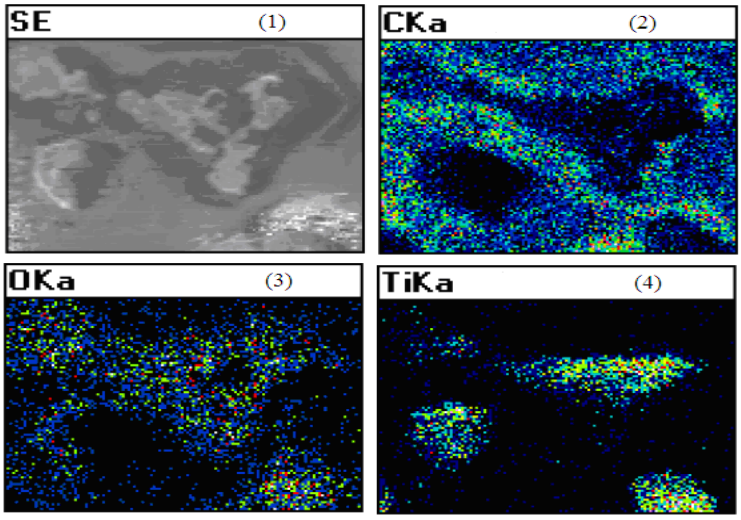

Figure 31 EDS spectrum (a) and elemental mapping (b) of TiO_2-strewn sheet sample.

3.2.2.3 X-ray powder diffraction (XRD)

The X-ray diffraction patterns of Degussa P25 TiO_2 in the powder form and the immobilized form on a rubber sheet surface are illustrated in Figure 32. The diffraction peaks of anatase and rutile phases are marked with 'A' and 'R', respectively. From Figure 32, the well crystallized anatase and rutile forms were observed in the TiO_2-strewn sheet indicating successful addition of TiO_2 powder onto the rubber sheet surface (Fig. 32a and 32b). A broad scattering peak ($2\theta = 19°$) of the X-ray beam by the low Z matrix of rubber also shows up in the patterns of TiO_2-strewn sheet. The surface of TiO_2-strewn sheet contains TiO_2 particles causing the average rubber matrix of the sheet to increase and, therefore, less scattering of the X-ray beam (Sriwong et al., 2008).

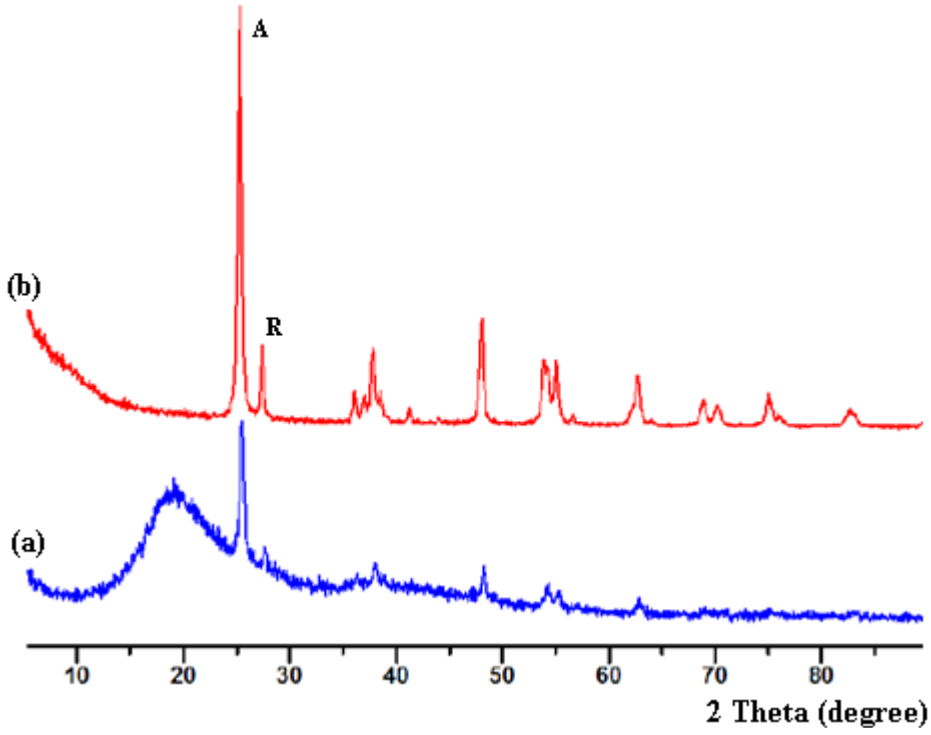

Figure 32 XRD patterns of (a) TiO_2-strewn sheet and (b) Degussa P25 powder.

3.2.3 Photocatalytic activity of TiO_2-strewn rubber sheets

3.2.3.1 Photocatalytic degradation of indigo carmine (IC) dye by TiO_2-strewn rubber sheets

The photocatalytic activities of all TiO_2-strewn rubber sheet samples were to be evaluated using IC dye as a model of organic dye pollutant in water. Two blanks experimental were performed, one with only the IC dye solution, and the other one with the pristine rubber sheet in IC dye solution. We found that they showed no significant change in dye absorbance spectra. This result confirmed that the photocatalytic activity to come from only the TiO_2 particles impregnated in the rubber sheet. The photocatalytic activity of TiO_2-strewn rubber sheet samples prepared with varying the time at strewing is shown in Figure 33. It can be observed that the TiO_2-strewn rubber sheet prepared with 2 h of the time at strewing showed better photocatalytic activity than the other sheets. As shown in Figures. 28(C), the sheet higher content of TiO_2 particles on the surface than the other sheets exhibited higher surface morphology and roughness, therefore, its observed higher photocatalytic activity was not unexpected. Generally, the photocatalytic reaction on the TiO_2 surface is very sensitive to its surface structure owning to the photocatalytic is a surface reaction. Thus, the higher the surface morphology and roughness the more the photocatalytic reaction takes place. In contrast, the lower the surface roughness with lower TiO_2 particles in the sheet surface will have lower photocatalytic activity. The order of activities of TiO_2-strewn rubber sheets as 2 h > 3 h > 1 h >> 0 h in varying the time at strewing. While the photocatalytic activity of TiO_2-strewn rubber sheet samples prepared with varying the time for drying at 100 °C is shown in Figure 34. It can be seen that the TiO_2-strewn rubber sheets prepared with 1 h, 2 h, and 3 h of the time for drying at 100 °C showed similar and good performances on the photocatalytic degradation of IC dye. Whereas, the TiO_2-strewn rubber sheet prepared with 0 h (no drying) showed slightly lower photocatalytic activity than the other sheets due to its lower surface with lower TiO_2 particles on the sheet. The order of activities of TiO_2-strewn rubber sheets as 3 h ≈ 2 h ≈ 1 h > 0 h in varying the time for drying at 100 °C.

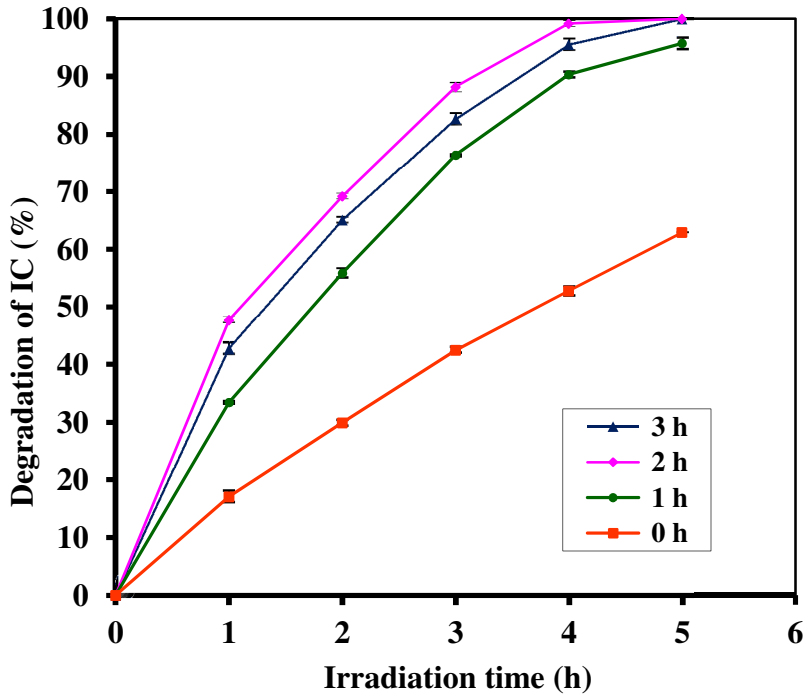

Figure 33 The efficiencies of photocatalytic degradation of IC dye by TiO_2-strewn rubber sheets prepared with varying the time at strewing under UV irradiation (n = 3).

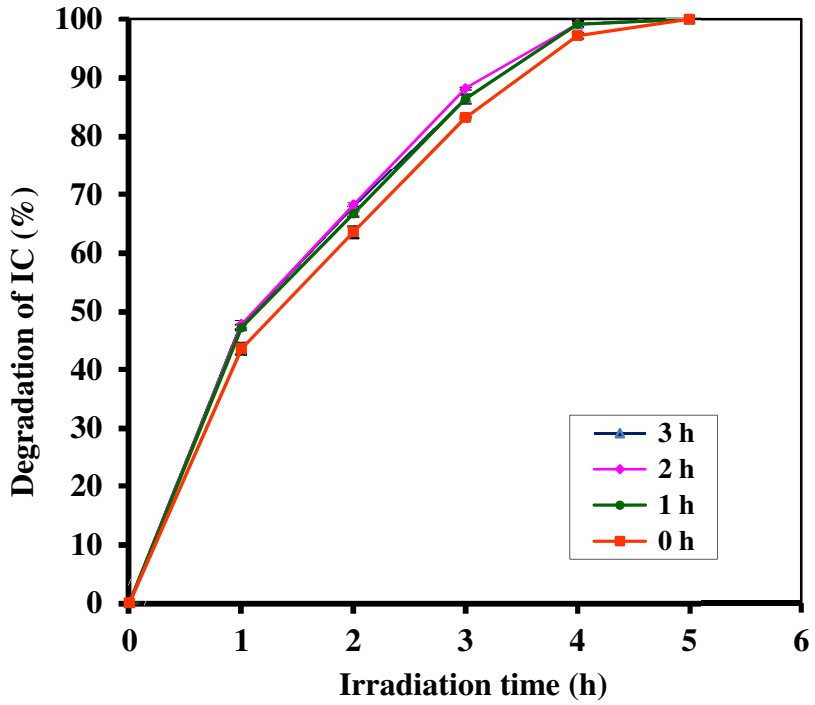

Figure 34 The efficiencies of photocatalytic degradation of IC dye by TiO_2-strewn rubber sheets prepared with varying the time for drying at 100 °C under UV irradiation (n = 3).

The photocatalytic activity of TiO_2-strewn rubber sheets prepared with varying the amount of Degussa P25 TiO_2 powder is shown in Figure 35. It can be seen from the Figure 35 that the photodegradation efficiency of IC dye by TiO_2-strewn rubber sheets increased with increasing amount of P25 TiO_2 powder. The TiO_2-strewn rubber sheets prepared with 0.10 g and 0.07g showed similar and better efficiencies due to they have high content of TiO_2 particles on the sheet surface. The order of activities of TiO_2-strewn rubber sheets prepared with varying amount of P25 TiO_2 powder as 0.10 g ≈ 0.07 g > 0.05g > 0.03 g.

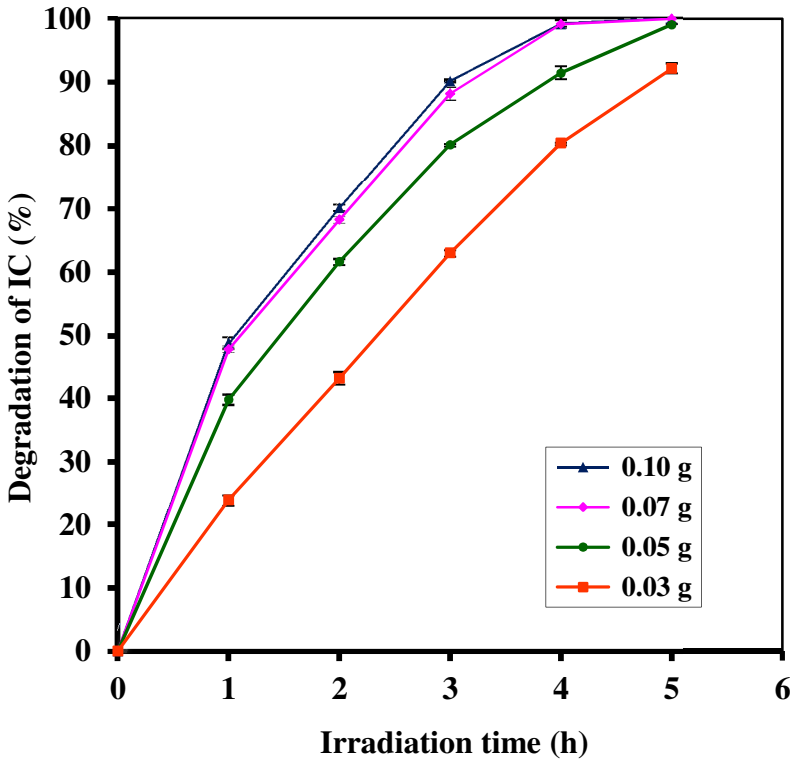

Figure 35 The efficiencies of photocatalytic degradation of IC dye by TiO_2-strewn rubber sheets prepared with varying amount of Degussa P25 TiO_2 powder under UV irradiation (n = 3).

From above studies we found that the optimal conditions for preparation of TiO_2-strewn rubber sheet were: 10 mL latex, 0.07 g Degussa P25 TiO_2 powder, 2 h strewing time, and 1 h drying time at 100 °C which has shown the highest photocatalytic activity than the other conditions. Therefore, these conditions were chosen to prepare the TiO_2-strewn rubber sheet for further studies.

3.2.3.2 The effects of pH on the photocatalytic activity of the TiO_2-strewn sheet

In real-life applications, the sheet may be used under varied pH conditions. Therefore, the prepared TiO_2-strewn sheet was put to test under varying pHs (from pH 3 to pH 8). The natural pH of IC dye solution was 6.53. The solution was adjusted to other pH by adding either diluted HCl or NaOH solution accordingly. The effects of pH on the photocatalytic degradation of IC dye in the presence of TiO_2-strewn sheet are shown in Figure 36. It can be seen that the degradation efficiency of IC dye decreased with the increasing of pH. It is known that the metal oxide particles in water exhibits amphoteric behavior and readily reacts with dye which can be described by the following chemical equilibria (Kiriakidou, et al., 1999; Toor, et al., 2006):

$$\text{pH} < \text{pzc:} \qquad \text{Ti-OH} + H^+ \rightarrow TiOH_2^+ \qquad (22)$$

$$\text{pH} > \text{pzc:} \qquad \text{Ti-OH} + OH^- \rightarrow TiO^- + H_2O \qquad (23)$$

Generally, for the charged surface of TiO_2 particles, a significant dependency of the photocatalytic efficiency on the pH value was observed since the overall surface charge and, hence, the adsorptive properties of TiO_2 particles depended strongly on the solution pH (Senthikumaar et al., 2005). According to the point of zero charge (pzc), the surface charge property of TiO_2 changes with solution pH. The pH_{pzc} for TiO_2 has been reported in the range 6.25-6.90. Thus, the TiO_2 surface is positively charged in acidic media (pH < pH_{pzc}), and negatively charged under alkaline conditions (pH > pH_{pzc}) (Sun et al., 2008). Therefore, it is expected that at pH below pH_{pzc}, TiO_2 particles at the TiO_2-strewn sheet surface acquires a positive charge (Eq. 22). Since TiO_2 particles are located near the sheet surface, hence, the electrostatic interaction between the surface of the strewn sheet and the anionic dye parent fragment leads to strong adsorption with a corresponding high photodegradation activity at pH 3. On the other hand, at pH above pH_{pzc}, electrostatic repulsion between the negative surfaces of strewn sheet and anionic dye fragment retards the photodegradation activity. The order of activity decreases as pH 3 > pH 5 > pH 6.53 > pH 8.

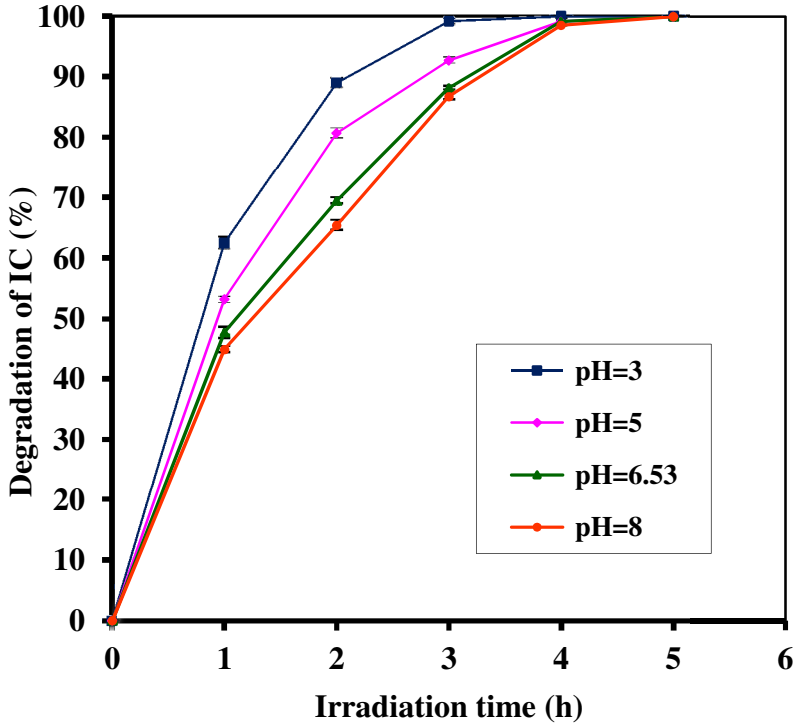

Figure 36 Photodegradation efficiencies of TiO_2-strewn sheet as a function of pH (dye concentration 2.5×10^{-5} M, (n = 3)).

3.2.3.3 The effects of initial concentration of IC dye on the photocatalytic activity of the TiO_2-strewn sheet

The effects of initial concentration on the photocatalytic degradation was investigated using concentrations 2.5×10^{-5}, 5.0×10^{-5}, and 7.5×10^{-5} M. The kinetics studies of the photocatalytic degradation at different initial concentrations by TiO_2-strewn sheet are shown in the Figure 37. It can be seen that on increasing the dye concentration, the photocatalytic activities of IC dye decreased. Hence, the photocatalysis process will work faster at lower concentration of pollutants. This behavior has been explained that with a high concentration of dye, the deeper colored solution would be less transparent to the UV light and the dye molecules could also absorb a significant amount of UV light causing less light to reach the catalyst resulting in the $OH^{\bullet}$ radicals forming on the surface of film to decrease, as a result, the reactive number of $OH^{\bullet}$ radicals attacking the dye molecules decreases and thus photodegradation efficiencies decreases (Konstantinou et al., 2004). The straight lines in Figure 37 confirms the first-order reaction of the degradation process with the rate

constants 0.9138 h^{-1}, 0.7077 h^{-1}, and 0.5590 h^{-1} for the dye concentration 2.5×10^{-5} , 5.0×10^{-5} , and 7.5×10^{-5} M, respectively.

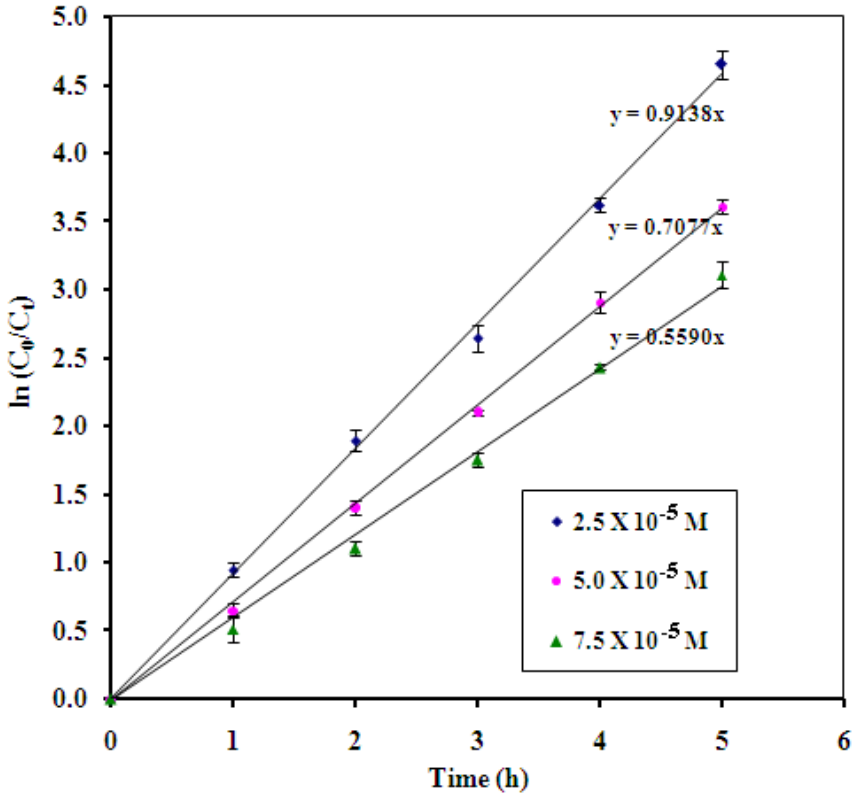

Figure 37 Reaction kinetics of the photocatalytic degradation of IC dye solution at different initial concentrations by TiO_2-strewn sheet (n = 3).

3.2.3.4 The effect of UV light intensity on the photocatalytic activity of the TiO_2-strewn sheet

The effect of UV light intensity on the photocatalytic degradation of IC dye was investigated by varying light intensity designated as: low, medium, and high. On increasing the light intensity, the photocatalytic activities increased as shown in the Figure 38. It has been reported by several groups (Toor et al., 2006; Liu et al., 2006; Jun et al., 2007), that the photodegradation rate increased with the increase of irradiation light intensity. High UV light intensity increases the photon influx entering the dye solution and consequently excites the TiO_2 particles at the sheet surface resulting in more of the $OH^{\bullet}$ radicals being formed. As the reactive number of $OH^{\bullet}$ radicals increases, the photodegradation efficiencies also increase

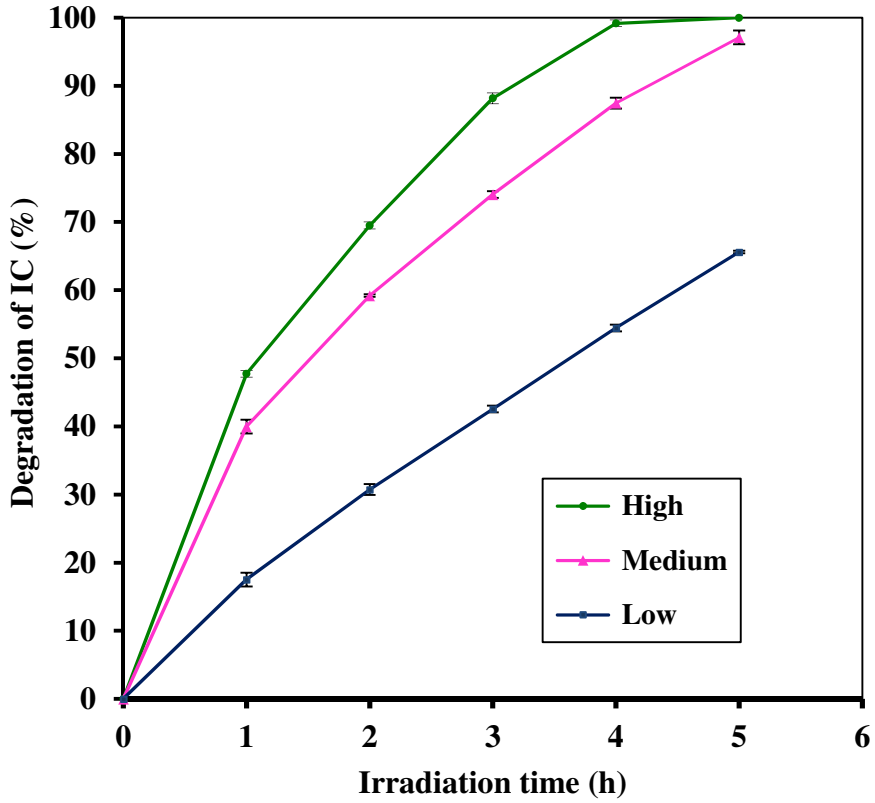

Figure 38 The effects of UV light intensity on the photocatalytic degradation of IC dye solution by the TiO_2-strewn sheet (n = 3).

3.2.3.5 Comparison between the Im-Anatase sheet, Im-P25 sheet, and TiO_2-strewn sheet on the photocatalytic activity

Since the P25 TiO_2 nanoparticles were on the sheet surface and contacted directly with dye molecules in the solution, the mechanism of dye degradation by P25 in this case was essentially the same as that which had been well documented as follows (Houas et al., 2001; Baiju et al., 2007; Khataee et al., 2010):

$$TiO_2 + h\upsilon \rightarrow TiO_2 + e^- + h^+ \quad (24)$$

$$OH^- + h^+ \rightarrow {}^\bullet OH \quad \text{(in alkaline solution)} \quad (25)$$

$$H_2O + h+ \rightarrow {}^\bullet OH + H^+ \quad \text{(in neutral solution)} \quad (26)$$

$$O_2 + e^- \rightarrow O_2^{\bullet -} \quad (27)$$

$$O_2^{\bullet -} + H^+ \rightarrow {}^\bullet O_2H \quad (28)$$

$$2\ {}^\bullet O_2H \rightarrow H_2O_2 + O_2 \quad (29)$$

$$H_2O_2 + e^- \rightarrow {}^{\bullet}OH + OH^- \quad (30)$$

$$\text{Dye} + {}^{\bullet}OH \rightarrow \text{degradation products} \quad (31)$$

These reactions sequence can be put together as shown in Figure 39 where the protruding TiO_2 surface is first irradiated with UV light causing the electron in the valence band being excited is into the conduction band. This generates an electron (e^-)/hole (h^+) pair (Eq. (24)) which, if they can survive from recombination, are highly active species to induce further reactions. The hole in the valence band can oxidize the hydroxide anion (or H_2O) near the surface to yield the very reactive hydroxyl radical ($^{\bullet}OH$) (Eqs. (25) or (26)) meanwhile the electron in the conduction band can reduce the surface adsorbed oxygen molecule to yield the superoxide radical ($O_2^{\bullet -}$) (Eq. (27)) which later yields the active $^{\bullet}OH$ radicals, Eqs. (28) - (30). The reactive $^{\bullet}OH$ radical is the main species that degrades the dye molecules, Eq. (31).

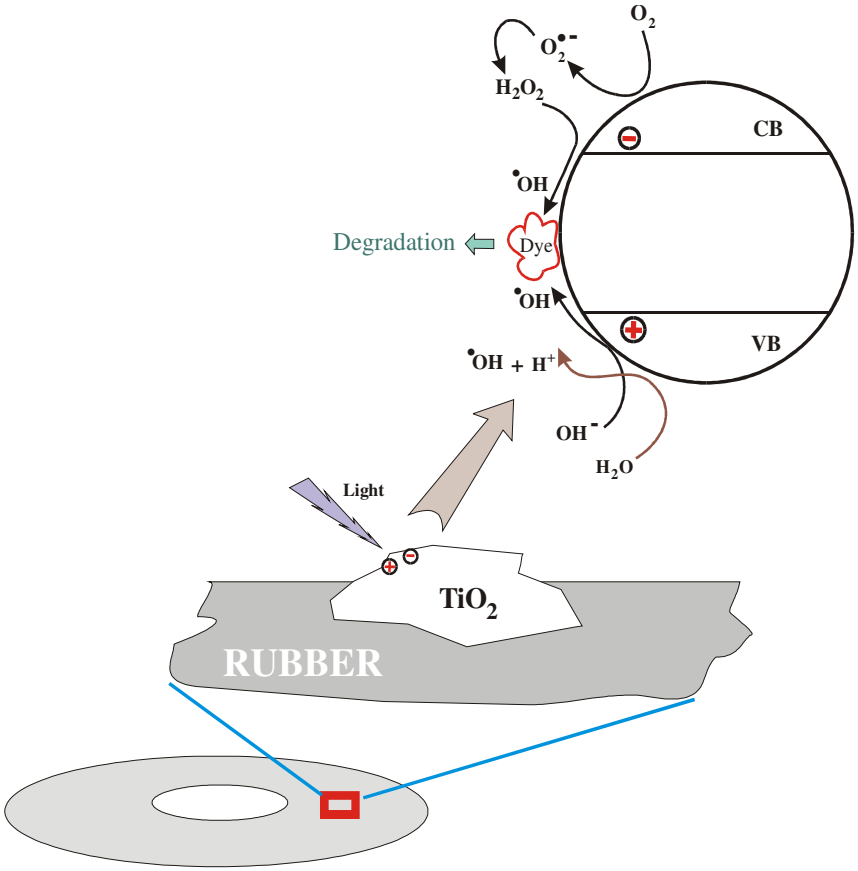

Figure 39 Degradation of dye by the TiO_2-strewn rubber sheet (Sriwong, et al., 2012).

The photocatalytic degradation efficiency of TiO_2-strewn sheet found in this work is higher than that of titania rubber sheets (referred to as Im-Anatase sheet and Im-P25 sheet) as we have reported recently (Sriwong et al., 2010). These efficiencies discrepancy are shown comparatively in Figure 40. The different efficiencies might be attributed to the location of the TiO_2 particles. TiO_2 particles of the TiO_2-strewn sheet that are externally located at the surface should have more chance to contact with IC dye molecules than those of both Im-Anatase sheet and Im-P25 sheet which are embedded rather deeply under the surface of rubber. Furthermore, in the preparation, only 0.07 g of TiO_2 was used for the TiO_2-strewn sheet while 0.1 g of TiO_2 was required to prepare the other two sheets by the previous method (in part 1).

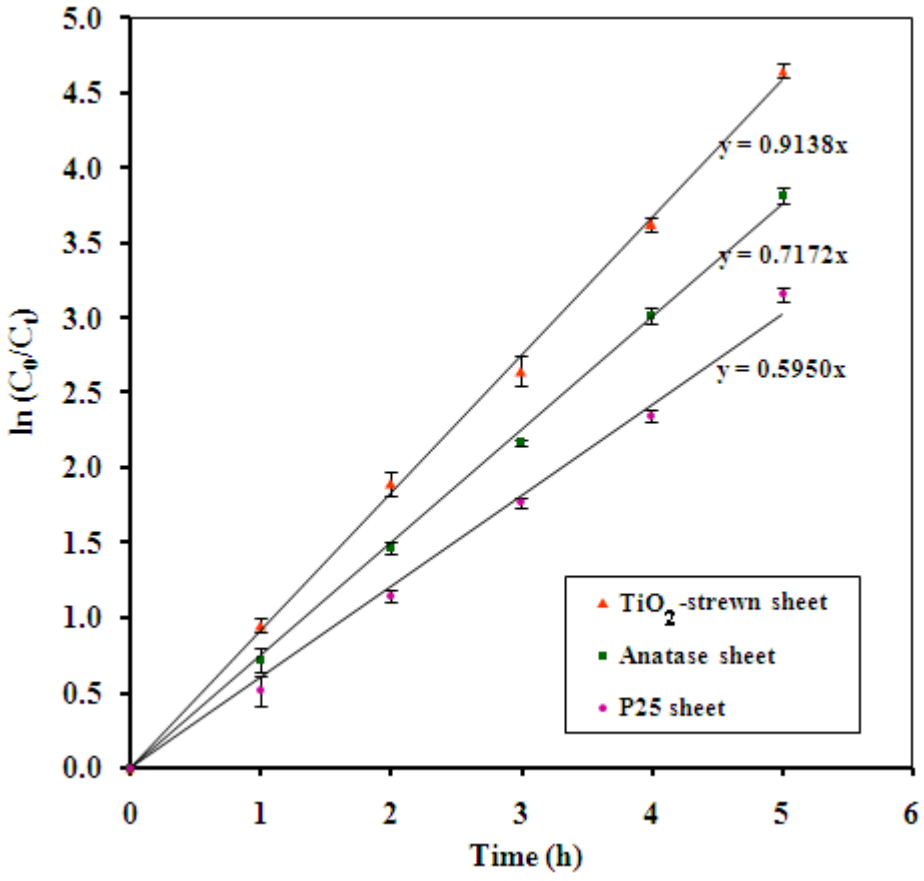

Figure 40 Comparisons of photodegradation efficiencies of indigo carmine (IC) dye (concentration 2.5×10^{-5} M) by Im-Anatase sheet, Im-P25 sheet, and TiO_2-strewn sheet (n = 3).

3.2.3.6 Recyclability of the TiO_2-strewn sheet on the photocatalytic degradation of IC dye solution

In this work, the TiO_2-strewn sheet can be used repeatedly for the photodegradation of IC dye solution. The sheet, after being used, remained clean and required no cleaning for subsequent uses. Photographs of new sheets and used sheets are shown in the Figure 41. The clean sheet surface results from repulsive force between the negative charge at the surface of the sheet and the negative charge on IC dye parent fragment. The hydrophobic properties of rubber sheet substrate may also contribute to the non-accumulation of dye molecules on the sheet surface. As a result, the sheet surface remains clean and the intermittently cleanings are not necessary. The sheet was tested for recyclability up to ten times the results of which are shown in the Figure 42. The photodegradation efficiencies of the sheet remained high throughout the recyclability test. One noticeable feature in Figure 42 is that the efficiency of the first use was slightly lower than those of the other subsequent uses. This may result from the fact that, when freshly prepared, the rubber surface as well as some of TiO_2 particles was still covered with trace of impurities. During the first use these impurities were destroyed in the photodegradation along with IC dye molecules in the solution. Hence, after the first use, the sheet surface appeared to be cleaner, i.e. less covered with impurities, with a higher number of TiO_2 particles contact with the dye solution and showed higher activity in the second use.

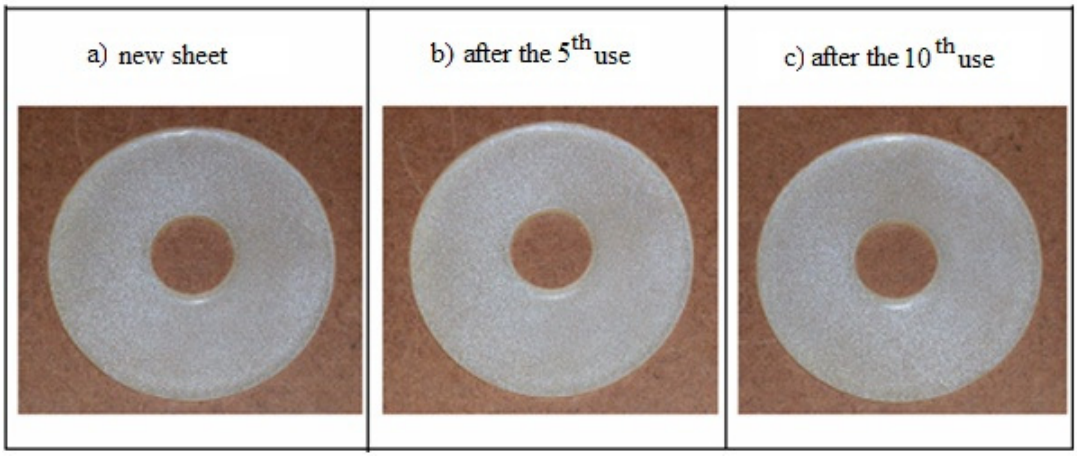

Figure 41 Photographs of the TiO_2-strewn sheet: a) new sheet, b) after the 5^{th} use, and c) after the 10^{th} use.

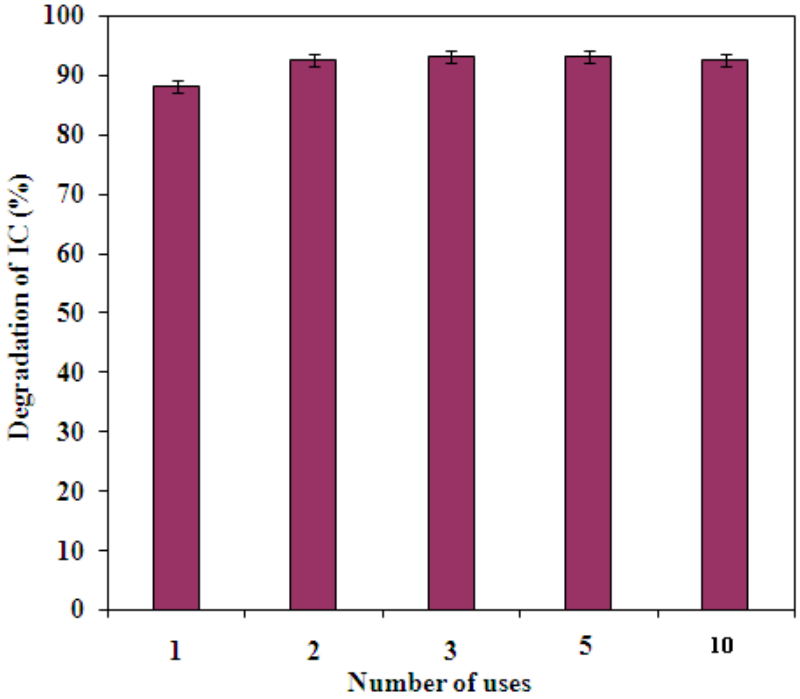

Figure 42 The photodegradation efficiencies of TiO_2-strewn sheet from the recyclability test (under UV- light 3 h, at concentration 2.5×10^{-5} M, (n = 3)).

In this part, the TiO_2-strewn rubber sheets were successfully prepared, used, and reused. However, the TiO_2-strewn rubber sheets (in this part) as well as the TiO_2 impregnated sheets (in part 1) were only one-side active. It might be a good idea to prepare a sheet that is active on usable on both sides of the sheet. This leads to another study to prepare very thin and flexible sheet which can be used either side as described in the following section.

3.3 Preparation and characterization of TiO_2-embedded rubber (ET) sheets

3.3.1 Preparation of TiO_2-embedded rubber (ET) sheets

In this present study, the TiO_2-embedded rubber sheet (hereinafter designed as ET sheet) was prepared from water-mixed diluted rubber latex and Degussa P25 TiO_2 powder suspended in ammonia solution. Then, the mixture was subjected to vacuum suction through a sintered glass and dried to remove of water and ammonia gas, finally, the ET sheet was obtained. The freshly prepared ET sheet has the same white

color as that of the rubber latex. The thickness of the 5 %wt ET sheet is 0.33 mm as estimated from the SEM cross section image. As the concentration of the latex increases so does the thickness of the sheet, i.e., the thickness of 10 %wt ET and 15 %wt ET sheets are 0.68 mm and 1.00 mm, respectively. To the naked eyes the sheet has smooth surface. The sheet can be bent or stretched and returns to its original shape easily. Figures 43(a), 43(b), and 43(c) show the photographs of ET sheet with its flexibility and elasticity properties, respectively.

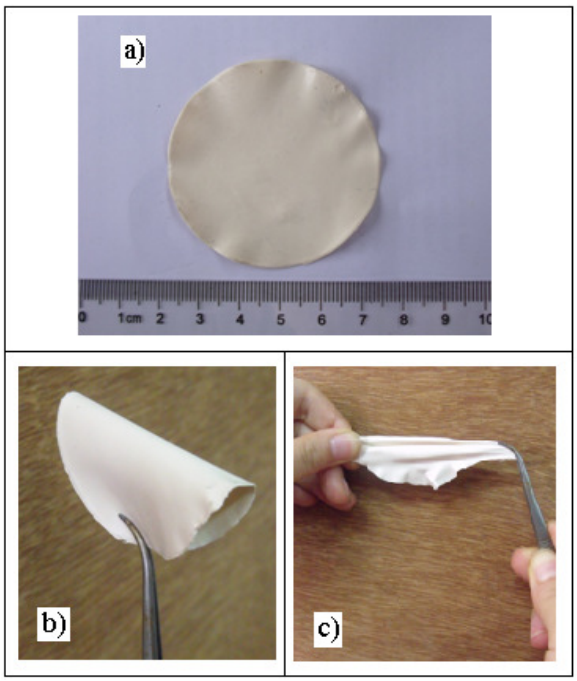

Figure 43 Photographs of (a) ET sheet, (b) showing flexibility, and (c) showing elasticity.

3.3.2 Characterization of TiO_2-embedded rubber (ET) sheets

3.3.2.1 Scanning electron microscopy (SEM)

Scanning electron microscopy is a technique used to investigate the surface morphology of all TiO_2-embedded rubber sheets. The SEM images of ET sheets are shown in Figure 44. It can be seen that the surface roughness and the content of TiO_2 particles decreased with increasing amount of rubber latex. The 5 %wt ET sheet with the highest TiO_2 particles content (Figures 44(a) and 44(d)) has the coarsest surface compared with the other two sheets. Furthermore, the TiO_2 particles appear densely on the 5 %wt ET sheet surface. The amount of rubber latex used in the

preparation of sheets has direct effect on the surface morphology of each sheet, i.e., when higher content of rubber latex was used the sheet became thicker and TiO_2 particles would appear less dense on the surface as most of them were buried rather deep under the surface of sheet (in Figures 44(b) and 44(c), respectively). Moreover, porous surface was observed only on the surface of 5 %wt ET sheet but not on the other two sheets with higher content of latex. This could be the 5 %wt ET sheet was so thin that air could pass through easily during the vacuum suction step causing some tiny holes on the surface (Figure 44(a) and 44(d)). It has been known that the surface roughness and the porous structure are very important for the photocatalytic activity of TiO_2 films (Ao, et al., 2008) since the photocatalytic activity would be increased with the enhanced surface morphology for the roughness and the porous structure.

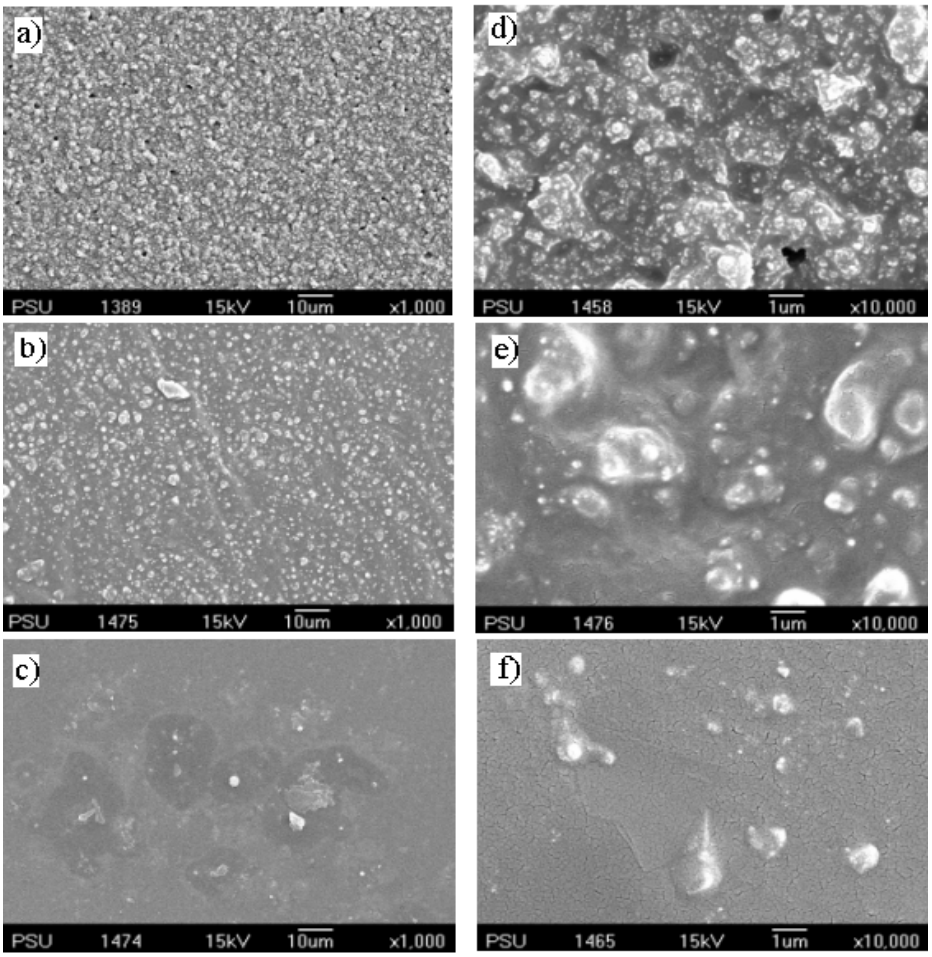

Figure 44 SEM images of ET sheets; low magnification (left column) and high magnification (right column) of 5 %wt ET sheet ((a) and (d)), 10 %wt ET sheet ((b) and (e)), and 15 %wt ET sheet ((c) and (f)).

3.3.2.2 Energy dispersive X-ray spectroscopy (EDS)

The EDS analysis was carried out to confirm the presence of elements in the flexible sheets. The EDS spectra and mapping of 5 %wt and 15 %wt ET sheets are shown in Figure 45 and Figure 46, respectively, which show that only three elements are present in the sheets (carbon, oxygen, and titanium). The 5 %wt ET sheet (Figure 45(a)) clearly shows strong Ti peaks than the 15 %wt ET sheet in Figure 46(a) corresponding to more distribution of Ti (TiO_2 particles) atoms on this sheet surface. This finding is further supported by EDS elemental mapping in Figure 45b and Figure 46(b), respectively. The 15 %wt sheet (Figure 46(a)), however, exhibits very strong carbon peak due to high concentration of rubber latex matrix on the sheet surface. Natural rubber consists mostly of *cis*-1,4 polyisoprene with a repeating hydrocarbon unit, ($-CH_2CH_3C{=}CHCH_2-$), which is the main source of carbon signal. This observation supports the conclusion from SEM results in Figures 44(c) and 44(f) that there is high concentration of rubber latex on the surface and very small amount of TiO_2 particles (very low Ti peak) on the surface of the 15 %wt ET sheet.

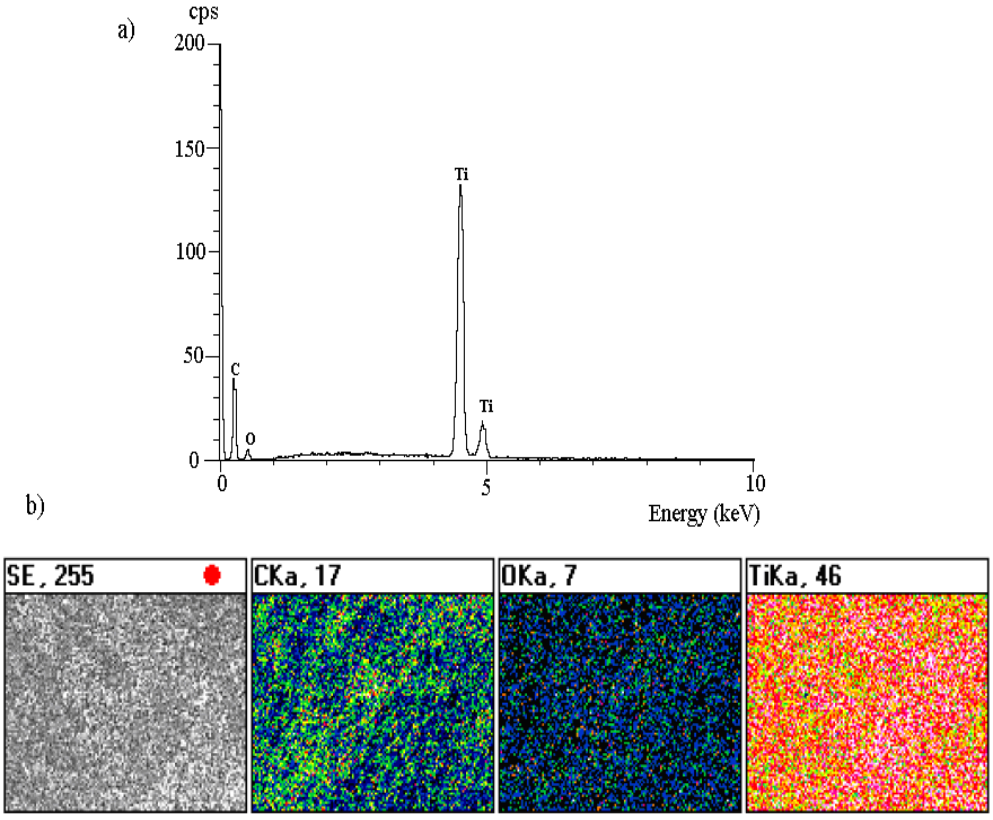

Figure 45 EDS spectra (a) and mapping images (b) of the 5 %wt ET sheet.

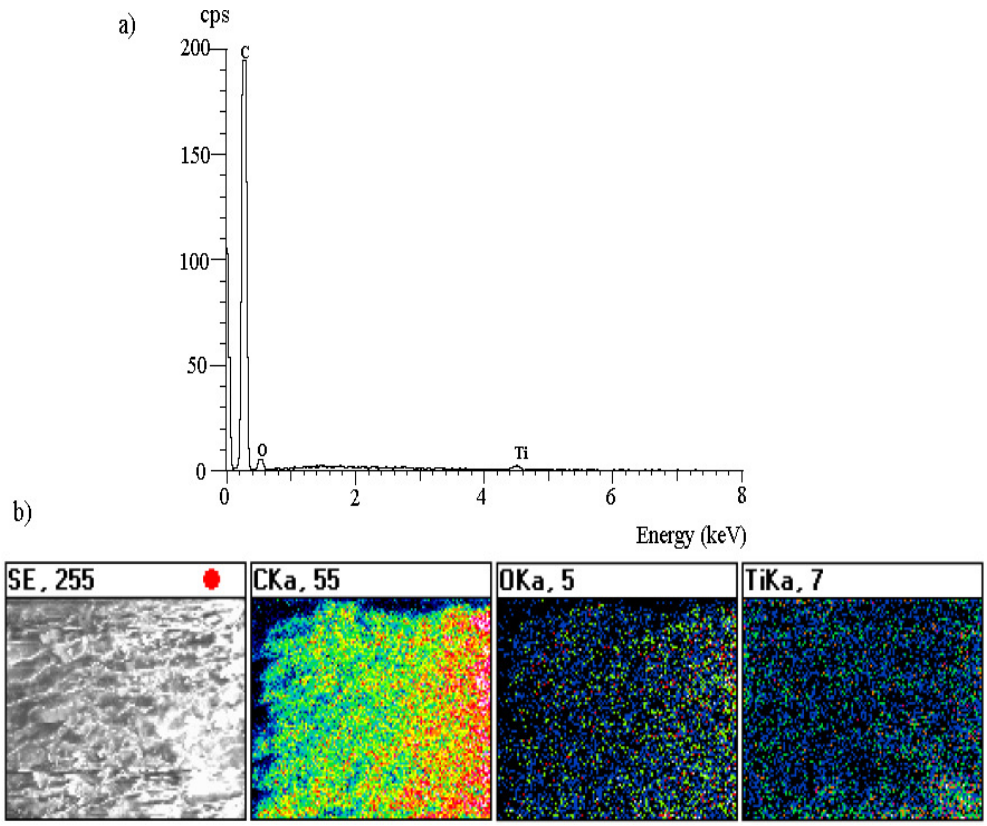

Figure 46 EDS spectra (a) and mapping images (b) of the 15 %wt ET sheet.

3.2.2.3 X-ray powder diffraction (XRD)

The X-ray diffraction patterns of the loose powder TiO_2 and TiO_2-embedded in the sheet are shown in Figure 47. The diffraction peaks of anatase and rutile phases are marked with 'A' and 'R', respectively. The anatase peaks appear at 2θ = 25.50° (101) and 48.0° while those of rutile at 2θ = 27.50° (101) and 54.50°. As shown in the figure, the well crystallized anatase and rutile forms were observed in all the ET sheets (Figures 47(b), 47(c), and 47(d)) and were identical to those of Degussa P25 powder in Figure 47(a). In addition, a broad scattering peak at 2θ = 19° of rubber matrix was also discernible in the patterns of all the ET sheet samples. The intensities of this broad peak increase with increasing concentration of rubber latex, i.e., the 5 %wt ET sheet (Figure 47(b)) has the lowest intensity compared with the 10 %wt ET and 15 %wt ET sheets, respectively. The XRD of pristine rubber sheet has been shown previously to have only a large broad peak near 2θ = 19° (Sriwong, et al., 2008) due to the fact that the rubber matrix is composed of low atomic number (low Z) elements

(Leyden, 1984). The matrix of 5 %wt ET sheet has the highest proportion of TiO_2 particles than those of the other sheets, therefore, the highest average Z-value of matrix in the former resulting in the lowest X-ray scattering and the lowest intensity peak at 2θ = 19° as shown in Figure 47(b).

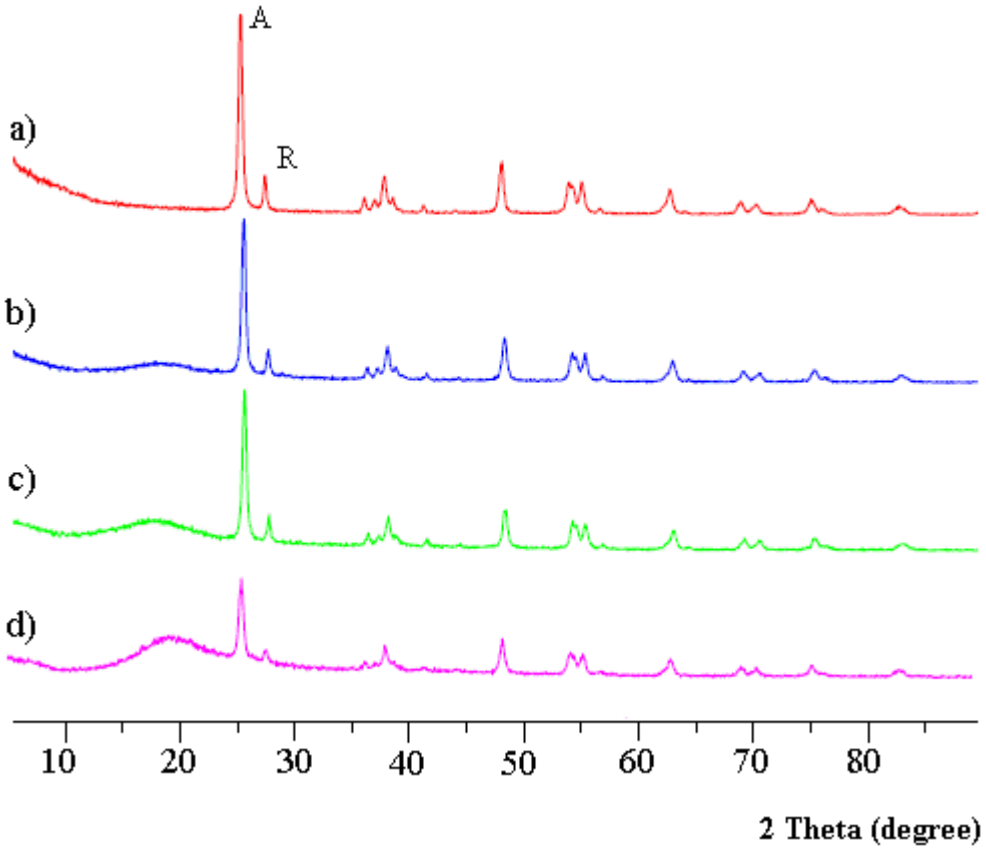

Figure 47 XRD patterns of (a) Degussa P25 TiO_2 powder; and Degussa P25 powder embedded in (b) 5 %wt ET sheet, (c) 10 %wt ET sheet, and (d) 15 %wt ET sheet.

3.3.3 Photocatalytic activity of TiO_2-strewn rubber sheets

3.3.3.1 Photocatalytic degradation of indigo carmine (IC) dye by TiO_2-embedded rubber (ET) sheets

The photocatalytic degradation of IC dye solution by the ET sheet under UV-light irradiation is shown in Figure 48. It can be seen from the figure that 5 %wt ET sheet has the highest photodegradation efficiency than the 10 %wt and 15 %wt ET sheets, respectively. As shown in Figures 44(a) and 44(d), the 5 %wt ET sheet with

very high content of TiO_2 particles on the surface has the highest surface morphology and surface roughness, therefore, it has the highest the photocatalytic activity than the other two sheets. Generally, the photocatalytic reaction on the TiO_2 surface is very sensitive to its surface structure because the photocatalytic is a surface reaction (Kwon, et al., 2004). Thus, the larger the surface structure with high surface morphology and surface roughness, the more the photocatalytic reaction takes place. In contrast, the lower the surface morphology and surface roughness as in the smooth surface sheet will have lower photodegradation activity. This is exactly what was observed in the study of the 10 %wt and 15 %wt ET sheets in comparison with the 5 %wt ET sheet.

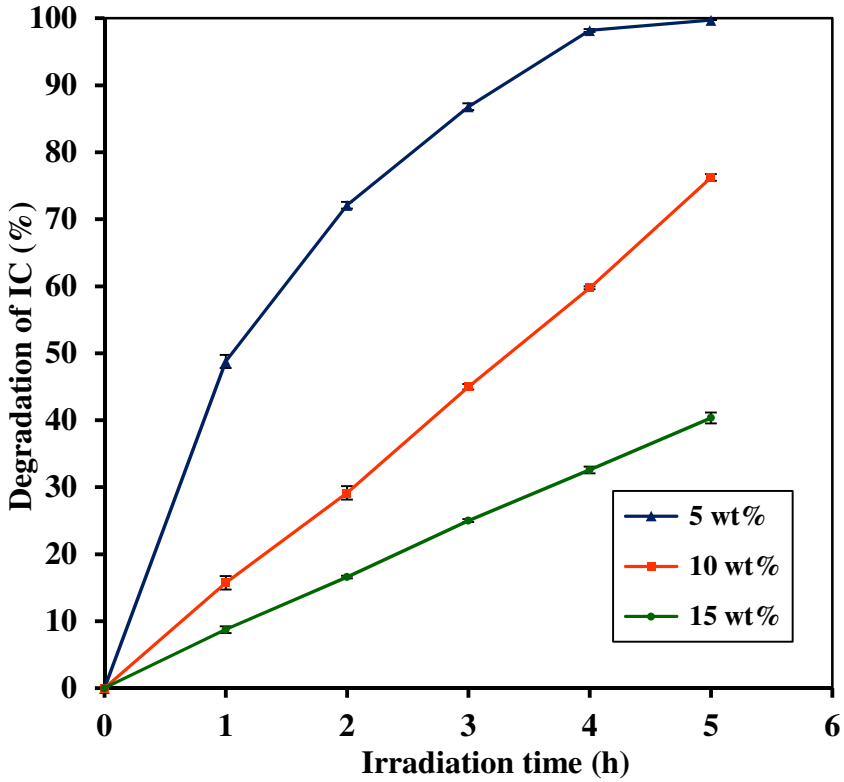

Figure 48 The efficiencies of photocatalytic degradation of IC dye by ET sheets under UV light irradiation (n = 3).

In the kinetics study, the apparent rate constant (k_{app}) has been chosen as the basic kinetics parameter for all the ET sheets under investigation. The apparent first-order kinetics equation is (Silva, et al., 2006; Baiju, et al., 2007; Ao, et al., 2008),

$$\ln\left(\frac{C_0}{C}\right) = k_{app} \times t, \qquad (32)$$

where C_0 is the initial concentration of dye, C is the concentration at time t, and k_{app} is the apparent rate constant. The straight lines obtained when ln (Co/C) was plotted against t confirmed the first-order kinetics of dye degradation as shown in Figure 49. The rate constant values calculated from Eq. (32) were 0.8247 h^{-1}, 0.2729 h^{-1}, and 0.1004 h^{-1} for the 5 %wt, 10 %wt, and 15 %wt ET sheets, respectively.

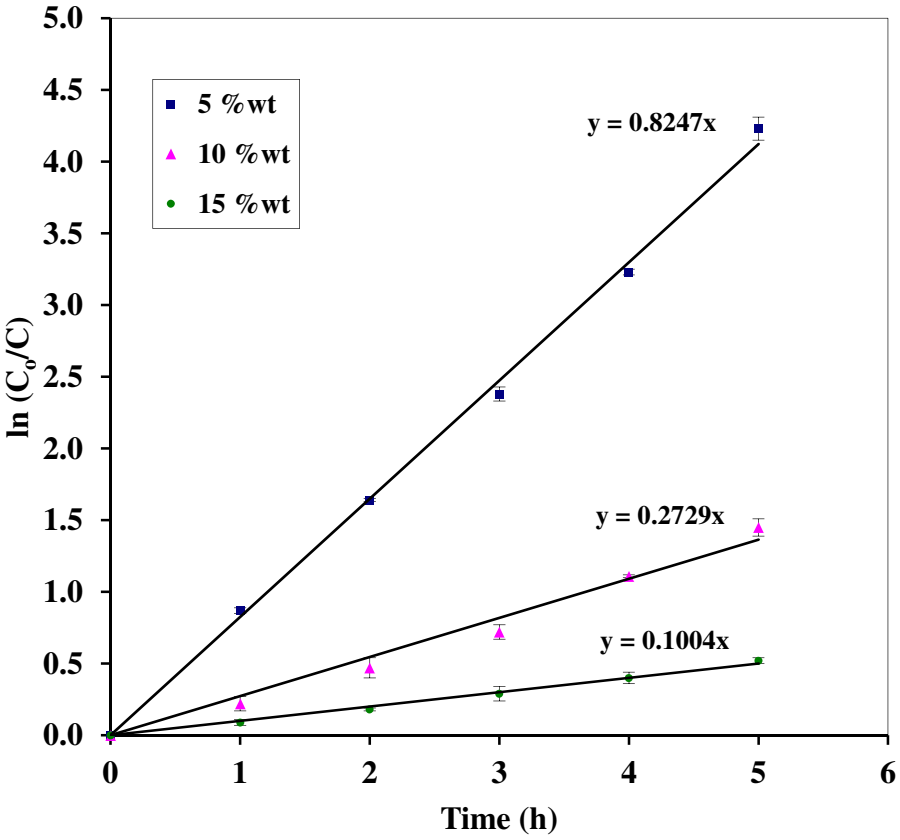

Figure 49 The kinetics plots rate of disappearance of IC dye by ET sheets (n = 3).

3.3.3.2 The effects of pH on the photocatalytic activity of the TiO_2-embedded (ET) sheet

To be useful for industrial applications, the sheet should be workable under various pH conditions. Therefore, the prepared ET sheet was put to test under varying pHs (from pH 3 to pH 8). The natural pH of IC dye solution was 6.53. The solution was adjusted to other pHs by adding either diluted HCl or NaOH solution accordingly. The effects of pH on the photocatalytic degradation of IC dye in the presence of 5 %wt ET sheet are shown in Figure 50. It can be seen that the degradation efficiency of IC dye decreases with the increasing of pH. The behavior of amphoteric metal oxide particles in water can be described by the following chemical equilibria (Kiriakidou, et al., 1999; Toor, et al., 2006):

$$\text{pH} < \text{pzc:} \qquad \text{Ti-OH} + H^+ \rightarrow \text{TiOH}_2^+ \qquad (33)$$

$$\text{pH} > \text{pzc:} \qquad \text{Ti-OH} + OH^- \rightarrow \text{TiO}^- + H_2O \qquad (34)$$

Generally, for the charged surface of TiO_2 particles, a significant dependency of the photocatalytic efficiency on the pH value was observed since the overall surface charge and, hence, the adsorptive properties of TiO_2 particles depended strongly on the solution pH (Ibhadon, et al., 2008). According to the point of zero charge (pzc), the surface charge property of TiO_2 changes with solution pH. The reported pH_{pzc} for TiO_2 is in the range 6.25-6.90. Thus, the TiO_2 surface is positively charged in acidic media ($pH < pH_{pzc}$) via the protonation depicted by equation (33) and negatively charged under alkaline conditions ($pH > pH_{pzc}$) via the proton abstraction by hydroxide ion depicted by equation (34) (Firiakidou, et al., 1999). Therefore, it is expected that at pH below pH_{pzc}, TiO_2 particles at the ET sheet surface would bear a positive charge. Since TiO_2 particles are located near the sheet surface, hence, the electrostatic interaction between the surface of the flexible ET sheet and the anionic dye parent fragment leads to strong adsorption with a corresponding high photodegradation activity at pH 3. On the other hand, at pH above pH_{pzc}, electrostatic repulsion between the negative surfaces of flexible ET sheet and anionic dye fragment retards the photodegradation activity. The order of activity decreases as pH 3 > pH 5 > pH 6.53 > pH 8.

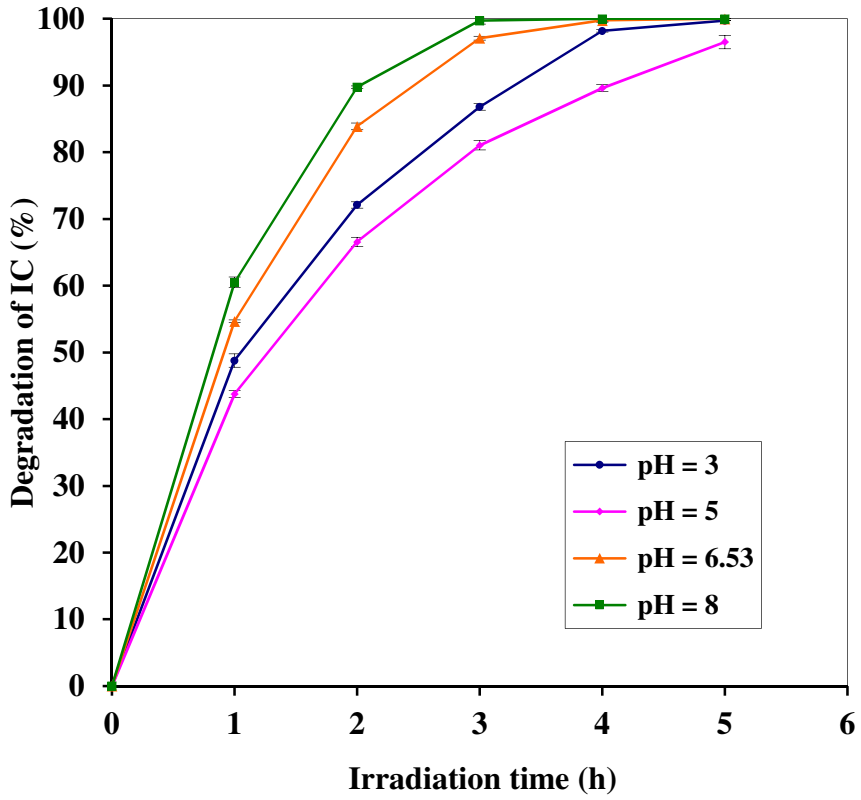

Figure 50 Effects of pH on the photodegradation efficiencies of IC dye by 5 %wt ET sheet (n = 3).

3.3.3.3 The effects of initial concentration of IC dye on the photocatalytic activity of the TiO_2-embedded (ET) sheet

The effect of initial concentration on the photocatalytic degradation was investigated using concentrations 2.5×10^{-5}, 5.0×10^{-5}, and 7.5×10^{-5} M. The efficiencies of the photocatalytic degradation at different initial concentrations by ET sheet are shown in the Figure 51. It can be seen that on increasing the dye concentration, the photocatalytic activities of IC dye decrease. Hence, the photocatalysis process will work faster at lower concentration of pollutants. This behavior has been explained that at high concentration of dye, the deeper colored solution would be less transparent to the UV light and the dye molecules could also absorb a significant amount of UV light causing less light reaching the catalyst resulting in the decrease of $OH^{\bullet}$ radical formed on the surface of film, as a result, the reactive number of $OH^{\bullet}$ radicals attacking the dye molecules decrease and thus photodegradation efficiencies decrease (Silva, et al., 2006).

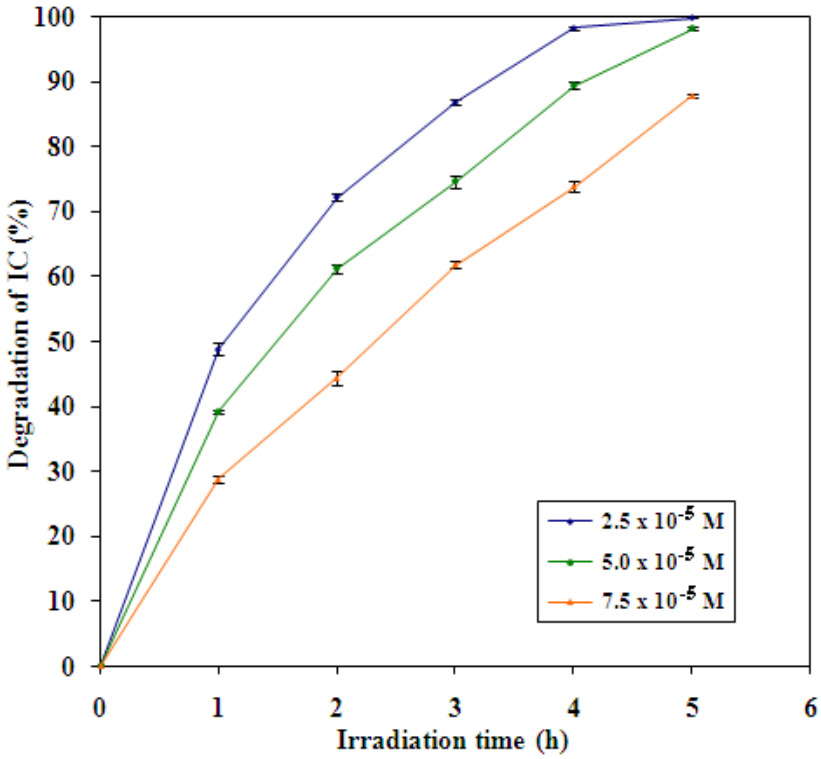

Figure 51 Effects of the initial concentration on the photodegradation efficiencies of IC dye by 5 %wt ET sheet (n = 3).

3.3.3.4 Recyclability of ET sheet on the photocatalytic degradation of IC dye

In this work, the ET sheet can be repeatedly used for the photodegradation of IC dye solution. The sheet, after used, remained clean and required no cleaning for the subsequent uses. Photographs of new and used sheets are shown in Figure 50. The clean sheet surface results from repulsive force between the potentially negative charge at the surface of sheet (due to the embedded TiO_2 particles) and the negative charge on the IC dye parent fragment. As a result, the dye molecular fragments do not adhere to the sheet surface rendering the sheet surface remains clean and the intermittently cleanings are not necessary. However, the surface of used sheets became off-white to pale yellow after several reuses compared to plain white of the new sheet (Figure 52). The sheet was tested for recyclability up to ten times the results of which are shown in Figure 53. The photodegradation efficiencies of the flexible sheet remained high throughout the recyclability tests. Note that, in Figure 53, the efficiency of the first use was slightly lower than those of the subsequent uses. The explanation for this observation is that when freshly prepared the rubber surface as well as some of

TiO_2 particles were still covered with traces of impurities. During the first use these impurities were destroyed in the photodegradation process along with IC dye molecules in the solution. Hence, after the first use, the sheet surface appeared to be cleaner, i.e. less or not at all covered with impurities, with higher number of TiO_2 particles contact with the dye solution, therefore, higher activity was observed in the second use and onward.

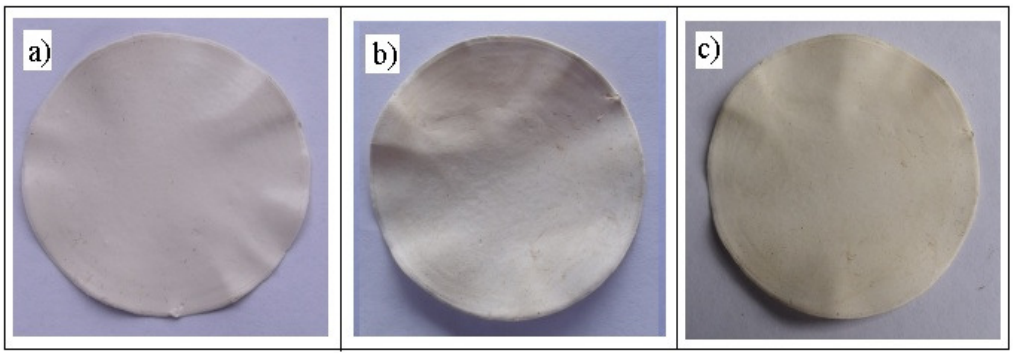

Figure 52 Photographs of the 5 %wt ET sheet; a) new sheet, b) after the 5th use, and c) after the 10th use.

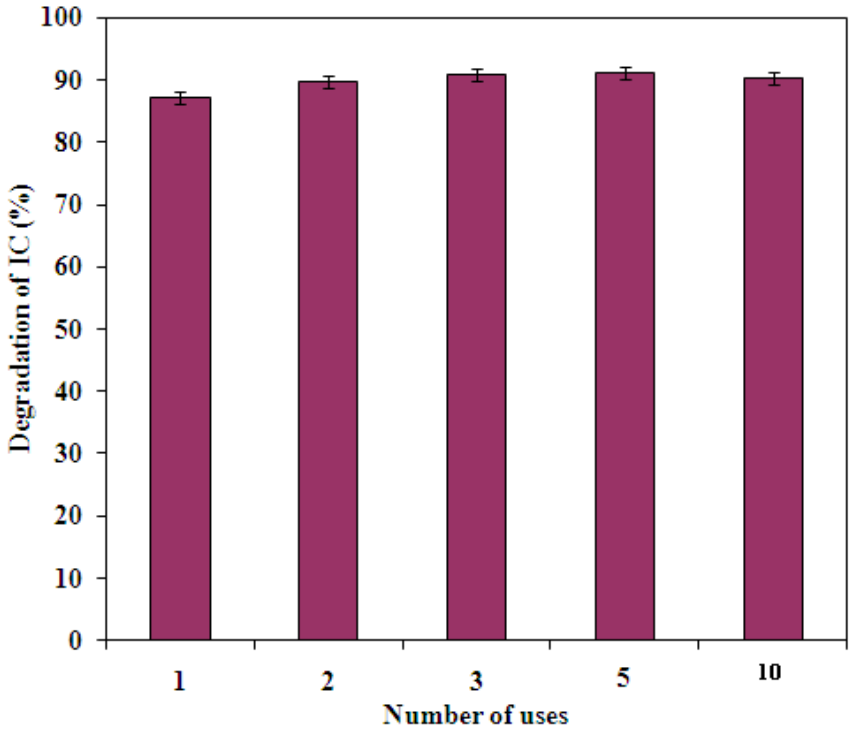

Figure 53 The efficiencies of IC dye degradation by 5 %wt ET sheet after repeated uses under UV light irradiation for 3 h (n = 3).

CHAPTER 4
CONCLUSIONS

This research is divided into three parts; part 1: preparation and characterization of TiO_2-impregnated rubber sheets, and then study their photocatalytic activity; part 2: preparation and characterization of TiO_2-strewn rubber sheets, and then study their photocatalytic activity; and part 3: preparation and characterization of TiO_2-embedded rubber sheets, and then study their photocatalytic activity.

In part 1, the preparation of both impregnated anatase sheet (Im-Anatase) and impregnated Degussa P25 sheet (Im-P25) has been described (Sriwong, et al., 2008). The impregnated rubber sheet was prepared by directly mixing TiO_2 powder with rubber latex (60% HA) and certain amount of distilled water. The characteristic of impregnated sheets was studied by the scanning electron microscopy/energy dispersive X-ray spectroscopy (SEM/EDS) and X-ray powder diffractometer (XRD) techniques. The surface morphology of Im-Anatase sheet showed evenly and well spread of anatase powder with higher surface roughness than the Im-P25 sheet. The photocatalytic activity of TiO_2-impregnated sheets was evaluated using indigo carmine (IC) dye as a model for organic dye pollutant in water. The results showed that the TiO_2-impregnated sheets could degrade IC dye solution under UV light irradiation. The Im-Anatase sheet showed higher degradation efficiency than the Im-P25 sheet. The effects of pH, initial concentration, and the intensity of UV light on the photodegradation were also investigated. Kinetics of the photocatalytic degradation was of the first-order reaction. The used TiO_2-impregnated sheet can be recovered and reused. The recycling uses did not require any cleaning between successive uses and no decline in the photodegradation efficiency was observed compared with freshly prepared TiO_2-impregnated sheet.

In part 2, the TiO_2-strewn sheet was prepared by the use of TiO_2 powder (Degussa P25) being strewn onto the sheet made form rubber latex (60% HA) through a steel sieve (60-mesh sieve). The effect of various parameters such as the time at strewing, the time for drying at 100 °C, and the amount of Degussa P25 TiO_2 powder were studied to optimize the preparation of TiO_2-strewn sheet for maximum

photocatalytic degradation of IC dye in aqueous solution. The characteristic of the TiO_2-strewn sheet was studied by using scanning electron microscopy/energy dispersive X-ray spectrometer (SEM/EDS) and X-ray powder diffractometer (XRD) techniques. The photocatalytic activity of TiO_2-strewn rubber sheet was evaluated using indigo carmine (IC) dye as a model for organic dye pollutant in water. The results showed that the TiO_2-strewn sheet could degrade IC dye solution under UV light irradiation. The order of activities of TiO_2-strewn rubber sheets as 2 h > 3 h > 1 h >> 0 h in varying the strewing time. The order of activities of TiO_2-strewn rubber sheets as 3 h ≈ 2 h ≈ 1 h > 0 h in varying the drying time at 100 °C. While the order of activities of TiO_2-strewn rubber sheets prepared with varying amount of P25 TiO_2 powder as 0.10 g ≈ 0.07 g > 0.05g > 0.03 g. The optimal conditions for preparation of TiO_2-strewn rubber sheet were: 10 mL latex, 0.07 g Degussa P25 TiO_2 powder, 2 h strewing time, and 1 h drying time at 100 °C showed the highest photocatalytic activity. The effects of pH, initial concentration, and the intensity of UV light on the photodegradation were also investigated. Kinetics of the photocatalytic degradation was of the first-order reaction. The used TiO_2-strewn sheet can be recovered and reused. The recycling uses did not require any cleaning between successive uses and no decline in the photodegradation efficiency was observed compared with freshly prepared TiO_2-strewn sheet.

In part 3, the TiO_2-embedded rubber (ET) sheet was prepared by mixing TiO_2 powder (Degussa P25) with small amount of natural rubber latex (60 %HA) followed by vacuum filtration through a sintered glass to form a thin paper-like and flexible sheet. The characteristic of the ET sheet was studied by scanning electron microscopy/energy dispersive X-ray spectrometer (SEM/EDS) and X-ray diffractometer (XRD) techniques. From the SEM results, the 5 %wt ET sheet contained very dense and better covered by titanium dioxide particles on the sheet surface rendering high surface morphology and surface roughness from which the highest photocatalytic efficiency was originated. The photocatalytic activity of ET sheet was evaluated using indigo carmine (IC) dye as a model for the organic dye pollutant in water. The results showed that the 5 %wt ET sheet has the highest degradation efficiency than other sheets. The effects of pH and initial concentration of dye solution on the photodegradation were also investigated. Kinetics of the photocatalytic degradation was of the first-order reaction. The used ET sheet can be recovered and reused with no decline in the

photodegradation efficiency over a long-term usage. The recyclability of the ET sheet should be attractive to the water treatment industry as it helps keep the operation cost low. The relatively low cost of the materials (photocatalyst powder and rubber latex) is a onetime investment and will last over a long period of time and usage.

From the conclusions above, we found that three types of TiO_2 immobilized rubber sheets were successfully prepared by three different methods. These methods - simple, low cost, and more effective - are based on the use of commercial TiO_2 powder and natural rubber latex (60 %HA) as starting materials. The rubber latex is interesting because of its versatility in daily life and available locally. Furthermore, since rubber latex is used to make the sheets, this should be another way of utilizing the rubber latex which Thailand is the number one producer in the world. From the photocatalytic activities test, all types of immobilized TiO_2 sheets could degrade IC dye solution under UV light irradiation. The photocatalytic activities of all types of TiO_2 sheets depended on the effects of pH, initial concentration of IC dye solution, and the intensity of UV light. Although all types of TiO_2 sheets showed less activities than the loose powder of the same catalysts (Sriwong, et al., 2008), it has one clear advantage over the loose powder that it can be easily recovered after used and can be reused many times. The recyclability of all immobilized TiO_2 sheets should be attractive to the water treatment industry as it helps keep the operation cost low. The relatively low cost of the materials (photocatalyst powder and rubber latex) is a onetime investment and will last over a long period of time and usage. We deem that this work could be used in Thailand as a method for the destruction of synthetic dye pollutants in the factories before releasing wastewater into the natural water system.

REFERENCES

Ao, Y.; Xu, J.; Fu, D.; Shen, X. and Yuan, C. 2008. "Low temperature preparation of anatase TiO_2-coated activated carbon", Applied Surface Science. 254 (2008), 4001-4006.

Ao, Y.; Xu, J.; Fu, D. and Yuan, C. 2008. "Preparation of porous titania thin film and its photocatalytic activity", Applied Surface Science. 255 (2008), 3137-3140.

Arabarzis, I. M.; Stergiopoulos, T.; Andreeva, D.; Kitova, S.; Neophytides, S. G. and Falaras, P. 2003. "Characterization and photocatalytic activity of Au/TiO_2 thin films for azo-dye degradation", Journal of Catalysis. 220 (2003), 127-135.

Baiju, K.V.; Shukla, S.; Sandhya, K.S.; James, J. and Warrier, K.G.K. 2007. "Photocatalytic activity of sol-gel-derived nanocrystalline titania", Journal of Physical Chemistry. 111 (2007), 7612-7622.

Baolong, Z.; Baishun, C.; Keyu, S.; Shangjin, H.; Xiaodong, L.; Zongjie, D. and Kelian, Y. 2003. "Preparation and characterization of nanocrystal grain TiO_2 porous microspheres", Applied Catalysis B: Environmental. 40 (2003), 253-258.

Baran, W.; Makoeski, A. and Wardas, W. 2008. "The effect of UV radiation absorption of cationic and anionic dye solution on their photocatalytic degradation in the presence TiO_2", Dyes and Pigments. 76 (2008), 226-230.

Barka, N.; Assabbane, A.; Nounah, A. and Ichou, Y. A. 2008. "Photocatalytic degradation of indigo carmine in aqueous solution by TiO_2 coated non-woven fibres", Journal of Hazardous Materials. 152 (2008), 1054-1059.

Bizani, E.; Fytianos, K.; Poulios, I. and Tsiridis, V. 2006. "Photocatalytic decolorization and degradation of dye solutions and wastewaters in the presence of titanium-dioxide", Journal of Hazardous Materials. 136 (2006), 85-94.

Buchner, W.; Schliebs, S.; Winter, G. and Buchel. K. H. 1989. Industrial Inorganic Chemistry. New York : VCH.

Byun, D.; Jin, Y.; Kim, B.; Lee, J.K. and Park.; D. 2000. "Photocatalytic TiO_2 deposition by chemical vapor deposition", Journal of Hazardous Materials. B73 (2000), 199-206.

Carneiro, P. A.; Osugi, M. E.; Sene, J. J.; Anderson, M. A. and Boldrin Zanoni, M. V. 2004. "Evaluation of color removal and degradation of a reactive texile azo dye on nanoporous TiO_2 thin-film electrodes", Electrochimica Acta. 49 (2004), 3807-3820.

Chatterjee, D.; and Mahata, A. 2002. "Visible light induced photodegradation of organic pollutants on dye adsorbed TiO_2 surface", Journal of Photochemistry and Photobiology A: Chemistry. 153 (2002), 199-204.

Chen, J.; Shunchen, Q.; Yuexiang, Z. and Youchang, X. 2011. "Phosphorous-modified TiO_2 with excellent thermal stability and its application to the degradation of pollutants in water", Chinese Journal of Catalysis. 32 (2011), 1173-1179.

Chiang, K.; Amal, R. and Tran, T. 2002. "Photocatalytic degradation of cyanide using titanium dioxide modified with copper oxide", Advances in Environmental Research. 6 (2002), 471-485.

Clark, R. J. H. 1968. The Chemistry of Titanium and Vanadium. Amsterdam : Elsevier. (1968), 526-528.

Deanna, C.H.; Alexander, G.A.; Kimberly, A.G.; Tijana, R. and Marion, C.T. 2003. "Explaining the enhanced photocatalytic activity of Degussa P25 mixed-phase TiO_2 using EPR", Journal of Physical Chemistry. 107 (2003), 4545-4549.

Ding, Z.; Lu, G. Q. and Greenfield, P. F. 2000. "Role of the crystallite phase of TiO_2 in heterogeneous photocatalysis for phenol oxidation in water", Journal of Physical Chemistry. 104 (2000), 4815-4820.

Ding, Z.; Hu, X.; Yue, P.L.; Lu, G.Q. and Greenfield, P.E. 2001. "Synthesis of anatase TiO_2 supported on porous solids by chemical vapor deposition", Catalysis Today. 68 (2001), 173-182.

Dumitriu, D.; Bally, A.R.; Hones, P. and Schmid, P.E. 2000. "Photodegradation of phenol by TiO_2 thin films prepared by sputtering", Applied Catalysis B: Environmental. 25 (2000), 83-92.

Faisal, F.; Abu Tariq, M. and Muneer, M. 2007. "Photocatalysed degradation of two selected dyes in UV-irradiated aqueous suspensions of titania", Dyes and Pigments. 72 (2007) 233-239.

Ge, L.; Xu, M.; Sun, M. and Fang, H. 2006. "Fabrication and characterization of nano TiO_2 thin films at low temperature", Materials Research Bulletin. 41 (2006), 1569-1603.

Ge, L.; Xu, M. and Fang, H. 2006. "Synthesis of novel photocatalytic $InVO_4$-TiO_2 thin films with visible light photoactivity", Materials Letters. 61 (2006), 63-66.

Gomes de Moraes, S.; Sanches Freire, R. and Duran, N. 2000. "Degradation and toxicity reduction of textile effluent by combined photocatalytic and ozonation processes", Chemospere. 40 (2000), 369-373.

Guo, H.; Kemell, M.; Heikkila, M. and Leskela, M. 2010. "Novel metal-modified TiO_2 Thin film photocatalyst on porous steel fiber support", Applied Catalysis B: Environmental. 95 (2010), 358-364.

Habibi, M.H.; Talebian, N. and Choi, J.H. 2007. "The effect of annealing on photocatalytic properties of nanostructured titanium dioxide thin films" Dyes and Pigments. 73 (2007), 103-110.

Herrmann, J.M.; Tahiri, H.; Ait-Ichou, Y.; Lassaletta, G.; Gonzalez-Elipe, A. R. and Fernanedz, A. 1997. "Characterization and photocatalytic activity in aqueous medium of TiO_2 and Ag- TiO_2 coatings on quartz", Applied Catalysis B: Environmental. 13 (1997), 219-228.

Houas, A.; Lachheb, H.; Ksibi, M.; Elaloui, E.; Guillard, C. and Hermann, J. M. 2001. "Photocatalytic degradation pathway of methylene blue in water", Applied Catalysis B: Environmental. 31 (2001), 145-157.

Hurum, D.C.; Agrios, A.G.; Crist, S.E.; Gray, K.A.; Rajh, K.A. and Thurnauer, M.C. 2006. "Probing reaction mechanisms in mixed phase TiO_2 by EPR", Journal of ElectronScopy and Relatived Phenomena. 150 (2006), 155-163.

Ishibai, Y.; Sato, J.; Nishikawa, T. and Miyagishi, S. 2008. "Synthesis of visible-light active TiO_2 photocatalyst with Pt-modification: role of TiO_2 substrate for high photocatalytic activity", Applied Catalysis B: Environmental. 79 (2008), 117-121.

Kang, H.; Kang, M.Y. and Han, K.H. 2000. "Identification of natural rubber and characterization of rubber biosynthetic activity in Fig Tree", Plant Physiology. 123 (2000), 1133-1142.

Kanna, M.; Wongnawa, S.; Buddee, S.; Dilokkhunakul, K. and Pinpithak, P. 2010. "Amorphous titanium dioxide: a recyclable dye remover for water treatment", Journal of Sol-Gel Science Technology. 53 (2010), 162-170.

Kiriakidou, F.; Kondarides, D.I.; Verykios X.E. 1999. "The effect of operational parameters and TiO_2-doping on the photocatalytic degradation of azo-dyes", Catalysis Today. 54 (1999), 119-130.

Kwon, C.H.; Shin, H.; Kim, J.H.; Choi, W.H. and Yoon, K.H. 2004. "Degradation of methylene blue via photocatalysis of titanium dioxide", Materials Chemistry and Physics. 86 (2004), 78-82.

Leyden, D.E. 1984. "Fundamentals of X-ray spectrometry as applied to energy dispersive techniques", Tracor Xray, Inc., Mountain View, California. (1984).

Li, S.; Ye, G. and Chen, G. 2009. "Low-temperature preparation and characterization of nanocrystalline Anatase TiO_2", Journal of Physical Chemistry: C. 113 (2009), 4031-4037.

Li, F.T.; Zhao, Y.; Liu, Y.; Hao, Y.J.; Liu, R.H. and Zhao, D.S. 2011. "Solution combustion synthesis and visible light-induced photocatalytic activity of mixed amorphous and crystalline $MgAl_2O_4$ nanopowders", Chemical Engineering Journal. 173 (2011), 750-759.

Losito, I.; Amorisco, A.; Palmisano, F. and Zambonin, G.P. 2005. "X-ray photoelectron spectroscopy characterization of composite TiO_2-poly (vinylidenefluoride) films synthesised for applications in pesticide photocatalytic degradation. Applied Surface Science. 240 (2005), 180-188.

Luis, A.M.; Neves, M.C.; Mendoca, M.H. and Monteiro, O.C. 2011. "Influence of calcination parameters on the TiO_2 photocatalytic properties", Materials Chemistry and Physics. 125 (2011), 20-25.

Matsuo, S.; Sakaguchi, N.; Yamada, K.; Matsuo, T. and Wakita, H. 2004. "Role in photocatalisis and coordination structure of metal ions adsorbed on titanium dioxide particles: a comparison between lanthanide and iron ions", Applied Surface Science. 228 (2004), 233-244.

Michael, L.; Hitchman. and Tian, F. 2002. "Studies of TiO_2 thin films prepared by chemical vapor deposition for photocatalytic and photoelectrocatalytic degradation of 4-chlorophenol", Journal of Electroanalytical Chemistry. 538-539 (2002), 165-172.

Mills, A. and Wang, J. 1999. "Photobleaching of methylene blue sensitised by TiO_2: an ambiguous system", Journal of Photochemistry and Photobiology A: Chemistry. 127 (1999), 123-134.

Mittal, A. M.; Mittal, J. M. and Kurup, L. 2006. "Batch and Bulk removal of hazardous dye, indigo carmine from wastewater through adsorption", Journal of Hazardous Materials. 137 (2006), 591-602.

Muruganandham, M.; Shobana, N. and Swaminathan, M. 2005. "Optimization of solar photocatalytic degradation conditions of Reactive Yellow 14 azo dye in aqueous TiO_2", Journal of Molecular Catalysis A: Chemical. 246 (2005), 154-161.

Nagaveni, K.; Sivalingam, G. and Heged, M.S. 2004. "Solar photocatalytic degradation of dyes:high activity of combustion synthesized nano TiO_2", Applied Catalysis B: Environmental. 48 (2004), 83-93.

Nawamawat, K.; Sakdapipanich, J.T.; Ho, C.C.; Ma, Y.; Song, J. and Vancso, J.G. 2011. "Surface nanostructure of *Hevea brasiliensis* natural rubber latex particles", Colloids and Surfaces A: Physicochemical and Engineering Aspects. 309 (2011), 157-166.

Ohno, T.; Sarukawa, K.; Tokieda, K. and Matsumura, M. 2001. "Morphology of a TiO_2 photocatalyst (Degussa, P25) consisting of anatase and rutile crystalline phases", Journal of Catalysis. 203 (2001) 82-86.

Ohtani, B.; Prieto-Mahaney, O.O.; Li, D. and Abe, R. 2010. "What is Degussa (Evonic) P25? Crystalline composition analysis, reconstruction from isolated pure particles and mechanisms", Journal of Photochemistry and Photobiology A: Chemistry. 216 (2010), 179-182.

Oliveira, E.G.L.; Rodrigues, J.J. and Oliveira, H.P. 2011. "Influence of surfactant on the fast photodegradation of rhodamine B induced by TiO_2 dispersions in aqueous solution", Chemical Engineering Journal. 172 (2011), 96-101.

Othman, I.; Mohamed, R. M.; Ibrahim, I. A. and Mohamed, M. M. 2006. "Synthesis and modification of ZSM-5 manganese and lanthanum and their effects on decolorization of indigo carmine dye", Applied Catalysis A: General. 299 (2006), 95-102.

Othman, I.; Mohamed, R. M.; Ibrahim, I. A. and Mohamed, M. M. 2007. "Study of photocatalytic oxidation of indigo carmine dye on Mn-supported TiO_2", Journal of Photochemistry and Photobiology A: Chemistry. 189 (2007), 80-85.

Paola, A.D.; Addamo, M.; Bellardita, M.; Cazzanelli, E. and Palmisano, L. 2007. "Preparation of photocatalytic brookite thin flims", Thin Solid Films. 515 (2007), 3527-3529.

Parida, K. M.; Sahu, N.; Biswal, N. R.; Naik, B. and Pradhan, A. C. 2008. "Preparation, characterization, and photocatalytic activity of sulfate-modified titania for degradation of methyl orange under visible light", Journal of Colloid and Interface Science. 318 (2008), 231-237.

Partsinis. S.E. 1996. “Flame Synthesis of nanosize particles: precise control of particle size”, Journal of Aerosol Science. 27 (1996), s153-s154.

Perrella, F.W. and Gaspari, A.A. 2002. “Natural rubber latex protein reduction with an emphasis on enzyme treatment”, Methods. 27 (2002), 77-86.

Prado, A.G.S.; Bolzon, L.B.; Pedroso, C.P.; Moura, O.A. and Costa, L.L. 2008. “Nb_2O_5 as efficient and recyclable photocatalyst for indigo carmine degradation”, Applied Catalysis B: Environmental. 82 (2008), 219-224.

Putta, T.; Lu, M.C. and Anotai, J. 2011. “Photocatalytic activity of tungsten-doped TiO_2 with hydrothermal treatment under blue light irradiation”, Journal of Environmental Management. 92 (2011), 2272-2276.

Qamar, M.; Saquib, M. and. Muneer, M. 2005. “Photocatalytic degradation of two selected derivative, chromotrope 2B and amino black 10B, in aqueous suspensions of titanium dioxide”, Dyes and Pigments. 65 (2005), 1-9.

Ranjit, K. T.; Willner, I.; Bossmann, S. H. and Braun, A. M. 2001. “Lanthanide oxide doped titanium dioxide photocatalysts: Effective photocatalysts for the enhanced degradation of salicylic acid and *t*-cinamic acid”, Journal of Catalysis. 204 (2001), 305-313.

Ren, L.; Zeng, Y.P. and Jiang, D. 2009. “Preparation, characterization and photocatalytic activities of Ag-deposited porous TiO_2 sheets”, Catalysis Communications. 10 (2009) 645-649.

Ripple, M.M.; Costa, C.A.R. and Galembeck, F. 2004. “Natural rubber latex modification by sodium polyphosphate: a SPM study on the improved latex adhesion to glass sheet”, Polymer. 45 (2004), 3367-3375.

Saepurahman; Abdullah, M.A. and Chong, F.K. 2010. "Preparation and characterization of tungsten-loaded titanium dioxide photocatalyst for enhanced dye degradation", Journal of Hazardous Materials. 176 (2010), 451-458.

Sanguansap, K.; Suteewong, T.; Saendee, P.; Buranabunya, U. and Tangboriboonrat, P. 2005. "Composite natural rubber based latex particles: a novel approach", Polymer. 46 (2005), 1373-1378.

Sankapal, S.B.; Steiner, M.Ch. and Ennaoui, A. 2005. "Synthesis and characterization of anatase-TiO_2 thin films", Applied Surface Science. 239 (2005), 165-170.

Sansatsadeekul, J.; Sakdapipanich, J. and Rojruthai, P. 2011. "Characterization of associated proteins and phospholipids in natural rubber latex", Journal of Bioscience and Bioengineering. 111 (2011), 628-634.

Sameiro, M.; Goncalves, T.; Pinto, M.S. and Peter, N. 2005. " Degradation of *C.I. Reactive Orange 4* and its simulated dyebath wastewater by heterogeneous photocatalysis", Dyes and Pigments. 64 (2005), 135-139.

Seabra, M.P.; Rego, E.; Ribeiro, A. and Labrincha, J.A. 2011. "Photodegradation of orange II solutions by TiO_2 active layer jet spray on aluminium sheets", Chemical Engineering Journal. 171 (2011), 175-180.

Sen, S.; Mahanty, S.; Roy, S.; Heintz, O. and Bourgeois, D. 2005. "Investigation on sol-gel synthesized Ag-doped TiO_2 cermet thin films", Thin Solid Films. 474 (2005), 245-249.

Senthilkumaar, S. and Porkodi, K. 2005. "Heterogeneous photocatalytic decomposition of Crystal Violet in UV-illuminated sol-gel derived nanocrystalline TiO_2 suspensions", Journal of Colloid and Interface Science. 288 (2005), 184-189.

Senthilkumaar, S.; Porkodi, K. and Vidyalakshmi, R. 2005. "Photodegradation of a textile dye catalyzed by sol-gel derived nanocrystalline TiO_2 via ultrasonic irradiation", Journal of photochemistry and Photobiology A: Chemistry. 170 (2005), 225-232.

Shi, J.; Zheng, J.; Wu, P.; and Ji, X, 2008. "Immobilization of TiO_2 films on activated carbon fiber and their photocatalytic degradation properties for dye compounds with different molecular size", Catalysis Communications. 9 (2008), 1846-1850.

Silva, C.G.; Wang, W. and Faria, J.L. 2006. " Photocatalytic and photochemical degradation of mono-, di- and tri-azo dyes in aqueous solution under UV irradiation", Journal of Photochemistry and Photobiology A: Chemistry. 181 (2006), 314-324.

Sriwong, C.; Wongnawa, S. and Patarapaiboolchai, O. 2008. "Photocatalytic activity of rubber sheet impregnated with TiO_2 particles and its recyclability", Catalysis Communications. 9 (2008), 213-218.

Sriwong, C.; Wongnawa, S. and Patarapaiboolchai, O, 2010. "Degradation of indigo carmine dye by rubber sheet impregnated with TiO_2 particles", ScienceAsia. 36 (2010), 52-58.

Sriwong, C.; Wongnawa, S. and Patarapaiboolchai, O, 2012. "Rubber sheet strewn with TiO_2 particles: Photocatalytic activity and recyclability", Journal of Environmental Sciences. 24 (2012), 464-472.

Sriwong, C.; Wongnawa, S. and Patarapaiboolchai, O, 2012. "Recyclable thin TiO_2-embedded rubber sheet and dye degradation", Chemical Engineering Journal. (2012), doi:10.1016/j.cej.2012.03.005.

.

Sruanganurak, A.; Sanguansap. and Tangboriboonrat, P. 2006. "Layer-by-layer assembled nanoparticles: a novel method for surface modification of natural rubber latex film", Colloids and Surfaces A: Physicochemical and Engineering Aspects. 301 (2007), 147-152.

Stylidi, M.; Kondarides, D.I. and Verykios, X.E. 2003. "Pathways of solar light-induced photocatalytic degradation of azo drys in aqueous TiO_2 suspensions", Applied Catalysis B: Environmental. 40 (2003), 271-286.

Sung-Suh, H.M.; Choi, J.R.; Hah, H.J.; Koo, S.M. and Bac, Y.C. 2004. "Comparison of Ag deposition effects on the photocatalytic activity of nanoparticulate TiO_2 under UV light irradiation", Journal of Photochemistry and Photobiology A: Chemistry. 163 (2004), 37-44.

Suwanchawalit, C.; Patil, A.J.; Kumar, R.K.; Wongnawa, S. and Stephen, M. 2009. "Fabrication of ice-templated macroporous TiO_2-chitosan scaffolds for photocatalytic applications", Journal of Materials Chemistry. 19 (2009), 8478-8483.

Tehrani, F.M.K.; Rashidzadeh, M.; Nemati, A.; Irandoukht, A. and Faridnia, B. 2011. "Characterization and photocatalytic activity of nanosized titanium dioxide thin films", International Journal of Environmental Science and Technology. 8 (2011), 545-552.

Tian, B.; Tong, T.; Chen, F. and Zhang, J. 2007. "Effect of water washing treatment on the photocatalytic activity of Au/TiO_2 catalysts", Acta-Physico-Chimica Sinica. 23 (2007), 978-982.

Toor, A.P.; Verma, A.; Jotshi, C.K.; Bajpai, P.K. and Singh, V. 2006. "Photocatalytic degradation of Direct Yellow 12 dye using UV/TiO_2 in shallow pond slurry reactor", Dyes and Pigments. 68 (2006), 53-60.

Tsuji, H.; Sugahara, H.; Gotoh, Y. and Ishikawa, J. 2003. "Improvement of photocatalytic efficiency of rutile titania by silver negative-ion implantation", Nuclear Instruments and Methods in Physics Research: B. 206 (2003), 249-253.

Vautier, M.; Guillard, C. and Herrmann, J.M. 2001. "Photocatalytic degradation of dye in water: case study of indigo and indigo carmine", Journal of Catalysis. 201 (2001), 46-59.

Wang, T.; Wang, H.; Zhao, X. and Chao, S. 1998. "The effect of properties of semiconductor oxide thin films on photocatalytic decomposition of dyeing waste water", Thin Solid Films. 334 (1998), 103-108.

Wang, W.; Serp, P.; Kalck, P. and Faria, J.L. 2005. "Visible light photodegradation of phenol on MWNT-TiO_2 composite catalysts prepared by a modified sol-gel method", Journal of Molecular Catalyst A: Chemical. 235 (2005), 194-199.

Wang, H.; Wang, H.L.; Jiang, W.F. and Li, Z.Q. 2009. "Photocatalytic degradation of 2,4-dinitrophenol (DNP) by multi-walled carbon nanotubes (MWCNTs)/TiO_2 composite in aqueous solution under solar irradiation", Water Research. 43 (2009), 204-210.

Weng, W.; Ma, M.; Du, P.; Zhao, G.; Shen, G.; Wang, J. and Han, G. 2005. "Superhydrophilic Fe doped titanium dioxide thin films prepared by a spray pyrolysis deposition", Surface & Coatings Technology. 198 (2005), 340-344.

Wu, J.C.S. and Chen, C.H. 2004. "A visible-light response vanadium-doped titania nanocatalyst by sol-gel method", Journal of Photochemistry and Photobiology A: Chemistry. 163(2004), 509-515.

Xu, N.; Shi, Z.; Fan, Y.; Dong, J.; Shi, J. and H U, M. Z. C. 1999. "Effects of particle size of TiO_2 on photocatalytic degradation of methylene blue in aqueous suspension", Industry and Engineering Chemistry Research. 38 (1999), 373-379.

Yang, S.; Liu, Y.; Guo, Y.; Zhao, J.; Xu, H. and Wang, Z. 2002. "Preparation of rutile titania nanocrystals by liquid method at room temperature", Materials Chemistry and Physics. 9430 (2002), 1-6.

Yang, J.H.; Han, Y.S. and Choy,J.H. 2006. "TiO_2 thin-films on polymer substrates and their photocatalytic activity", Thin Solid Films. 495 (2006), 266-271.

Yang, G.; Jiang, Z.; Shi, H.; Jones, M.O.; Xiao, T.; Edwards, P.P. and Yan, Z. 2010. "Study on the photocatalysis of F–S co-doped TiO_2 prepared using solvothermal method", Applied Catalysis B: Environmental. 96 (2010), 458-465.

Yanqing, Z.; Erwel, S.; Zhinzhan, C.; Wenjun, L. and Xingfang, H. 2001. "Influence of solution concentration on the hydrothermal preparation of titania crystallines", Journal of Material Chemistry. 11 (2001), 1547-1551.

Yeang, H.Y.; Arif, S.A.M.; Yusof, F. and Sunderasan, E. 2002. "Allergenic proteins of natural rubber latex", Methods. 27 (2002), 32-45.

Yogi, C.; Kojima, K.; Wada, N.; Tokumoto, H.; Takai, T.; Mizoguchi, T. and Tamiaki, H. 2008. "Photocatalytic degradation of methylene blue by TiO_2 film And Au particles-TiO_2 composite film", Thin Solid Films. 516 (2008), 5881-5884.

Yu, J.; Yu, H.; Ao, C.H.; Lee, S.C.; Yu, J.C. and Ho, W. 2005. "Preparation, characterization and photocatalytic activity of in situ Fe-doped TiO_2 thin films", Thin Solid Films. 496 (2006), 273-280.

Yu, Z. and Chuang, S.S.C. 2008. "The effect of Pt on the photocatalytic degradation Path way of methylene blue over TiO_2 under ambient conditions", Applied Catalysis B: Environmental. 83 (2008), 277-285.

Yuan, R.; Guan, R. and Shen, W. 2005. "Photocatalytic degradation of methylene blue by a combination of TiO_2 and activated carbon fibers", Journal of Colloid and Interface Science. 282 (2005), 87-91.

Yuan, Z.; Zhang, J.; Li, B. and Li, J. 2007. "Effect of metal ion dopants on Electrochemical properties of anatase TiO_2 films synthesized by a modified sol-gel method", Thin Solid Films. 515 (2007), 7091-7095.

Zainal, Z.; Hui, L.H.; Hussein, M.Z. and Ramli, I. 2005. "Removal of dyes using immobilized titanium dioxide illuminated by fluorescent lamps. Journal of Hazardous Materials. B125 (2005), 113-120.

Zhang, X.; Zhang, F. and Chan K.Y. 2006. "The synthesis of Pt-modified titanium dioxide thin films by microemulsion templating, their characterization and visible-light photocatalytic properties", Materials Chemistry and Physics. 97 (2006), 384-389.

APPENDICES

RESEARCH ARTICLE

ScienceAsia 36 (2010): **52–58**

doi: 10.2306/scienceasia1513-1874.2010.36.052

Degradation of indigo carmine by rubber sheet impregnated with TiO_2 particles

Chaval Sriwong[a], **Sumpun Wongnawa**[a,*], **Orasa Patarapaiboolchai**[b]

[a] Department of Chemistry and Centre for Innovation in Chemistry, Faculty of Science, Prince of Songkla University, Hat Yai, Songkhla 90112, Thailand

[b] Polymer Science Program, Faculty of Science, Prince of Songkla University, Hat Yai, Songkhla 90112, Thailand

*Corresponding author, e-mail: sumpun.w@psu.ac.th

Received 9 Aug 2009
Accepted 24 Feb 2010

ABSTRACT: The photocatalytic degradation of indigo carmine was investigated by using rubber sheet impregnated with titanium dioxide particles. The characteristics of the impregnated sheet were studied using scanning electron microscopy and X-ray diffraction. The degradation was monitored by measuring the change of dye concentration as a function of irradiation time under UV light. The anatase impregnated sheet showed higher degradation efficiency than the P25 impregnated sheet. The effects of solution pH, dye initial concentration, and intensity of UV light on the photodegradation were investigated. Kinetics of photocatalytic degradation was of a first-order reaction. The used TiO_2-impregnated sheets can be recovered and reused with no decline in the photodegradation efficiency.

KEYWORDS: immobilized titanium dioxide, titanium dioxide photocatalyst, photocatalytic degradation, dye degradation

INTRODUCTION

Applications of semiconducting catalysts for environmental protection and remediation have attracted much attention in recent years. Heterogeneous photocatalysis using semiconducting materials is efficient and broadly used for environmental applications such as air purification, water disinfection, hazardous water remediation, and water purification[1–4]. This process is based on the incidence of radiation of an adequate wavelength on semiconducting materials to shift an electron from the valence band to the conduction band thus producing an electron-hole pair that is responsible for the start of the degradation catalysis of organic compounds. Among the semiconducting materials, one of the most used is titanium dioxide due to its commercial availability, low cost, chemical stability, photostability, and high efficiency in photocatalytic processes[5–7]. A disadvantage of the use of TiO_2 in powder form as a photocatalyst in large scale processes is the difficulty in separating it from the reaction system, precluding its recovery and reuse. The loose photocatalyst powder can also cause human health problems[8,9]. In order to avoid the use of photocatalyst powders, efforts have been made to coat TiO_2 thin films on various substrates such as glass[10–12], plastics[13], and polymers[14]. However, these substrates are expensive and have some limitations in applications. Photocatalyst TiO_2 thin films have been prepared by various techniques such as chemical vapour deposition[15], spray pyrolysis deposition[16], flame synthesis[17], sol-gel dip coating[18–20]. However, these methods also have some disadvantages for industrial applications. Chemical vapour deposition, spray pyrolysis deposition, and flame synthesis all require costly apparatus and complex procedures for the deposition of TiO_2 films. The sol-gel dip coating method needs repeated coating to produce a thick film and a high annealing temperature for crystallization. Furthermore, the heating process precludes the fabrication of TiO_2 films on substrates with low thermal stability such as plastics and polymers[14]. To overcome these obstacles, simple, less expensive, and more effective methods to prepare immobilized TiO_2 powder on a certain type of substrate are under investigation worldwide.

In our previous work[21], we reported the preparation of rubber sheet impregnated by commercial TiO_2 powders and their photocatalytic activity in the degradation of methylene blue (MB), a cationic dye usually used as a model to test for photocatalytic activity. In the present work, the scope was extended to cover indigo carmine (IC) which is an anionic dye usually used in the textile, food, and cosmetics industries. Indigo carmine is regarded as a highly toxic dye that may lead to tumours at the site of application, cause

skin or eye irritation, and permanent injury to cornea and conjunctiva, and can be fatal if consumed. The toxicity tests of IC dye revealed long-term toxicity in mice and short-term toxicity in pigs[22–24].

In this report, the degradation of IC dye was investigated by using rubber sheets impregnated with commercial TiO_2 particles. The effect of various parameters such as solution pH, dye initial concentration, and intensity of UV light were studied. After being used, the sheet remained clean and ready for reuse. The sheet was tested for reuse up to ten times with no decrease in degradation efficiency.

MATERIAL AND METHODS

Materials

Titanium dioxide P25 was a gift donated from Degussa AG (Frankfurt), anatase was purchased from Carlo Erba (AR grade). Indigo carmine ($C_{16}H_8N_2Na_2O_8S_2$, MW = 466.36 g/mol) was purchased from Fluka and rubber latex (60% HA) from Chana Latex Co. Ltd. (Songkhla, Thailand). The dye and latex were used as received.

Preparation and characterization of TiO_2-impregnated rubber sheet

The preparation of both impregnated anatase sheet (Im-Anatase) and impregnated Degussa P25 sheet (Im-P25) has been described previously[21]. The surface morphology of TiO_2-impregnated rubber sheets were characterized by scanning electron microscopy (SEM) (JEOL-JSM 5800LV, Japan) while X-ray diffraction (XRD) (X′ Pert MPD, Ni filtered Cu Kα radiation, Phillips) was used for the identification of crystalline phase of TiO_2 particles embedded in the sheets.

Photocatalytic study

The same experimental set up was employed for the photocatalytic studies as described previously[21]. The concentration of IC dye solution was 2.5×10^{-5} M. Five fluorescent blacklight tubes served as the source of UV light. These blacklight tubes were turned on 1, 3, or 5 tubes at a time to provide, respectively, low, medium, or high intensity of UV light. In most of the experiments, high intensity was used to shorten the experiment times. The concentration of IC dye after photodegradation was analysed by using a UV-Vis spectrophotometer (Specord S100, Analytik Jena) by measuring the change in absorbance at 610 nm. The control experiment was carried out by irradiating an aqueous solution of IC dye and replacing the TiO_2-impregnated rubber sheet with a pristine rubber sheet where no observable loss of dye was observed.

RESULTS AND DISCUSSION

Characterization of TiO_2-impregnated rubber sheet

The impregnated rubber sheet was prepared by mixing TiO_2 powder with latex and a certain amount of distilled water. Then, the mixture was poured into the Petri-dish mould. When the latex sheet solidified, it was taken out of the mould and flipped upside down before being used so that the bottom surface would face upward and contact with the dye solution. This flipped-up bottom surface was characterized. The SEM images of the surface and cross-section of Im-Anatase and Im-P25 sheets are shown in Fig. 1. The surface morphology of Im-Anatase sheet showed evenly and well-spread anatase powder with higher surface roughness than that of the Im-P25 sheet. This results from the physical difference of anatase and P25 powders. The former has a higher agglomeration and density than P25, which exists as light and fluffy-like particulates. When added to the latex, the anatase particles sank to the bottom faster and accumulated close to the bottom surface. The P25 particles, however, sank to the bottom slower so the number of particles to reach and accumulate at the bottom surface was smaller than in the case of anatase. This is clearly shown in Fig. 1a (right) where a distinct layer of anatase particles can be seen at the surface of the sheet (arrow) while that in P25 is less visible (Fig. 1b, right). The rough surface of Im-Anatase sheet (Fig. 1a, left) resembles the cracks running through a sun-dried mud surface. With these cracks, the anatase powders that gather near the surface will have more chance to contact the dye molecules than those of the Im-P25 which are buried rather deep under the smoother surface of the rubber. This surface difference is responsible for a better performance of Im-Anatase sheet over Im-P25 sheet in the subsequent dye degradation studies.

The X-ray diffraction patterns of TiO_2 in powder form and in the impregnated rubber sheets are illustrated in Fig. 2. The anatase peaks appear at 2θ = 25.50° (101) and 48.0° while those of rutile appear at 2θ = 27.50° (110) and 54.5°. Well crystallized anatase can be observed in the Im-Anatase sheet indicating successful impregnation of anatase powder into the rubber sheet (compare Figs. 2a and 2c). The same result is seen for Im-P25 sheet as shown in Fig. 2d (compare with Fig. 2b). The XRD of pristine rubber sheet has been shown previously to have only a large broad scattering peak near 2θ = 19°[21] due to the fact that the rubber matrix is composed of low atomic number (low Z) elements. This broad scattering peak

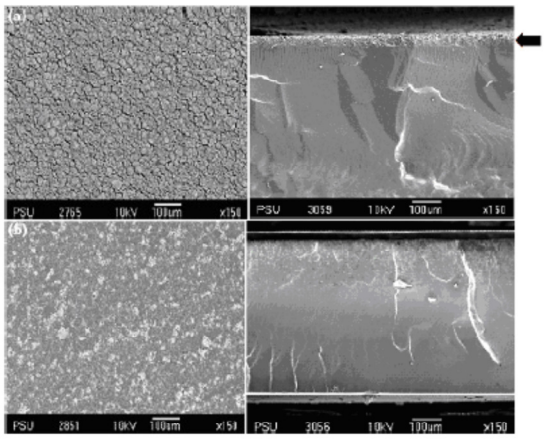

Fig. 1 SEM images of surface (left) and cross-section (right) of (a) Im-Anatase sheet and (b) Im-P25 sheet.

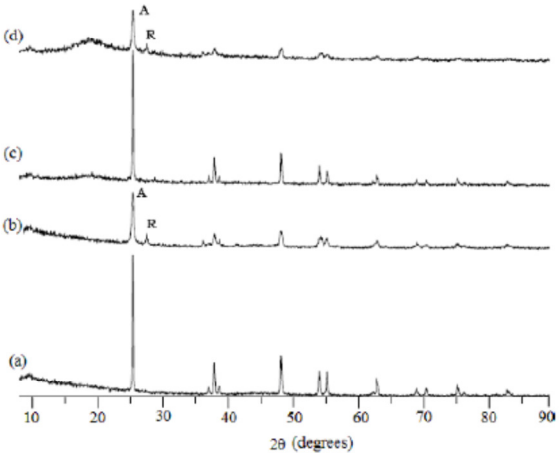

Fig. 2 XRD patterns of (a) commercial anatase powder, (b) Degussa P25 powder, (c) Im-Anatase sheet, and (d) Im-P25 sheet. A: anatase phase; R: rutile phase.

also appears in the patterns of both impregnated sheets but with smaller intensity due to inclusion of TiO_2 particles in the impregnated sheets. The surface of Im-Anatase sheet has a higher content of TiO_2 particles than that of Im-P25 causing the average Z-value of matrix in the former to increase. This results in lower X-ray scattering in the case of Im-Anatase.

Photocatalytic degradation of indigo carmine (IC) by TiO_2-impregnated rubber sheet

The photodegradation efficiencies of IC by Im-Anatase sheet and Im-P25 sheet under UV light irradiation are shown in Fig. 3. The Im-Anatase sheet has higher surface roughness than the Im-P25 sheet (Fig. 1). The cracked surface of Im-Anatase sheet

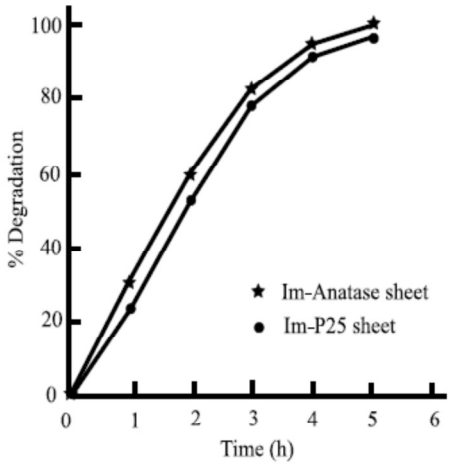

Fig. 3 The efficiencies of photocatalytic degradation of IC dye by impregnated rubber sheets under UV irradiation.

has grooves running all over the surface. These grooves give the sheet at least two advantages: (i) after falling into the groove, the dye molecules cannot easily escape from the surface, and (ii) along the groove surface, the oxygen atoms have a better chance to protrude from the latex texture and their negative charges can attract or repel charges of the dye molecular fragment (Fig. 4). The smoother surface of Im-P25 with TiO_2 particles embedded deeper in the surface will have weaker electrostatic forces to interact with the dye molecules. Therefore, the higher surface roughness can help to gather more dye molecules onto the sheet surface and more photocatalytic reaction can take place. This is reflected by the slightly better performance of Im-Anatase over Im-P25 as shown in Fig. 3.

The kinetics of the degradation was studied and the data were tested with the first-order kinetic expression[2,28],

$$\ln[C_t] = \ln[C_0] - k_{\mathrm{app}}t,$$

where $[C_0]$ is the initial concentration of dye, $[C_t]$ is the concentration at time t, and k_{app} is the apparent rate constant. The straight lines obtained when $\ln[C_t]$ was plotted against t confirmed the first-order kinetics of dye degradation. The rate constants for IC dye degradation were found to be 0.717 ± 0.004 h^{-1} and 0.595 ± 0.004 h^{-1} for the Im-Anatase and Im-P25 sheets, respectively ($n = 3$).

Effect of pH

All of the experiments were carried out at the natural pH of IC dye solution which is 6.4. However, in real life situations the effluents from factories may cover

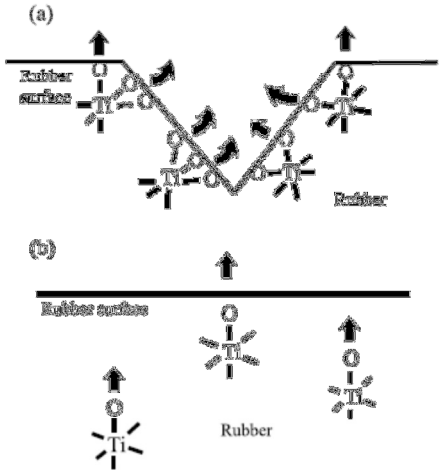

Fig. 4 Effect of rough and smooth surfaces: (a) Im-Anatase (b) Im-P25. Arrows represent electrostatic forces from the negatively charged oxygen atoms.

a wide range of pHs. To assess the efficiencies of degradation by the TiO_2 impregnated rubber sheet, solutions of several pH values (3, 5, 6.4, and 8) were investigated. Both Im-Anatase and Im-P25 showed parallel behaviour (Figs. 5a and 5b) with the efficiencies decreasing as the pH values increased in the order: (pH) $3 > 5 > 6.4 > 8$.

Generally, for a charged surface containing TiO_2 particles, a significant dependence of the photocatalytic efficiency on the pH value is observed, since the overall surface charge and hence the adsorptive properties of TiO_2 particles depend strongly on the solution pH[29–31]. It is known that the metal oxide particles in water exhibit amphoteric behaviour and readily reacts with dye by a mechanism which can be described by the following chemical equilibria[29–31]:

$$\equiv TiOH + H^+ \rightleftharpoons \equiv TiOH_2^+ \qquad (1)$$

$$\equiv TiOH + OH^- \rightleftharpoons \equiv TiO^- + H_2O. \qquad (2)$$

The charge of TiO_2 depends on the solution pH. The pH at the point of zero charge (pH_{PZC}) for TiO_2 has been reported to be in the range 6.25–6.90[32]. Thus, the TiO_2 surface is positively charged in acidic media ($pH < pH_{PZC}$), and negatively charged under alkaline conditions ($pH > pH_{PZC}$). This argument, valid for the powder form in contact with solution, should also be applicable when the powder is in a rubber sheet. The effect, however, should be less pronounced for the impregnated sheet than in the powder form. In the case of the impregnated sheet, the TiO_2 particles closer to

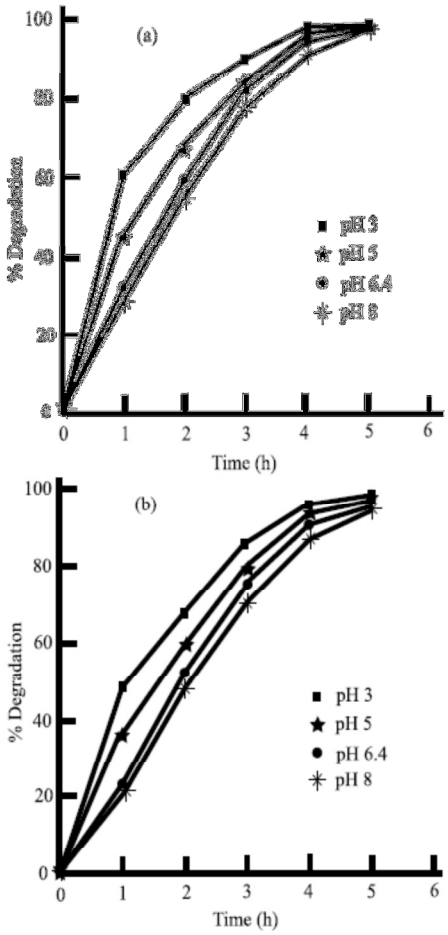

Fig. 5 Effect of pH on the photodegradation efficiency of IC dye by (a) Im-Anatase sheet and (b) Im-P25 sheet.

the surface may have part of oxygen atoms protrude from the rubber surface (Fig. 4). (This assertion is justified by the fact that the photocatalytic reaction did indeed take place but with less efficiency than in the loose powder form.) Therefore, it is expected that at a pH below pH_{PZC}, the surface of impregnated sheet acquires a positive charge, indicated by (1), and hence attracts the negatively charged IC dye skeleton resulting in a large number of dye molecules being attracted (or adsorbed) onto the sheet surface. As the dye concentration at the surface increases the photodegradation activity also increases, as observed at pH 3. At a pH above pH_{PZC}, electrostatic repulsion between the negative charge at the surface of impregnated sheet, as shown in (2), and anionic dye skeleton retards the accumulation of dye molecules at the surface resulting in decrease of the photodegradation activity.

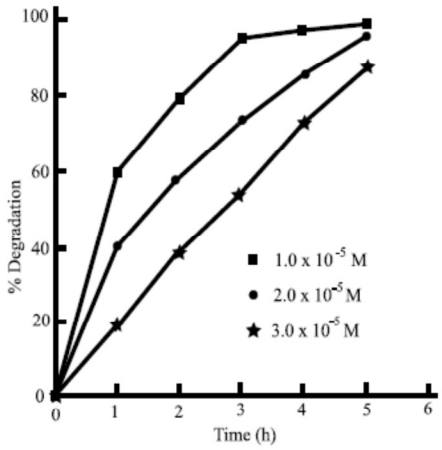

Fig. 6 Effect of IC dye initial concentration on the photocatalytic efficiency of Im-Anatase sheet.

Effect of dye initial concentration

The effects of the initial concentration of IC dye on the photocatalytic efficiency was investigated with concentrations 1.0×10^{-5} M, 2.0×10^{-5} M, and 3.0×10^{-5} M (Fig. 6). It was found that on increasing the dye concentration the degradation efficiencies of dye decreases. Hence, the photo-oxidation process will work faster at a low concentration of pollutants. These results are in agreement with previous reports[2,31,33] that photodegradation of textile dye Reactive Red 2, C.I. Acid Yellow 17, and Direct Yellow 12 decreased with increasing concentrations. At high concentrations of dye, the deeper coloured solution would be less transparent to UV light and the dye molecules may absorb a significant amount of UV light causing less light to reach the catalyst and thus reducing the $OH^{\bullet}$ radical formation. Since $OH^{\bullet}$ radicals are of prime importance in the attack of the dye molecules, lowering the amount $OH^{\bullet}$ radicals would cause the photodegradation efficiency to decrease[34].

Effect of UV light intensity

On increasing the light intensity, the degradation efficiency of dye increases. It has been reported that the photocatalytic reaction rate depends largely on the irradiation absorption of the photocatalyst leading to an increase in the degradation rate with increasing light intensity during photocatalytic degradation[31,33,35]. The high UV light intensity increases the photon influx entering the dye solution and consequently excites the TiO_2 particles in the sheet resulting in more $OH^{\bullet}$ radicals being formed at the surface of the film. As the reactive number of $OH^{\bullet}$ radicals attacking the dye molecules increases, the photodegradation efficiency also increases. The activity increases with increasing intensity of UV light.

Recyclability of the TiO_2-impregnated rubber sheets on the photocatalytic degradation of IC dye

Both types of sheet were tested for their recyclability up to 10 times. The sheets showed no sign of deterioration or decrease in performance. We thus anticipate that the sheets could be used much more than 10 times. One striking result was that the sheet surface remained rather clean after being used. As a result, the sheet surface need no cleaning between uses and so could be used immediately for the next cycle. The reason for this can be traced back to the repulsive force between the negative charge on the skeleton of the dye fragment and the oxygen atoms on the catalyst surface. This repulsion greatly diminishes the accumulation of dye fragments on the sheet surface.

The highest performance was only obtained after the third use and remained at that high efficiency until the tenth use (Fig. 7). This trend can be expected to continue even after the tenth use. The lower results of the first few uses may result from the fact that the rubber surface was covered with traces of impurities during the preparation and the impurities were destroyed during the first and the second uses by the photodegradation reaction together with IC dye molecules in the solution.

The recyclability of the impregnated rubber sheet should be attractive to the water treatment industry as it helps keep the operational cost low. The low cost of raw materials (photocatalyst powder and rubber latex) enables a one time investment which will last over a long period of uses.

Comparison between MB and IC degradation by TiO_2 impregnated rubber sheet

In another study we carried out (unpublished) the rate constants of MB degradation by TiO_2 impregnated rubber sheet were found to be 1.086 ± 0.002 h^{-1} for Im-Anatase and 0.764 ± 0.006 h^{-1} for Im-P25 sheets ($n = 3$). These figures indicate that the rubber sheets exhibit higher photocatalytic activities towards MB than IC dye. Our results agree with other studies which showed that MB degradation efficiency was higher than other dyes containing the $-SO_3^-$ group[30]. It has also been shown elsewhere that under similar conditions the rate of degradation of MB is faster than that for IC[25,36].

When the rubber sheet was used with MB, a significant amount of dye adhered to the sheet surface. However, the surface could be cleaned easily and

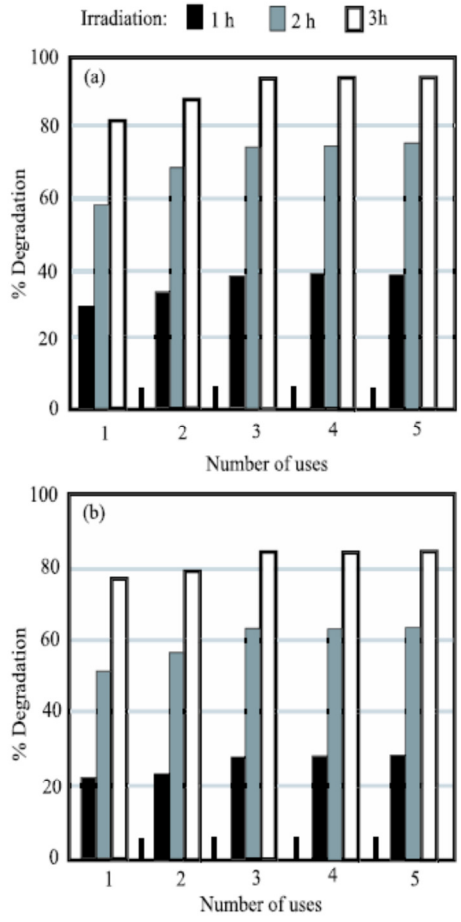

Fig. 7 The efficiencies of IC dye degradation by (a) Im-Anatase sheet and (b) Im-P25 sheet after repeated use under UV light irradiation for 1–3 h.

reused[21]. The number times the sheet could be reused for MB dye appeared to be less than for IC dye.

The trend on pH for MB was the opposite of the IC behaviour, i.e., the efficiency for MB degradation increased with increasing pH. These differences can be explained based on the charge type on the dye fragment. MB is a cationic dye whereas IC is anionic. The positive charge of the MB fragment attracts the negatively charged oxygen atom of TiO_2 impregnated in the rubber surface promoting accumulation of dye molecules onto the surface. As more molecules flock together on the catalyst surface, a higher rate of degradation should result. In the IC case, the negative charge on the dye skeleton repels with the impregnated TiO_2 in the rubber surface discouraging accumulation of dye molecules on the sheet surface. As a result the surface remains clean, but the degradation rate was less than the MB case.

Acknowledgements: Financial support from the Thailand Research Fund through the Royal Golden Jubilee PhD Programme (PHD/0003/2550), the Centre for Innovation in Chemistry (PERCH-CIC), Commission on Higher Education, Ministry of Education, and the Graduate School of Prince of Songkla University are gratefully acknowledged.

REFERENCES

1. Mills A, Elliott N, Parkin IP, O'Neill SA, Clark RJ (2002) Novel TiO_2 CVD films for semiconductor photocatalysis. *J Photochem Photobiol A* **151**, 171–9.
2. Senthilkumaar S, Porkodi K (2005) Heterogeneous photocatalytic decomposition of Crystal Violet in UV-illuminated sol-gel derived nanocrystalline TiO_2 suspension. *J Colloid Interface Sci* **288**, 184–9.
3. Yu J, Yu H, Ao CH, Lee SE, Yu JC, Ho W (2006) Preparation, characterization and photocatalytic activity of in situ Fe-doped TiO_2 thin films. *Thin Solid Films* **46**, 273–80.
4. Parida KM, Sahu N, Biswal NR, Naik B, Pradhan AC (2008) Preparation, characterization, and photocatalytic activity of sulfate-modified titania for degradation of methyl orange under visible light. *J Colloid Interface Sci* **318**, 231–7.
5. Nakaoka Y, Nasaka Y (1997) ESR investigation into the effect of heat treatment and crystal structure on radicals produced over irradiated TiO_2 powder. *J Photochem Photobiol A* **110**, 299–305.
6. Nagaveni K, Sivalingam G, Heged MS (2004) Solar photocatalytic degradation of dye: high activity combustion synthesized nano TiO_2. *Appl Catal B* **48**, 83–93.
7. Yuan Z, Zhang J, Li B, Li J (2007) Effect of metal ion dopants on photochemical properties of anatase TiO_2 film synthesized by a modified sol-gel method. *Thin Solid Films* **515**, 7091–5.
8. Yuan R, Guan R, Shen W, Zheng J (2005) Photocatalytic degradation of methylene blue by a combination of TiO_2 and activated carbon fibers. *J Colloid Interface Sci* **282**, 87–91.
9. Habibi MH, Talebian N, Choi JH (2007) The effect of annealing on photocatalytic properties of nanostructured titanium dioxide thin films. *Dyes Pigments* **73**, 103–10.
10. Wang T, Wang H, Xu P, Zhao X, Liu Y, Chao S (1998) The effect of properties of semiconductor oxide thin films on photocatalytic decomposition of dying waste water. *Thin Solid Films* **334**, 103–8.
11. Losito I, Amorisco A, Palmisano F, Zambonin PG (2005) X-ray photoelectron spectroscopy characterization of composite TiO_2-poly (vinylidenefluoride) film synthesized for applications in pesticide photocatalytic degradation. *Appl Surf Sci* **240**, 180–8.
12. Sankapal SB, Steiner MC, Ennaoui A (2005) Synthesis and characterization of anatase TiO_2 thin films. *Appl Surf Sci* **239**, 165–70.

13. Kwon CH, Shin H, Kim JH, Choi WS, Yoon KH (2004) Degradation of methylene blue via photocatalysis of titanium dioxide. *Mater Chem Phys* **86**, 78–82.
14. Yang H, Han YS, Choy JH (2006) TiO_2 thin-films on polymer substrates and their photocatalytic activity. *Thin Solid Films* **495**, 266–71.
15. Ding Z,Hu X, Yue PY, Lu PQ, Greenfield PE (2001) Synthesis of TiO_2 supportedon porous solids by chemical vapor deposition. *Catal Today* **68**, 173–82.
16. Weng W, Ma M, Du P, Zhao G, Shen G,Wang J,Han G (2005) superhydrophilic Fe doped titanium dioxide thin films prepared by a spay pyrolysis deposition. *Surf Coating Tech* **198**, 340–4.
17. Pratsinis SE (1996) Flame synthesis of nanosize particle: precise control of particle size. *J Aerosol Sci* **27**, S153–4.
18. Sen S, Mahanty S, Roy S, Heintz O, Bourgeois S, Chaumont D (2005) Investigation on sol-gel synthesized Ag-doped TiO_2 cermet thin films. *Thin Solid Films* **474**, 245–9.
19. Ge L, Xu M, Sun M, Fang H (2006) Fabrication and characterization of nano TiO_2 thin films at low temperature. *Mater Res Bull* **41**, 1596–603.
20. Yogi C, Kojima K, Wada N, Tokumoto H, Takai T, Mizoguchi T, Tamiaki H (2008) Photocatalytic degradation of methylene blue by TiO_2 film and Au-particles composite film. *Thin Solid Films* **519**, 5881–4.
21. Sriwong C, Wongnawa S, Patarapaiboolchai O (2008) Photocatalytic activity of rubber sheet impregnated with TiO_2 particles and its recyclability. *Catal Comm* **9**, 213–8.
22. Othman I, Mohamed RM, Ibrahim IA, Mohamed MM (2006) Synthesis and modification of ZSM-5 with manganese and lanthanum and their effects on decolorization of indigo carmine dye. *Appl Catal A* **299**, 95–102.
23. Mittal A, Mittal J, Kurup L (2006) Batch and bulk removal of hazardous dye, indigo carmine from wastewater through adsorption. *J Hazard Mater* **137**, 591–602.
24. Othman I, Mohamed RM, Ibrahem FM (2007) Study of photocatalytic oxidation of indigo carmine dye on Mn-supported TiO_2. *J Photochem Photobiol A* **189**, 80–5.
25. Houas A, Lachheb H, Ksibi M, Elaloui E, Guillard C, Herrmann JM (2001) Photocatalytic degradation pathway of methylene blue in water. *Appl Catal B* **31**, 145–57.
26. Anpo M, Takeuchi M (2003) The design and development of highly reactive titanium oxide photocatalysts operating under visible light irradiation. *J Catal* **216**, 505–16.
27. Randorn C, Wongnawa S, Boonsin P (2004) Bleaching of methylene blue by hydrated titanium dioxide. *Sci Asia* **30**, 149–56.
28. Silva CG, Wong W, Faria JL (2006) Photocatalytic and photochemical degradation of mono-, di- and tri-azo dye in aqueous solution by UV irradiation. *J Photochem Photobiol A* **181**, 314–24.
29. Kiriakidou F, Kondarides DI, Verykios XE (1999) The effect of operational parameters and TiO_2 doping on the photocatalytic degradation of azo-dyes. *Catal Today* **54**, 119–30.
30. Lachheb H, Puzenat E, Houas A, Ksibi M, Elaloui E, Guillard C, Herrmann JM (2002) Photocatalytic degradation of various types of dyes (Alizarin S, Crocein Orange G, Methyl red, Congo red, Methylene blue) in water by UV-irradiated titania. *Appl Catal B* **39**, 75–90.
31. Toor AP, Verma A, Jotshi CK, Bajpai PK, Singh V (2006) Photocatalytic degradation of Direct Yellow 12 dye using UV/TiO_2 in a shallow pound slurry reactor. *Dyes Pigments* **68**, 53–60.
32. Sun J, Qiao L, Sun S, Wang G (2008) Photocatalytic degradation of Orange G on nitrogen-doped TiO_2 catalyst under visible light and sunlight irradiation. *J Hazard Mater* **155**, 312–9.
33. Liu CC, Hsieh YH, Lai PF, Li CH, Kao CL (2006) Photodegradation treatment of azo dye wastewater by UV/TiO_2 process. *Dyes Pigments* **68**, 191–5.
34. Konstantinou IK, Albanis TA (2004) TiO_2-assisted photocatalytic degradation of azo dye in aqueous solution: kinetic and mechanistic investigations: A review. *Appl Catal B* **49**, 1–14.
35. Jun W, Gang Z, Zhaohong Z, Xiangdong Z, Guan Z, Teng M, Yuefeng J, Peng Z (2007) Investigation on degradation of azo fuchsine dye using visible light in the presence of heat-treated anatase TiO_2 powder. *Dyes Pigments* **75**, 335–43.
36. Vautier M, Guillard C, Herrmann JM (2001) Photocatalytic degradation of dyes in water: case study of indigo and of indigo carmine. *J Catal* **201**, 46–59.

Available online at www.sciencedirect.com
ScienceDirect
Journal of Environmental Sciences 2012, 24(3) 464–472
JOURNAL OF ENVIRONMENTAL SCIENCES
ISSN 1001-0742
CN 11-2629/X
www.jesc.ac.cn

Rubber sheet strewn with TiO_2 particles: Photocatalytic activity and recyclability

Chaval Sriwong[1], Sumpun Wongnawa[1,*], Orasa Patarapaiboolchai[2]

1. Department of Chemistry and Center for Innovation in Chemistry, Faculty of Science, Prince of Songkla University, Hat Yai, Songkhla 90112, Thailand
2. Department of Materials Science and Technology, Faculty of Science, Prince of Songkla University, Hat Yai, Songkhla 90112, Thailand

Received 24 February 2011; revised 12 May 2011; accepted 12 June 2011

Abstract

A new method for the preparation of rubber sheet strewn with titanium dioxide particles (TiO_2-strewn sheet) is presented. This simple and low cost method is based on the use of TiO_2 powder (Degussa P25) being strewn onto the sheet made from rubber latex (60% HA) through a steel sieve. The characteristic of the TiO_2-strewn sheet was studied by using scanning electron microscopy/energy dispersive X-ray spectrometer (SEM/EDS) and X-ray diffractometer (XRD) techniques. The photocatalytic activity of TiO_2-strewn rubber sheet was evaluated using Indigo Carmine (IC) dye as a model for organic dye pollutant in water. The results showed that the TiO_2-strewn sheet could degrade IC dye solution under UV light irradiation. The effects of pH, initial concentration, and the intensity of UV light on the photodegradation were also investigated. Kinetics of the photocatalytic degradation was of the first-order reaction. The used TiO_2-strewn sheet can be recovered and reused. The recycling uses did not require any cleaning between successive uses and no decline in the photodegradation efficiency was observed compared with freshly prepared TiO_2-strewn sheet.

Key words: immobilized titanium dioxide; TiO_2 rubber composite; dye degradation; photocatalytic degradation; indigo carmine

DOI: 10.1016/S1001-0742(11)60794-8

Introduction

Over the past decade, the application of semiconductor photocatalysts to treat environmental contaminants has overwhelmingly prevailed as another alternative for the pollution treatment technology. Amongst the various semiconductor photocatalysts, TiO_2 has been considered as one of the most promising photocatalysts due to its stability, non-toxicity, low cost, and high efficiency in the photocatalysis process (Nagaveni et al., 2004; Zhu et al., 2004; Senthikumaar and Porkodi, 2005; Yuan et al., 2007; Parida et al., 2008; Wu and Cho, 2008). However, a disadvantage of the use of TiO_2 powder form as a photocatalyst in large scale processes is the difficulty in separating it from reaction systems, which precludes the recovery and reuse of the catalyst (Ge et al., 2006; Zhang et al., 2006; Choi et al., 2007; Ryu et al., 2008; Shi et al., 2008). The loose powder form of photocatalyst can cause serious human health problems (Yuan et al., 2005; Habibi et al., 2007). To avoid the use of photocatalyst in powder form, several efforts have been made to coat TiO_2 as thin films on various substrates (Wang et al., 1998; Kwon et al., 2004; Lositi et al., 2005; Sankapal et al., 2005; Yang et al., 2006), as well as employing several techniques such as chemical vapor deposition (CVD) (Ding et al., 2001), spray pyrolysis deposition (Weng et al., 2005), flame synthesis (Partsinis, 1996), sol-gel dip coating, (Sen et al., 2005; Yogi et al., 2008). However, the above methods have some disadvantages for industrial applications. The chemical vapor deposition, spray pyrolysis deposition, and flame synthesis methods require special and rather expensive apparatus and complex procedures for the deposition of TiO_2 film, while the sol-gel dip coating method needs repeated coatings to get a thick film and requires a high annealing temperature for crystallization. Furthermore, the heating process precludes the fabrication of TiO_2 films on substrates with low thermal stability such as plastics and polymers (Yang et al., 2006). An alternative to immobilize TiO_2 photocatalyst on organic substrates is to immobilize it along with magnetic materials. This way, TiO_2 photocatalyst can be recovered by applying magnetic field to collect photocatalyst particles from the used slurry. Among the first magnetic materials in this application were Fe_3O_4 and γ-Fe_2O_3 (Beydoun et al., 2000, 2001; Beydoun and Amal, 2002; Chen et al., 2001; Gao et al., 2003). Recently, $NiFe_2O_4$, a superparamagnetic material, was used with good results (Xu et al., 2008). All these methods have not yet been finalized and are still under investigation presently. Industrial application still awaits the most suitable immobilized photocatalyst. Therefore, a simple, less expensive, and more effective method for the

* Corresponding author. E-mail: sumpun.w@psu.ac.th

preparation of immobilized TiO_2 powder onto a substrate was investigated in our laboratory.

Recently our group reported the efficiency of the titania rubber sheet prepared from the method of embedding TiO_2 particles in rubber sheets (Sriwong et al., 2008, 2010) but that was still inferior to the sheet prepared by the novel method to be reported in this article. The difference can be traced to the fact that, in the new method, TiO_2 particles externally adhered to the surface of the sheet and were only covered with very thin clear film of latex while with the previous method TiO_2 particles were embedded within the rubber matrix. In comparing the two methods, the TiO_2 particles in the new method had a better contact with dye molecules in the solution and, hence, the higher degradation efficiency *(vide infra)*.

In this study, the TiO_2-strewn rubber sheet was prepared by strewing TiO_2 powder (Degussa P25) onto the sheet of rubber latex (60% HA). The efficiency of Indigo Carmine (IC) degradation by this sheet under UV light was evaluated. The effects of various parameters such as pH, initial concentration, and the intensity of UV light were also studied. Indigo Carmine was used as a model dye in this research due to the fact that it is usually used in the textile industry for dyeing of cloths (blue jeans) and other blue denim, in the food industry (typical products includes milk dessert, sweets, biscuits), and in the cosmetics industry. Indigo Carmine has been regarded as a highly toxic indigoid class of dye. It can cause skin or eye irritation and permanent injury to the cornea and conjunctiva. Moreover, IC dye can be fatal if consumed as it is carcinogenic in nature and can lead to reproduction, developmental of neuron, and acute toxicity (Mittal et al., 2006; Othman et al., 2006, 2007; Barka et al., 2008). The structure of IC dye molecule is a sodium salt which the parent fragment bears negative charges as illustrated in Fig. 1. In addition, the reaction kinetics and recycling uses of the TiO_2-strewn rubber sheet on the photodegradation for IC dye solution were presented.

1 Materials and methods

1.1 Chemicals and equipments

Rubber latex (60% HA, Chana Latex Co., Ltd., Thailand), Indigo Carmine dye (Fluka, USA), and titanium dioxide (Degussa P25, Degussa AG, Germany) were used. The surface morphologies of rubber sheets were characterized by using scanning electron microscopy (SEM) (JSM 5800LV, JEOL, Japan). The crystalline phases of TiO_2 were identified and confirmed by X-ray diffraction (XRD) technique (X'Pert MPD, Phillips, the Netherlands).

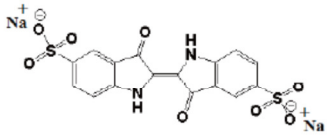

Fig. 1 Molecular structure of indigo carmine (IC) dye.

1.2 Preparation of TiO_2-strewn sheet

The TiO_2-strewn sheet was prepared from P25 TiO_2 powder and rubber latex. Rubber latex (10 mL) was poured into a Petri dish mould (3.5-inch diameter) and was left at room temperature about 2 hr for gelation to form. Then, 0.07 g of P25 TiO_2 was strewn onto the surface of the rubber sheet by using a 60-mesh sieve and allowed to dry at room temperature for 6 hr. Afterwards, the strewn rubber sheet was taken out from the mould and dried at 100°C for 1 hr. After cooling to room temperature, the sheet surface was lightly sprayed with distilled water to wash out some of the P25 TiO_2 particles that were left unbound until the strewn surface was free of loose particles. The sheet then was dried at 100°C for 10 min and ready for use, as shown in Fig. 2.

1.3 Photocatalytic study

In the photocatalytic studies, the TiO_2-strewn sheet was placed in a Petri dish (4-inch diameter) containing 60 mL of IC dye solution of known concentration. The solution was then stirred for 15 min in the dark to allow the adsorption-desorption equilibrium in the closed compartment for photoreaction. Subsequently, the irradiation was initiated using UV light (fluorescent blacklight 20 W, GE, USA) and magnetically stirred. At a given time interval (every 1 hr), 3 mL of dye solution was collected. The concentrations of IC dye after photodegradation were analyzed using a UV-Vis spectrophotometer (Specord S100, Analytik Jena, Germany). Controlled experiments were also performed to ensure the proper interpretation of results. The photoreaction compartment was fitted with five blacklight fluorescent tubes at fixed positions and evenly distributed in the compartment. These blacklight tubes can be turned on individually for one, three, or five tubes to provide low, medium, or high intensity of UV light. Normally, the highest intensity (five tubes) was employed to shorten the experimental time.

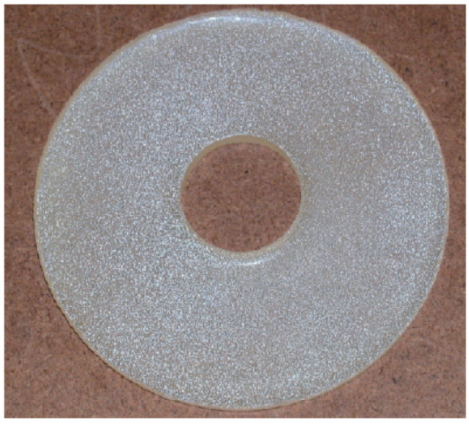

Fig. 2 Photograph of TiO_2-strewn sheet.

2 Results and discussion

2.1 Characterization of TiO_2-strewn sheet

The solidified rubber sheet served as a substrate upon which P25 TiO_2 powder was deposited. Drying at 100°C for 1 hr removed moisture from the rubber sheet to some extent. The heat drying process softened the sheet and caused subtle melting at the surface which helped increase the binding of TiO_2 particles to the sheet. On a close inspection with the naked eye one can see a colorless thin film covering the TiO_2 particles. The SEM images of the pristine rubber sheet and the TiO_2-strewn sheet are comparatively shown in Fig. 3. The surface morphology of the pristine rubber sheet is very smooth without any particles adhering to the surface (Fig. 3a). On the contrary, for the strewn sheet, TiO_2 particles can be seen spread evenly over the sheet surface causing high surface unevenness and roughness (Fig. 3b, c).

The energy dispersive X-ray spectrometer (EDS) analysis was carried out to determine the presence of elements in the TiO_2-strewn sheet. The EDS spectrum in Fig. 4a shows that only three elements were present in the sheet, i.e., carbon, oxygen, and titanium, as evidenced from their corresponding K lines. Figure 4b1 shows a SEM micrograph of an island of TiO_2 nanoparticles submerged in rubber.

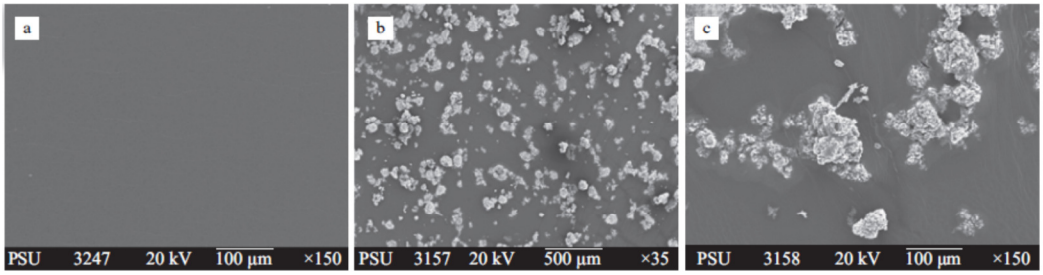

Fig. 3 SEM images of surface morphology of pristine rubber sheet (a), TiO_2-strewn sheet at 35× magnification (b), and TiO_2-strewn sheet at 150× magnification (c).

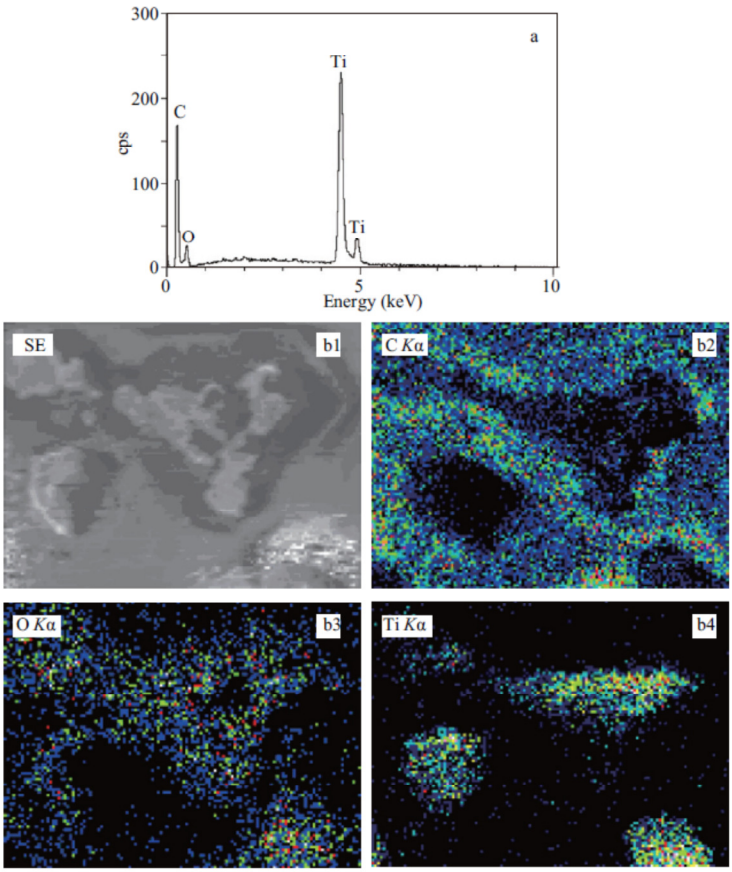

Fig. 4 EDS spectrum (a), and elemental mapping of TiO_2-strewn sheet (b).

This is supported by Fig. 4b2 which shows distribution of carbon atoms on the sheet surface surrounding the TiO_2 island (the island is seen as a black area in this figure). Oxygen and titanium atoms are seen in the area occupied by the TiO_2 island, Fig. 4b3 and b4, respectively. Titanium atoms are distributed over a narrower area within the TiO_2 island than the oxygen atoms distribution. In summary, the EDS data indicate that TiO_2 particles are located on the rubber surface with parts of the TiO_2 islands protruding from the surface (area of lighter color in Fig. 4b4).

The X-ray diffraction patterns of TiO_2 in the powder form and the immobilized form on a rubber sheet surface are illustrated in Fig. 5. The diffraction peaks of anatase and rutile phases are marked with 'A' and 'R', respectively. From Fig. 5, the well crystallized anatase and rutile forms were observed in the TiO_2-strewn sheet indicating successful addition of TiO_2 powder onto the rubber sheet surface (lines a and b in Fig. 5). A broad scattering peak ($2\theta = 19°$) of the X-ray beam by the low Z matrix of rubber also shows up in the patterns of TiO_2-strewn sheet. The surface of TiO_2-strewn sheet contains TiO_2 particles causing the average rubber matrix of the sheet to increase and, therefore, less scattering of the X-ray beam (Sriwong et al., 2008).

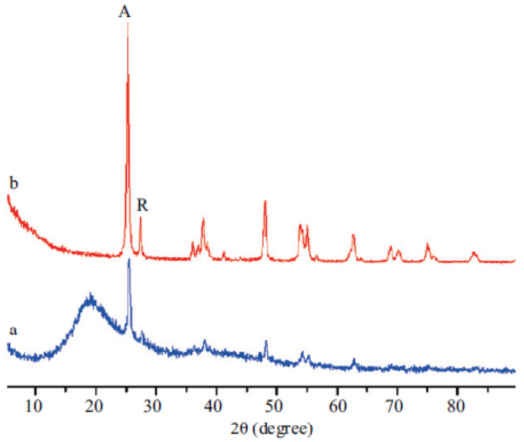

Fig. 5 XRD patterns of TiO_2-strewn sheet (line a), Degussa P25 powder (line b).

2.2 Photocatalytic degradation of IC by TiO_2-strewn sheet

2.2.1 Testing the photocatalytic activity of the TiO_2-strewn sheet

Results from the photocatalytic degradation of IC dye solution by the TiO_2-strewn sheet under UV light irradiation are shown in Fig. 6. The IC dye was degraded by the TiO_2-strewn sheet whereas in the case of pristine rubber sheet no observable loss of the dye could be detected. These results implied that the photocatalytic activity of the TiO_2-strewn sheet comes from the TiO_2 particles in the rubber sheet. As an example, the spectral changes of IC dye solution at 7.5×10^{-5} mol/L concentration degraded by TiO_2-strewn sheet under UV light as a function of irradiation time is shown in Fig. 7. Note that the intensity of the maximum peak at 610 nm decreases with increasing irradiation time due to the degradation of the IC dye molecules.

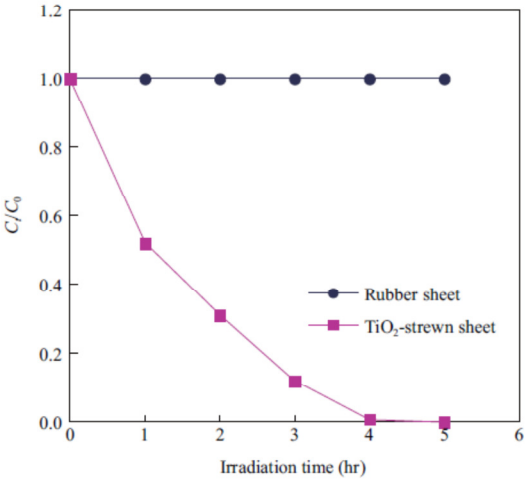

Fig. 6 Photodegradation of IC dye solution under UV light by pristine rubber sheet, and TiO_2-strewn sheet.

Since the P25 TiO_2 nanoparticles were on the sheet surface and contacted directly with dye molecules in the solution, the mechanism of dye degradation by P25 in this case was essentially the same as that which had been well documented as follows (Houas et al., 2001; Baiju et al., 2007; Khataee and Kasiri, 2010):

$$TiO_2 + h\nu \longrightarrow TiO_2 + e^- + h^+ \quad (1)$$

$$OH^- + h^+ \longrightarrow \cdot OH \text{ (in alkaline solution)} \quad (2)$$

$$H_2O + h^+ \longrightarrow \cdot OH + H^+ \text{(in neutral solution)} \quad (3)$$

$$O_2 + e^- \longrightarrow O_2^{\cdot -} \quad (4)$$

$$O_2^{\cdot -} + H^+ \longrightarrow {}^{\cdot}O_2H \quad (5)$$

$$2\,{}^{\cdot}O_2H \longrightarrow H_2O_2 + O_2 \quad (6)$$

$$H_2O_2 + e^- \longrightarrow \cdot OH + OH^- \quad (7)$$

$$\text{Dye} + \cdot OH \longrightarrow \text{Degradation products} \quad (8)$$

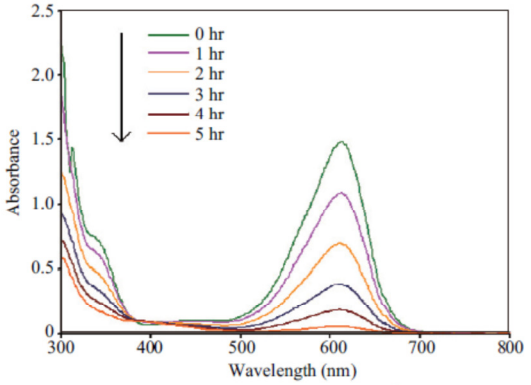

Fig. 7 Spectral change of IC dye solution (7.5×10^{-5} mol/L) degraded by TiO_2-strewn sheet under UV light as a function of irradiation time.

These reactions sequence can be put together as shown in Scheme 1 where the protruding TiO_2 surface is first irradiated with UV light causing the electron in the va-

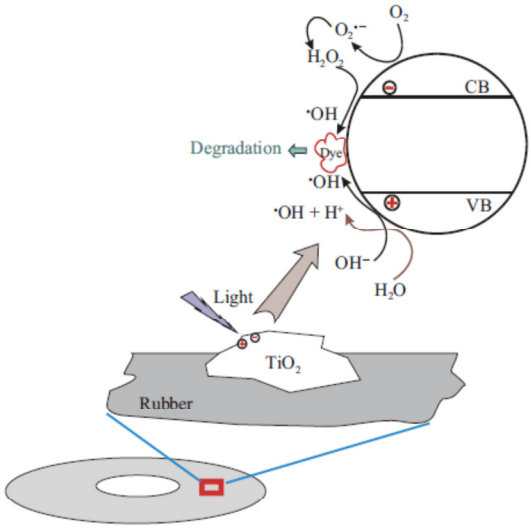

Scheme 1 Degradation of dye by TiO_2-strewn rubber sheet.

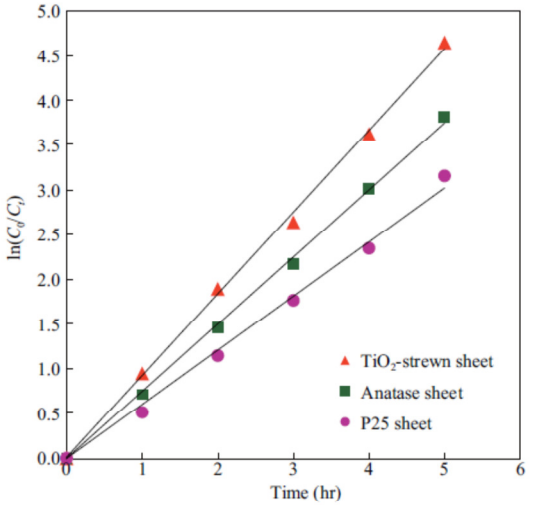

Fig. 8 Comparisons of photodegradation efficiencies of IC dye solution (2.5×10^{-5} mol/L) by TiO_2-strewn sheet, Im-Anatase sheet, and Im-P25 sheet.

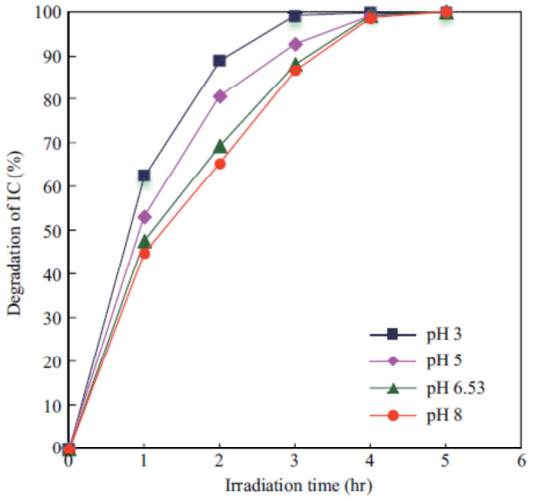

Fig. 9 Photodegradation efficiencies of TiO_2-strewn sheet as a function of pH (under UV light irradiation 3 hr; dye concentration 2.5×10^{-5} mol/L).

lence band being excited into the conduction band. This generates an electron (e^-) / hole (h^+) pair (Eq. (1)) which, if they can survive from recombination, are highly active species to induce further reactions. The hole in the valence band can oxidize the hydroxide anion (or H_2O) near the surface to yield the very reactive hydroxyl radical (•OH) (Reactions (2) and (3)) meanwhile the electron in the conduction band can reduce the surface adsorbed oxygen molecule to yield the superoxide radical ($O_2^{\bullet}$) (Reaction (4)) which later yields the active •OH radicals (Reactions (5)–(7)). The reactive •OH radical is the main species that degrades the dye molecules (Reaction (8)).

The photocatalytic degradation efficiency of TiO_2-strewn sheet found in this work is higher than that of titania rubber sheets (referred to as Im-Anatase sheet and Im-P25 sheet) as we have reported recently (Sriwong et al., 2010). These efficiencies discrepancy are shown comparatively in Fig. 8. The different efficiencies might be attributed to the location of the TiO_2 particles. TiO_2 particles of the TiO_2-strewn sheet that are externally located at the surface should have more chance to contact with IC dye molecules than those of both Im-Anatase sheet and Im-P25 sheet which are embedded rather deeply under the surface of rubber. Furthermore, in the preparation, only 0.07 g of TiO_2 was used for the TiO_2-strewn sheet while 0.1 g of TiO_2 was required to prepare the other two sheets by the method of Sriwong et al. (2008).

2.2.2 Effects of pH on the photocatalytic activity of the TiO_2-strewn sheet

In real-life applications, the sheet may be used under varied pH conditions. Therefore, the prepared TiO_2-strewn sheet was put to test under varying pH (from 3 to 8). The natural pH of IC dye solution was 6.53. The solution was adjusted to other pH by adding either diluted HCl or NaOH solution accordingly. The effects of pH on the photocatalytic degradation of IC dye in the presence of TiO_2-strewn sheet are shown in Fig. 9. It can be seen that the degradation efficiency of IC dye decreased with increasing pH. It is known that the metal oxide particles in water exhibit amphoteric behavior and readily react with dye which can be described by the following chemical equilibria (Kiriakidou et al., 1999; Silva et al., 2006; Toor et al., 2006):

$$\text{pH} < \text{pzc:} \quad \text{Ti-OH} + H^+ \longrightarrow \text{TiOH}_2^+ \tag{9}$$

$$\text{pH} > \text{pzc:} \quad \text{Ti-OH} + OH^- \longrightarrow \text{TiO}^- + H_2O \tag{10}$$

Generally, for the charged surface of TiO_2 particles, a significant dependency of the photocatalytic efficiency on the pH value was observed since the overall surface charge and, hence, the adsorptive properties of TiO_2 particles depended strongly on the solution pH (Senthilkumaar and Porkodi, 2005). According to the point of zero charge (pzc), the surface charge property of TiO_2 changes with

solution pH. The pH_{pzc} for TiO_2 has been reported in the range 6.25–6.90. Thus, the TiO_2 surface is positively charged in acidic media (pH < pH_{pzc}, and negatively charged under alkaline conditions (pH > pH_{pzc} (Sun et al., 2008). Therefore, it is expected that at pH below pH_{pzc}, TiO_2 particles at the TiO_2-strewn sheet surface acquires a positive charge. Since TiO_2 particles are located near the sheet surface, hence, the electrostatic interaction between the surface of the strewn sheet and the anionic dye parent fragment (Fig. 1) leads to strong adsorption with a corresponding high photodegradation activities at pH 3. On the other hand, at pH above pH_{pzc}, electrostatic repulsion between the negative surfaces of strewn sheet and anionic dye fragment retards the photodegradation activity. The order of activity decreases as pH 3 > pH 5 > pH 6.53 > pH 8.

2.2.3 Effect of initial concentration of IC dye on the photocatalytic activity of the TiO_2-strewn sheet

The effect of initial concentration on the photocatalytic degradation was investigated using concentrations 2.5×10^{-5}, 5.0×10^{-5}, and 7.5×10^{-5} mol/L. The kinetics studies of the photocatalytic degradation at different initial concentrations by TiO_2-strewn sheet are shown in Fig. 10. It can be seen that with increasing dye concentration, the photocatalytic activities of IC dye decreased. Hence, the photocatalysis process will work faster at lower concentration of pollutants. This behavior has been explained that with a high concentration of dye, the deeper colored solution would be less transparent to the UV light and the dye molecules could also absorb a significant amount of UV light causing less light to reach the catalyst resulting in the $OH^{\bullet}$ radicals forming on the surface of film to decrease, as a result, the reactive number of $OH^{\bullet}$ radicals attacking the dye molecules decreases and thus photodegradation efficiencies decreases (Konstantinou and Albanis, 2004). The straight lines in Fig. 10 confirm the first-order reaction of the degradation process with the rate constants 0.9138 hr^{-1}, 0.7077 hr^{-1}, and 0.5590 hr^{-1} for the dye concentration 2.5×10^{-5}, 5.0×10^{-5}, and 7.5×10^{-5} mol/L, respectively.

2.2.4 Effect of UV light intensity on the photocatalytic activity of the TiO_2-strewn sheet

The effect of UV light intensity on the photocatalytic degradation of IC dye was investigated by varying light intensity designated as: low, medium, and high. With increasing light intensity, the photocatalytic activities increased as shown in Fig. 11. It has been reported by several groups (Toor et al., 2006; Liu et al., 2006; Wang et al., 2007) that the photodegradation rate increased with the increase of irradiation light intensity. High UV light intensity increases the photon influx entering the dye solution and consequently excites the TiO_2 particles at the sheet surface resulting in more $OH^{\bullet}$ radicals being formed. As the reactive number of $OH^{\bullet}$ radicals increases, the photodegradation efficiencies also increase.

2.2.5 Recyclability of the TiO_2-strewn sheet on the photocatalytic degradation of IC dye solution

In this work, the TiO_2-strewn sheet can be used repeatedly for the photodegradation of IC dye solution. The sheet, after being used, remained clean and required no cleaning for subsequent uses. Photographs of new sheets and used sheets are shown in the Fig. 12. The clean sheet surface results from repulsive force between the negative charge at the surface of the sheet and the negative charge on IC dye parent fragment. The hydrophobic properties of rubber sheet substrate may also contribute to the non-accumulation of dye molecules on the sheet surface. As a result, the sheet surface remains clean and the intermittently cleanings are not necessary. The sheet was tested for recyclability up to ten times the results of which are shown in Fig. 13. The photodegradation efficiencies of the sheet remained high throughout the recyclability test. One noticeable feature in Fig. 13 is that the efficiency of the first use was slightly lower than those of the other subsequent uses. This may result from the fact that, when freshly prepared, the rubber surface as well as some of TiO_2 particles was still covered with trace of impurities.

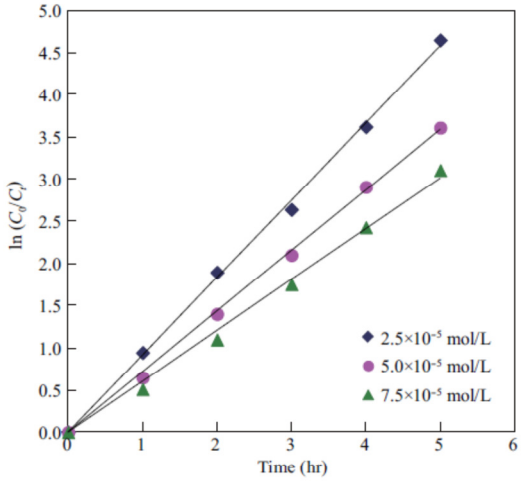

Fig. 10 Reaction kinetics on the photocatalytic degradation of IC dye solution at different initial concentrations by TiO_2-strewn sheet.

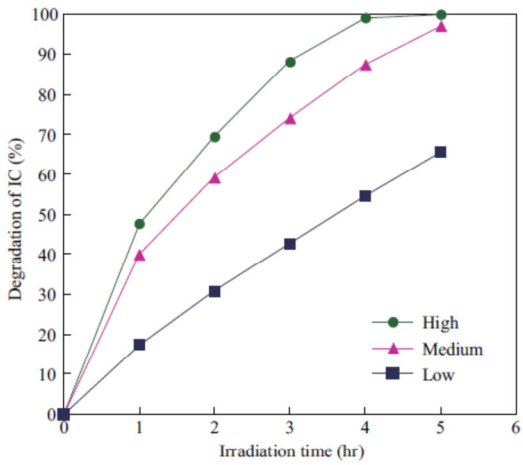

Fig. 11 Effects of UV light intensity on the photocatalytic degradation of IC dye solution by TiO_2-strewn sheet.

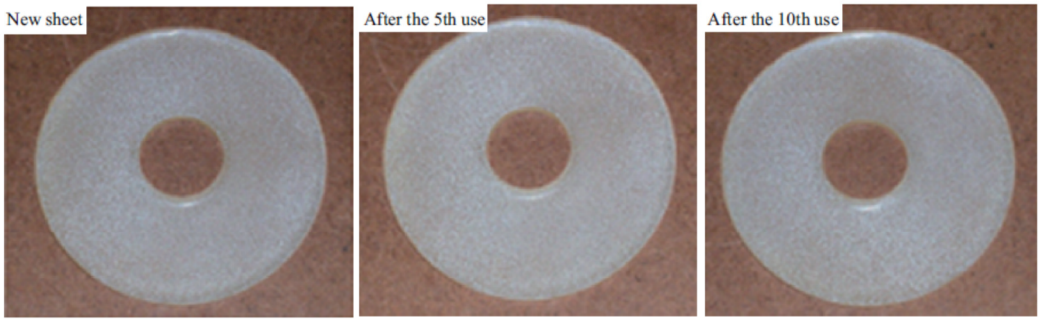

Fig. 12 Photographs of TiO_2-strewn sheet.

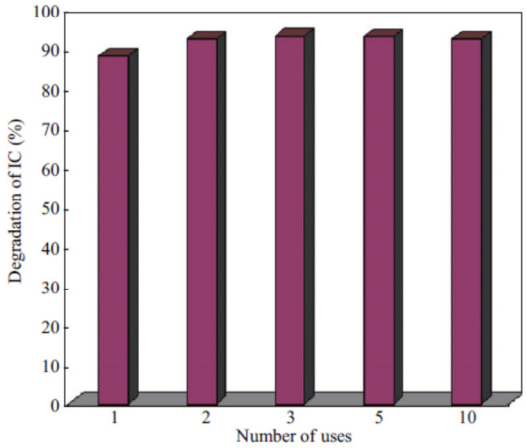

Fig. 13 Photodegradation efficiencies of TiO_2-strewn sheet from the recyclability test (under UV light, 3 hr, concentration 2.5×10^{-5} mol/L).

During the first use these impurities were destroyed in the photodegradation along with IC dye molecules in the solution. Hence, after the first use, the sheet surface appeared to be cleaner, i.e., less covered with impurities, with a higher number of TiO_2 particles contact with the dye solution and showed higher activity in the following use.

3 Conclusions

A novel, simple and low cost method for the preparation of TiO_2-strewn sheet is presented. The sheet still retains the photocatalytic property of TiO_2 particles by showing the photodegradation of IC dye solution under UV light illumination. From the SEM result, the TiO_2-strewn sheet contained densely titanium dioxide particles impregnated on the surface of the sheet rendering high surface unevenness and surface roughness from which high photocatalytic efficiency was originated. Dependencies of photocatalytic degradation of IC dye on the pH of dye solution, initial concentration of dye solution, and intensity of UV light were investigated. Although the TiO_2-strewn rubber sheet showed less activity than the loose powder of the same catalyst (Sriwong et al., 2008), it had one clear advantage over the loose powder in that it can be easily recovered after used and can be reused many times. The recyclability of the strewn rubber sheet should be attractive to the water treatment industry as it helps keep the operation cost low.

Acknowledgments

This research is supported by the Thailand Research Fund through the Royal Golden Jubilee Ph.D. Program (No. PHD/0003/2550), the Graduate School-PSU, and the Center for Innovation in Chemistry (PERCH-CIC), Commission on Higher Education, Ministry of Education. Sample of Degussa P25 used throughout this project was donated by Degussa AG, Frankfurt, Germany, through its agency in Bangkok, Thailand.

References

Baiju K V, Shukla S, Sandhya K S, James J, Warrier K G K, 2007. Photocatalytic activity of sol-gel derived nanocrystalline titania. *Journal of Physical Chemistry C*, 111(21): 7612–7622.

Barka N, Assabbane A, Nounah A, Ichou Y A, 2008. Photocatalytic degradation of indigo carmine in aqueous solution by TiO_2 coated non-woven fibres. *Journal of Hazardous Materials* 152(3): 1054–1059.

Beydoun D, Amal R, Low G, McEvoy S, 2000. Novel photocatalyst: titania-coated magnetite. Activity and photodissolution. *Journal of Physical Chemistry B*, 104(18): 4387–4396.

Beydoun D, Amal R, Scott J, Low G, McEvoy S, 2001. Studies on the mineralization and separation efficiencies of a magnetic photocatalyst. *Chemical Engineering Technology*, 24(7): 745–748.

Beydoun D, Amal R, 2002. Implication of heat treatment on the properties of a magnetic iron oxide-titanium dioxide photocatalyst. *Material Science Engineering B*, 94(1): 71–81.

Chen F, Xie Y D, Zhao J C, Lu G X, 2001. Photocatalytic degradation of dyes on a magnetically separated photocatalyst under visible and UV irradiation. *Chemosphere*, 44(5): 1159–1168.

Choi H, Stathatos E, Dionysiou D D, 2007. Photocatalytic TiO_2 films and membranes for the development of efficient wastewater treatment and reuses system. *Desalination*, 202(1-3): 199–206.

Ding Z, Hu X J, Yue P L, Lu G Q, Greenfield P F, 2001. Synthesis of anatase TiO_2 supported on porous solids by chemical

vapor deposition. *Catalysis Today*, 68(1-3): 173–182.

Gao Y, Chen B H, Li H L, Ma Y X, 2003. Preparation and characterization of a magnetically separated photocatalyst and its catalytic properties. *Materials Chemistry and Physics*, 80(1): 348–355.

Ge L, Xu M X, Sun M, Fang H B, 2006. Fabrication and characterization of nano TiO_2 thin films at low temperature. *Materials Research Bulletin*, 41(9): 1596–1603.

Habibi M H, Talebian N, Choi J H, 2007. The effect of annealing on photocatalytic properties of nanostructured titanium dioxide thin films. *Dyes and Pigments*, 73(1): 103–110.

Houas A, Lachheb H, Ksibi M, Elaloui E, Guillard C, Herrmann J M, 2001. Photocatalytic degradation pathway of methylene blue in water. *Applied Catalysis B: Environmental*, 31(2): 145–157.

Wang J, Zhao G, Zhang Z H, Zhang X D, Zhang G, Ma T et al., 2007. Investigation on degradation of azo fuchsine using visible light in the presence of heat-treated anatase TiO_2 powder. *Dyes and Pigments*, 75(2): 335–343.

Khataee A R, Kasiri M B, 2010. Photocatalytic degradation of organic dyes in the presence of nanostructured titanium dioxide: Influence of the chemical structure of dyes. *Journal of Molecular Catalysis A: Chemistry*, 328(1-2): 8–26.

Kiriakidou F, Kondarides D I, Verykios X E, 1999. The effect of operational parameters and TiO_2-doping on the photocatalytic degradation of azo-dyes. *Catalysis Today*, 54(1): 119–130.

Konstantinou I K, Albanis T A, 2004. TiO_2-assisted photocatalytic degradation of azo dyes in aqueous solution: kinetic and mechanistic investigations: A review. *Applied Catalysis B: Environmental*, 49(1): 1–14.

Kwon C K, Shin H, Kim J H, Choi W S, Yoon K H, 2004. Degradation of methylene blue via photocatalysis of titanium dioxide. *Materials Chemistry and Physics*, 86(1): 78–82.

Liu C C, Hsieh Y H, Lai P F, Li C H, Kao C L, 2006. Photodegradation treatment of azo dye wastewater by UV/TiO_2 process. *Dyes and Pigments*, 68(2-3): 191–195.

Losito I, Amorisco A, Palmisano F, Zambonin P G, 2005. X-ray photoelectron spectroscopy characterization of composite TiO_2-poly (vinylidenefluoride) films synthesised for applications in pesticide photocatalytic degradation. *Applied Surface Science*, 240(1-4): 180–188.

Mittal A M, Mittal J M, Kurup L, 2006. Batch and bulk removal of hazardous dye, indigo carmine from wastewater through adsorption. *Journal of Hazardous Materials*, 137(1): 591–602.

Nagaveni K, Sivalingam G, Heged M S, Madras G, 2004. Solar photocatalytic degradation of dyes: high activity of combustion synthesized nano TiO_2. *Applied Catalysis B: Environmental*, 48(2): 83–93.

Othman I, Mohamed R M, Ibrahim I A, Mohamed M M, 2006. Synthesis and modification of ZSM-5 manganese and lanthanum and their effects on decolorization of indigo carmine dye. *Applied Catalysis A: General*, 299: 95–102.

Othman I, Mohamed R M, Ibrahem F M, 2007. Study of photocatalytic oxidation of indigo carmine dye on Mn-supported TiO_2. *Journal of Photochemistry and Photobiology A: Chemistry*, 189(1): 80–85.

Parida K M, Sahu N, Biswal N R, Naik B, Pradhan A C, 2008. Preparation, characterization, and photocatalytic activity of sulfate-modified titania for degradation of methyl orange under visible light. *Journal of Colloid and Interface Science*, 318(2): 231–237.

Partsinis S E, 1996. Flame synthesis of nanosize particles: precise control of particle size. *Journal of Aerosol Science*, 27(S1): s153–s154.

Ryu J, Park D S, Hahn B D, Choi J J, Yoon W H, Kim K Y et al., 2008. Photocatalytic TiO_2 thin films by aerosol-deposition: From micron-sized particles to nano-grained thin film at room temperature. *Applied Catalysis B: Environmental*, 83(1-2): 1–7.

Sankapal S B, Steiner M C, Ennaoui A, 2005. Synthesis and characterization of anatase-TiO_2 thin films. *Applied Surface Science*, 239(2): 165–170.

Sen S, Mahanty S, Roy S, Heintz O, Bourgeois S, Chaumont D, 2005. Investigation on sol-gel synthesized Ag-doped TiO_2 cermets thin films. *Thin Solid Films*, 474(1-2): 245–249.

Senthilkumaar S, Porkodi K, 2005. Heterogeneous photocatalytic decomposition of Crystal Violet in UV-illuminated sol-gel derived nanocrystalline TiO_2 suspensions. *Journal of Colloid and Interface Science*, 288(1): 184–189.

Shi J W, Zheng J T, Wu P, Ji X J, 2008. Immobilization of TiO_2 films on activated carbon fiber and their photocatalytic degradation properties for dye compounds with different molecular size. *Catalysis Communications*, 9(9): 1846–1850.

Silva C G, Wong W D, Faria J L, 2006. Photocatalytic and photochemical degradation of mono-, di- and tri-azo dyes in aqueous solution under UV irradiation. *Journal of Photochemistry and Photobiology A: Chemistry*, 181(2-3): 314–324.

Sriwong C, Wongnawa S, Patarapaiboolchai O, 2008. Photocatalytic activity of rubber sheet impregnated with TiO_2 particles and its recyclability. *Catalysis Communications*, 9(2): 213–218.

Sriwong C, Wongnawa S, Patarapaiboolchai O, 2010. Degradation of indigo carmine dye by rubber sheet impregnated with TiO_2 particles. *Science Asia*, 36(1): 52–58.

Sun J H, Qiao L P, Sun S P, Wang G L, 2008. Photocatalytic degradation of Orange G on nitrogen-doped TiO_2 catalysts under visible light and sunlight irradiation. *Journal of Hazardous Materials*, 155(1-2): 312–319.

Toor A P, Verma A, Jotshi C K, Bajpai P K, Singh V, 2006. Photocatalytic degradation of Direct 12 Yellow dye using UV/TiO_2 in a shallow pond slurry reactor. *Dyes and Pigments*, 68(1): 53–60.

Wang T M, Wang H Y, Xu P, Zhao X C, Liu Y L, Chao S, 1998. The effect of properties of semiconductor oxide thin films on photocatalytic decomposition of dyeing waste water. *Thin Solid Films*, 334(1-2): 103–108.

Weng W J, Ma M, Du P Y, Zhao G, Shen G X, Wang J X et al., 2005. Superhydrophilic Fe doped titanium dioxide thin films prepared by a spay pyrolysis deposition. *Surface Coating and Technology*, 198(1-3): 340–344.

Wu K R, Cho T P, 2008. Photocatalytic properties of visible light enabling layered titanium oxide/tin indium oxide films. *Applied Catalysis B: Environmental*, 80(3-4): 313–320.

Xu S H, Shangguan W F, Yuan J, Chen M X, Shi J W, Jiang Z, 2008. Synthesis and performance of novel magnetically separable nanospheres of titanium dioxide photocatalyst with egg-like structure. *Nanotechnology*, 19(9): 095606 (7pp).

Yang J H, Han Y S, Choy J H, 2006. TiO_2 thin-films on polymer substrates and their photocatalytic activity. *Thin Solid Films*, 495(1-2): 266–271.

Yogi C, Kojima K, Wada N, Tokumoto H, Takai T, Mizoguchi T et al., 2008. Photocatalytic degradation of methylene blue by TiO_2 film and Au particles-TiO_2 composite film. *Thin*

Solid Films, 516(17): 5881–5884.

Yuan R S, Guan R B, Shen W Z, Zheng J T, 2005. Photocatalytic degradation of methylene blue by a combustion of TiO_2 and activated carbon fibers. *Journal of Colloid and Interface Science*, 282(1): 87–91.

Yuan Z F, Zhang J L, Li B, Li J Q, 2007. Effect of metal ion dopants on photochemical properties of anatase TiO_2 films synthesized by a modified sol-gel method. *Thin Solid Films*, 515(18): 7091–7095.

Zhang X, Zhang F, Chan K Y, 2006. The synthesis of Pt-modified titanium dioxide thin films by microemulsion templating, their characterization and visible-light photocatalytic properties. *Materials Chemistry and Physics*, 97(2-3): 384–389.

Zhu J F, Zheng W, He B, Zhang J L, Anpo M, 2004. Characterization of Fe-TiO_2 photocatalysts synthesized by hydrothermal method and their photocatalytic reactivity for photodegradation of XRG dye diluted in water. *Journal of Molecular Catalysis A: Chemistry*, 216(1): 35–43.

Chemical Engineering Journal 191 (2012) 210–217

Contents lists available at SciVerse ScienceDirect

Chemical Engineering Journal

journal homepage: www.elsevier.com/locate/cej

Recyclable thin TiO_2-embedded rubber sheet and dye degradation

Chaval Sriwong[a], Sumpun Wongnawa[a,*], Orasa Patarapaiboolchai[b]

[a] Department of Chemistry for Innovation in Chemistry, Faculty of Science, Prince of Songkla University, Hat Yai, Songkhla 90112, Thailand
[b] Department of Materials Science and Technology, Faculty of Science, Prince of Songkla University, Hat Yai, Songkhla 90112, Thailand

ARTICLE INFO

Article history:
Received 24 October 2011
Received in revised form 5 March 2012
Accepted 5 March 2012

Keywords:
Immobilized titanium dioxide
Photocatalytic degradation
Indigo carmine
Dye degradation
TiO_2-embedded rubber sheet

ABSTRACT

A new method for the preparation of thin rubber sheet embedded with TiO_2 from natural rubber latex is presented. This method – simple and inexpensive – is based on the use of TiO_2 powder (Degussa P25) mixing with small amount of natural rubber latex (60% HA) followed by vacuum filtration through a sintered glass to form a thin paper-like and flexible sheet. The characteristic of this thin and flexible TiO_2 sheet (FT sheet) thus formed was studied by X-ray diffractometer (XRD) and scanning electron microscopy/energy dispersive X-ray spectrometer (SEM/EDS) techniques. The photocatalytic activity of FT sheet was evaluated using indigo carmine (IC) dye as a model for the organic dye pollutant in water. The results showed that the FT sheet containing TiO_2 5 wt% has the highest degradation efficiency than sheets containing higher TiO_2 concentrations. The effects of pH and initial concentration of dye solution on the photodegradation were also investigated. Kinetics of the photocatalytic degradation was of the first-order reaction. The used FT sheet can be recovered and reused with no decline in the photodegradation efficiency over a long-term usage.

1. Introduction

During the last two decades, heterogeneous photocatalysis has attracted considerable attention for the complete destruction of undesirable organic pollutants both in aqueous and gaseous phases with the help of solar or artificial light [1–3]. This technique is based on the use of UV irradiated semiconductors which titanium dioxide (TiO_2), generally, is one of the most used photocatalysts due to its chemical stability, non-toxicity, inexpensiveness, and high efficiency in the photocatalysis process [4,5]. Among different commercially available titanium dioxide powders, Degussa P25 shows the highest activity and it is commonly used in many kinds of photocatalytic reactions [6–9]. However, many disadvantages of the use of TiO_2 in powder form have been noted: (i) difficulty and high cost in the separation and recovery of the catalyst from suspension, (ii) non-reusable of the catalyst, (iii) easy aggregation of the suspended particles, (iv) difficulty in application to continuous flow systems, and (v) possibility to cause adverse human health problems by the loose powder [10–13]. To avoid the use of photocatalyst in powder form, several efforts have been made to coat TiO_2 as films on various substrates [14–20] as well as employing several techniques such as chemical vapor deposition (CVD) [21], spray pyrolysis deposition [22], flame synthesis [23], and sol–gel dip/spin coating [24,25]. These methods, however, have some disadvantages for industrial applications, for instance, the chemical vapor deposition, spray pyrolysis deposition, and flame synthesis methods require special and rather expensive apparatus and complex procedures for the deposition of TiO_2 film while the sol–gel dip/spin coating method needs repeated coating in order to get a thick film and requires high annealing temperature for crystallization. In addition, the heating process precludes the fabrication of TiO_2 film on substrates with low thermal stability such as plastics and hydrocarbon polymers [18]. Therefore, a simple, less expensive and more effective method for the preparation of immobilized TiO_2 powder is still an interesting topic under investigation in many laboratories including ours.

In this present work we report a preparation of a very thin (paper-like) and flexible TiO_2 sheet (hereinafter designated as FT sheet) and the efficiency of indigo carmine (IC) degradation by the said sheet under UV light. The novel FT sheet was prepared by different methods from that used in the previous reports [26,27]. The resulting new sheet is much thinner as a result of using less amount of latex, i.e., 0.84 mL of latex for new method against 5 mL for the previous method. The thinness of the sheet enables the exposure of TiO_2 particles on both sides of the sheet compared to the one-sided exposure in the previous report resulting in more reactive in dye degradation and longer useful life due to the two-sided utility. In the investigation of this new FT sheet, the effects of pH and initial concentration of IC dye solution were studied. The reaction kinetics and the recycling use of FT sheet on the photodegradation of IC dye were also presented. Indigo carmine dye was used as a model dye in this work due to its usually used in textile industry for dying of cloths (blue jeans) and other blue denim, in food industry (typical products including milk, dessert, sweets, biscuits), and cosmetics

* Corresponding author. Fax: +66 7455 8841.
E-mail address: sumpun.w@psu.ac.th (S. Wongnawa).

1385-8947/$ – see front matter © 2012 Elsevier B.V. All rights reserved.
doi:10.1016/j.cej.2012.03.005

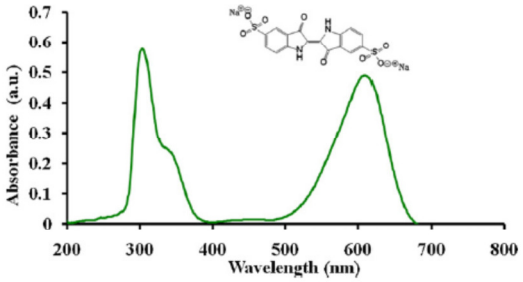

Fig. 1. Molecular structure and absorption spectrum of indigo carmine (IC) dye.

industry [28–31]. The molecular structure and absorption spectrum of IC dye are illustrated in Fig. 1.

2. Experimental

2.1. Chemicals and equipment

Titanium dioxide Degussa P25, a mixture of anatase and rutile (80:20) with surface area 50 m^2/g and mean particle diameter 30 nm, was obtained from Degussa AG, Germany. The natural rubber latex (60% HA) was purchased from Chana Latex Co. Ltd., Songkhla, Thailand. Indigo carmine (IC) dye was purchased from Fluka, USA. The crystalline phases of TiO_2 were identified by using X-ray diffraction technique (XRD) (X'Pert MPD, Phillips, The Netherlands). The surface morphologies of FT sheets were characterized by using scanning electron microscopy (SEM) (JEOL-JSM 5800LV, Japan) attached with energy dispersive X-ray spectrometer (EDS) (Oxford ISIS 300).

2.2. Preparation of FT sheet

The FT sheet was prepared from water-mixed rubber latex and TiO_2 powder suspended in ammonia solution. In a typical procedure to prepare the 5 wt% FT sheet, 0.84 mL of natural rubber latex (60% HA) was mixed with 9.16 mL of distilled water to make the total volume of 10 mL and was stirred for 15 min. The ammoniacal TiO_2 was prepared by mixing 0.5 g of TiO_2 powder (Degussa P25) with 5 mL ammonia solution and vigorously stirred for 15 min. The prepared 10 mL of water-mixed rubber latex was added to the TiO_2 suspension and then vigorously stirred for 15 min until the homogenized mixture formed. Subsequently, the mixture was subjected to vacuum suction through a sintered glass (150 mL, 4–5.5 ASM) and dried in the oven at 60 °C about 3 h to remove trace of water and ammonia gas. After drying, FT sheet was carefully taken out from the sintered glass and left to dryness at room temperature overnight. The sheet obtained was designated as 5 wt% FT sheet. The 10 wt% and 15 wt% FT sheets were prepared likewise using appropriate amount of natural rubber latex, 1.68 mL and 2.52 mL, respectively. (The 5 wt% sheet means the sheet contains 5% by weight of latex. When less than 5 wt% of latex was used the sheet was too thin and not sufficiently strong enough to withstand the vacuum suction resulting in a cracked sheet. On the other hand, for higher than 15 wt% of latex, the sheet showed low activity as is illustrated in Section 3.2.1.)

2.3. Photocatalytic studies

In the photocatalytic studies, FT sheet was placed in a Petri dish (4 in. diameter) containing 60 mL of 2.5×10^{-5} M IC dye. The solution was then stirred for 15 min in the dark to allow the adsorption equilibrium in a closed compartment (0.9 m × 0.9 m × 0.9 m) to avoid interference from ambient light after which the irradiation was initiated by switching on the UV light (fluorescent blacklight, 20 W, F20T12-BLB, GE, USA) and magnetically stirred. At a given time interval (every 1 h), 3 mL of dye solution was collected for analysis. The concentrations of IC dye were analyzed using a UV–vis spectrophotometer (Specord S100, Analytik Jena, Germany) from the changes in absorbance at 610 nm against the calibration graph constructed from several standard solutions of IC at various concentrations. The percentage of degradation was calculated by Eq. (1):

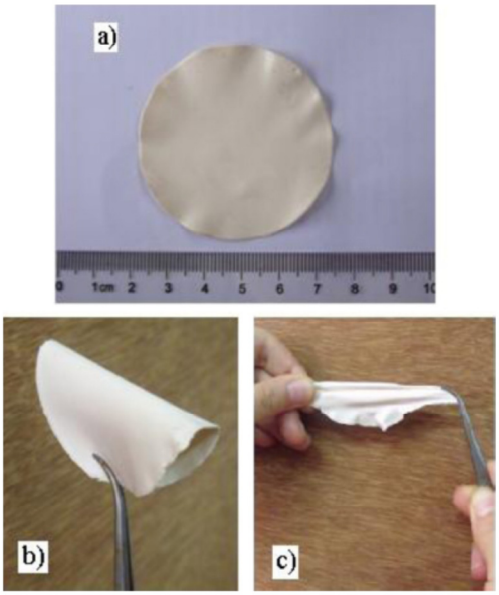

Fig. 2. Photographs of: (a) FT sheet, (b) showing flexibility, and (c) showing elasticity.

$$\%\,\text{Degradation} = \frac{C_0 - C_t}{C_0} \times 100 \quad (1)$$

where C_0 is the initial concentration of IC dye and C_t is the concentration at a specific time interval of the collected sample.

The controlled experiments, without TiO_2 or without light, were also performed to confirm that the decolorization of IC dye was truly the result of catalytic activity.

3. Results and discussion

3.1. Characterization of FT sheets

The freshly prepared FT sheet has the same white color as that of the rubber latex. The thickness of the 5 wt% sheet was 0.33 mm as estimated from the SEM cross section image. As the concentration of the latex increased so was the thickness of the sheet, i.e., the thickness of 10 wt% and 15 wt% was 0.68 mm and 1.00 mm, respectively. To the naked eyes the sheet had smooth surface. The bent or stretched sheet readily returns to its original shape. The flexibility and elasticity properties of FT sheet are illustrated in Fig. 2a–c.

The X-ray diffraction patterns of the loose powder TiO_2 and TiO_2 embedded in the sheet are shown in Fig. 3. The diffraction peaks of anatase and rutile phases are marked with 'A' and 'R',

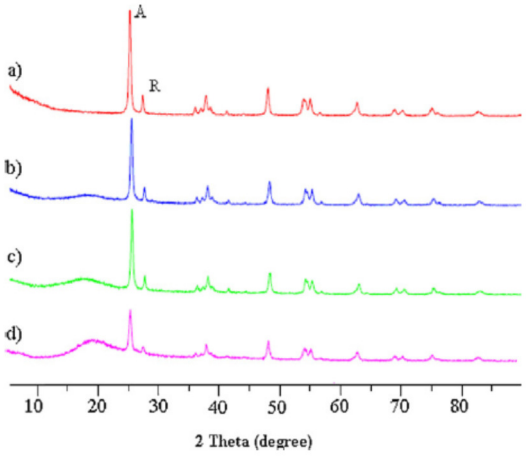

Fig. 3. XRD patterns of (a) TiO_2 P25 powder and TiO_2 P25 powder embedded in (b) 5 wt% sheet, (c) 10 wt% sheet, and (d) 15 wt% sheet.

respectively. The anatase peaks appear at $2\theta = 25.50^\circ$ (1 0 1) and 48.0° while those of rutile appear at $2\theta = 27.50^\circ$ (1 0 1) and 54.50°. As shown in the figure, the well crystallized anatase and rutile forms were observed in all the FT sheets (Fig. 3b–d) and were identical to those of Degussa P25 powder in Fig. 3a. In addition, a broad scattering peak at $2\theta = 19^\circ$ of rubber matrix was also discernible in the patterns of all the FT sheet samples. The intensity of this broad peak increases with increasing concentration of rubber latex, i.e., the 5 wt% sheet (Fig. 3b) exhibits the lowest intensity compared with the 10 wt% and 15 wt%, respectively. The XRD of pristine rubber sheet has been shown in our previous work elsewhere which shows only a large broad peak near $2\theta = 19^\circ$ [26] due to the fact that the rubber matrix is composed of low atomic number (low Z) elements. The matrix of 5 wt% sheet has the highest content of TiO_2 particles than those of the other sheets, therefore, the highest average Z-value of matrix resulting in the lowest X-ray scattering and the lowest intensity peak at $2\theta = 19^\circ$ as shown in Fig. 3b.

The SEM images of FT sheets are shown in Fig. 4. It can be seen that the surface roughness and the 'near surface' TiO_2 particles decreased with increasing amount of rubber latex. The 5 wt% sheet with the highest 'near surface' number of TiO_2 particles (Fig. 4a and d) has the coarsest surface compared with the other two sheets. The amount of rubber latex used in the preparation of sheets has direct effect on the surface morphology of each sheet, i.e., when higher content of rubber latex was used the sheet became thicker and TiO_2 particles readily submerged in the latex resulting in less amount of TiO_2 particles appeared near the sheet surface (Fig. 4b and c). Moreover, porous surface was observed only on the surface of 5 wt% sheet but not on the other two sheets with higher content of latex. This could be that the 5 wt% sheet contained minimal amount of latex barely sufficient to provide full coverage of all TiO_2 particles at the surface and to fill all the void spaces between particles (Fig. 4a and d). It has been known that the surface roughness and the porous structure are very important for the photocatalytic activity of TiO_2 films [1] since the photocatalytic activity would be increased with the enhanced surface morphology by the roughness and the porous structure.

The EDS analysis was carried out to confirm the presence of elements in the flexible sheets. The EDS spectra and mapping of 5 wt% and 15 wt% FT sheets are shown in Fig. 5 and Fig. 6, respectively, from which only three elements were detected in the sheets (carbon, oxygen, and titanium). The 5 wt% sheet (Fig. 5a) clearly shows stronger Ti peaks than the 15 wt% sheet in Fig. 6a corresponding to more atoms of Ti (TiO_2 particles) being exposed to electron beam on this sheet surface. This finding is further supported by EDS elemental mapping in Fig. 5b and Fig. 6b, respectively. The 15 wt% sheet (Fig. 6a), however, exhibits very strong carbon peak due to high concentration of rubber latex matrix on the sheet surface. Natural rubber consists mostly of *cis*-1,4 polyisoprene with a repeating hydrocarbon unit ($-CH_2CH_3C{=}CHCH_2-$), which is the main source of carbon signal. This observation supports the conclusion from SEM results in Fig. 4c and f that there is high concentration of rubber latex on the surface and very small amount of TiO_2 particles (very low Ti peak) on the surface of the 15 wt% sheet.

Table 1
The rate constants of IC dye degradation by the FT sheets.

FT sheets	k_{app} (h^{-1})	R^2
5 wt% sheet	0.8247	0.9977
10 wt% sheet	0.2729	0.9827
15 wt% sheet	0.1004	0.9935

3.2. Photocatalytic degradation of IC by FT sheet

3.2.1. Testing the photocatalytic activities of FT sheet

The photocatalytic degradation of IC dye solution by the FT sheet under UV-light irradiation is shown in Fig. 7. It can be seen from the figure that 5 wt% FT sheet showed higher photodegradation efficiency than the 10 wt% and 15 wt% sheets, respectively. As shown in Fig. 4a and d, the 5 wt% sheet with very high content of TiO_2 particles on the surface exhibited highest surface roughness, therefore, its observed highest photocatalytic activity was not unexpected. Generally, the photocatalytic reaction on the TiO_2 surface is very sensitive to its surface structure because the photocatalytic is a surface reaction [15]. Thus, the higher the surface roughness the more the photocatalytic reaction takes place. In contrast, the lower the surface roughness as in the smooth surface sheet will have lower photodegradation activity. This is exactly what was observed in the study of the 10 wt% and 15 wt% sheets in comparison with the 5 wt% sheet.

The detailed study of degradation mechanism of IC dye was not performed in this work, however, this dye had been investigated thoroughly and reported that it was almost completely mineralized by P25 TiO_2 when irradiated with UV light to CO_2, NH_4^+, NO_3^-, and SO_4^{2-} [32].

In the kinetics study, the apparent rate constant (k_{app}) has been chosen as the basic kinetics parameter for all the FT sheets under investigation. The k_{app} arises from the Langmuir–Hinshelwood first-order kinetics equation as [1,33–35]:

$$\ln\left(\frac{C_0}{C}\right) = k_{app} \times t \quad (2)$$

where C_0 is the initial concentration of dye, C is the concentration at time t, and k_{app} is the apparent rate constant. The straight lines obtained when $\ln(C_0/C)$ was plotted against t confirmed the first-order kinetics of dye degradation as shown in Fig. 8. The rate constant values calculated from Eq. (2) are summarized in Table 1 for all the three FT sheets.

3.2.2. Effect of pH on the photocatalytic activity of FT sheet

To be useful for industrial applications, the sheet should be workable under various pH conditions. Therefore, the prepared FT sheet was put to test under varying pHs (from pH 3 to pH 8). The natural pH of IC dye solution was 6.53. The solution was adjusted to other pHs by adding either diluted HCl or NaOH solution accordingly. The effects of pH on the photocatalytic degradation of IC dye

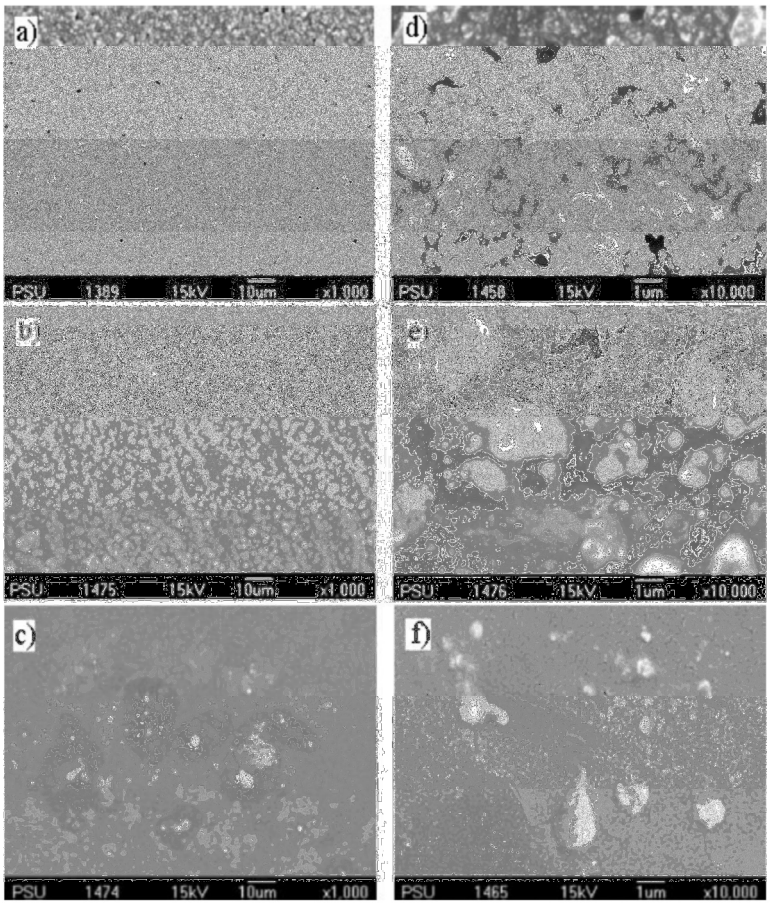

Fig. 4. SEM images of FT sheets; low magnification (left column) and high magnification (right column) of 5 wt% sheet (a and d), 10 wt% sheet (b and e), and 15 wt% sheet (c and f).

in the presence of TiO_2 sheet are shown in Fig. 9. It can be seen that the degradation efficiency of IC dye decreases with the increasing of pH. The behaviour of amphoteric metal oxide particles in water can be described by the following chemical equilibria [36–38]:

$$pH < pzc: \quad Ti{-}OH + H^+ \rightarrow TiOH_2^+ \tag{3}$$

$$pH > pzc: \quad Ti{-}OH + OH^- \rightarrow TiO^- + H_2O \tag{4}$$

Generally, for the charged surface of TiO_2 particles, a significant dependency of the photocatalytic efficiency on the pH value was observed since the overall surface charge and, hence, the adsorptive properties of TiO_2 particles depended strongly on the solution pH [39]. According to the point of zero charge (pzc), the surface charge property of TiO_2 changes with solution pH. The reported pH_{pzc} for TiO_2 is in the range 6.25–6.90. Thus, the TiO_2 surface is positively charged in acidic media ($pH < pH_{pzc}$) via the protonation depicted by Eq. (3) and negatively charged under alkaline conditions ($pH > pH_{pzc}$) via the proton abstraction by hydroxide ion depicted by Eq. (4) [40]. Therefore, it is expected that at pH below pH_{pzc}, TiO_2 particles at the FT sheet surface would bear a positive charge. Since TiO_2 particles are located near the sheet surface, hence, the electrostatic interaction between the surface of the FT sheet and the anionic dye parent fragment (see Fig. 1) leads to strong adsorption with a corresponding high photodegradation activity at pH 3. On the other hand, at pH above pH_{pzc}, electrostatic repulsion between the negative surface of FT sheet and anionic dye fragment retards the surface adsorption of dye molecules resulting in low photodegradation activity. The order of activity decreases as pH 3 > pH 5 > pH 6.53 > pH 8.

3.2.3. *Effect of initial concentration of IC dye on the photocatalytic activity of FT sheet*

The effect of initial concentration of dye on the photocatalytic degradation was investigated using various concentrations of dye solution: 2.5×10^{-5}, 5.0×10^{-5}, and 7.5×10^{-5} M. The efficiencies of the photocatalytic degradation at these concentrations by FT sheet are shown in Fig. 10. It can be seen that on increasing the dye concentration, the photocatalytic activity of IC dye decreases. Hence, the photocatalysis process will work faster at lower concentration of pollutants. This behavior has been explained that at high concentration of dye, the deeper colored solution would be less transparent to the incoming UV light and the dye molecules could also absorb a significant amount of UV light. This means less light

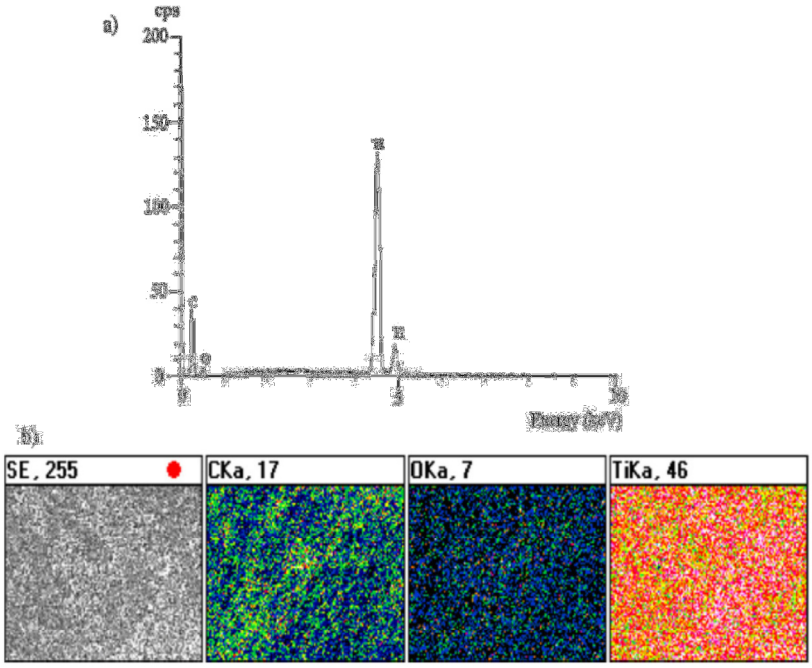

Fig. 5. EDS spectra (a) and mapping images (b) of the 5 wt% FT sheet.

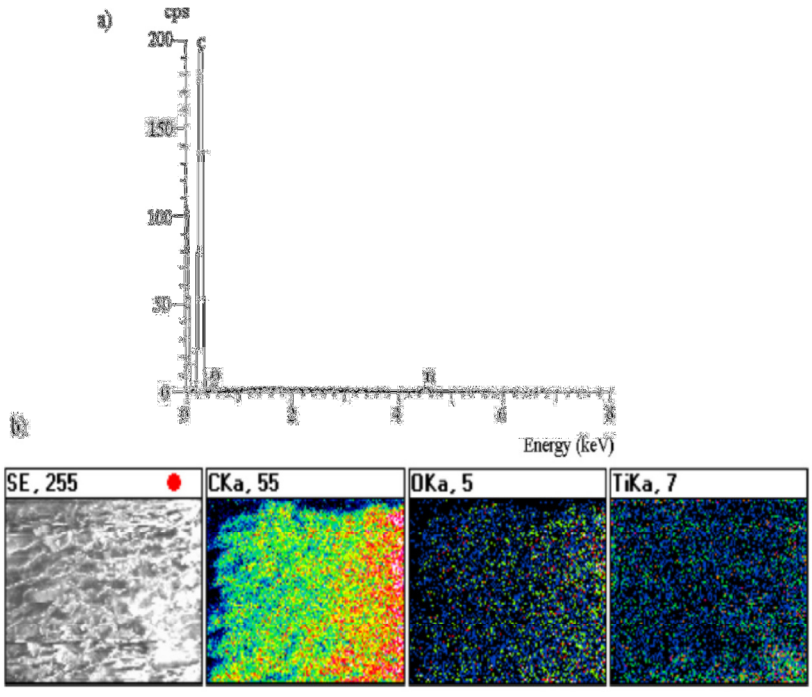

Fig. 6. EDS spectra (a) and mapping images (b) of the 15 wt% FT sheet.

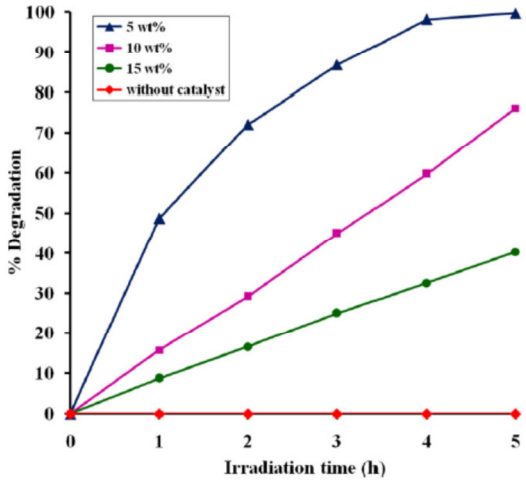

Fig. 7. The efficiencies of photocatalytic degradation of IC dye by FT sheets under UV irradiation.

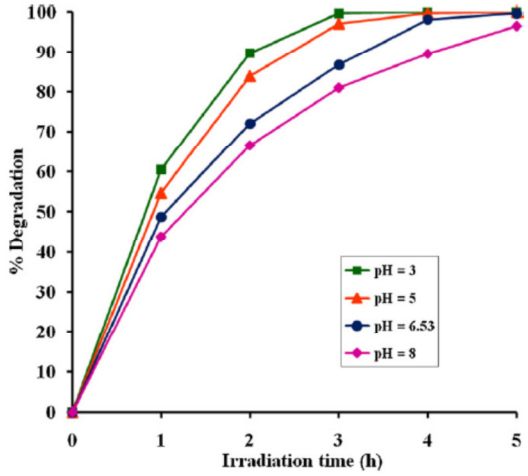

Fig. 9. Effects of pH on the photodegradation efficiencies of IC dye by 5 wt% FT sheet.

will reach the catalyst resulting in the decrease of OH• radical to be formed on the surface of catalyst particles, as a result, the reactive number of OH• radicals attacking the dye molecules decrease and thus photodegradation efficiency decreases [41].

3.2.4. Recyclability of FT sheet on the photocatalytic degradation of IC dye solution

In this work, the FT sheet can be repeatedly used for the photodegradation of IC dye solution. The sheet, after used, remained clean and required no cleaning for the subsequent uses. Photographs of new and used sheets are shown in Fig. 11. The clean sheet surface results from repulsive force between the potentially negative charge at the surface of sheet (due to the embedded TiO_2 particles) and the negative charge on the IC dye parent fragment. As a result, the dye molecular fragments do not adhere to the sheet surface rendering the sheet surface remains clean and the intermittently cleanings are not necessary. However, the surface of used sheets became off-white to pale yellow after several reuses compared to plain white of the new sheet (Fig. 11). The sheet was tested for recyclability up to ten times the results of which are shown in Fig. 12. The photodegradation efficiency of the FT sheet remained high throughout the recyclability tests. Note that, in Fig. 12, the efficiency of the first use was slightly lower than those of the subsequent uses. The explanation for this observation is that when freshly prepared the rubber surface as well as some of TiO_2 particles were still covered with traces of impurities. During the first use these impurities were destroyed in the photodegradation process along with IC dye molecules in the solution. Hence, after the first use, the sheet surface appeared to be cleaner, i.e., less or not at all covered with impurities, yielding higher number of TiO_2 particles contact with the dye solution, therefore, higher activity was observed in the second use and onward.

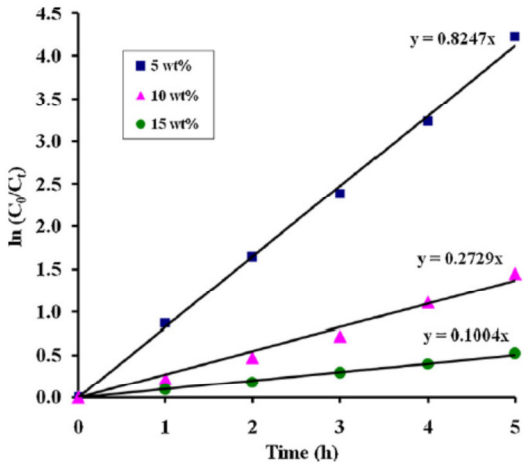

Fig. 8. Plots of rate of disappearance of IC dye by FT sheets.

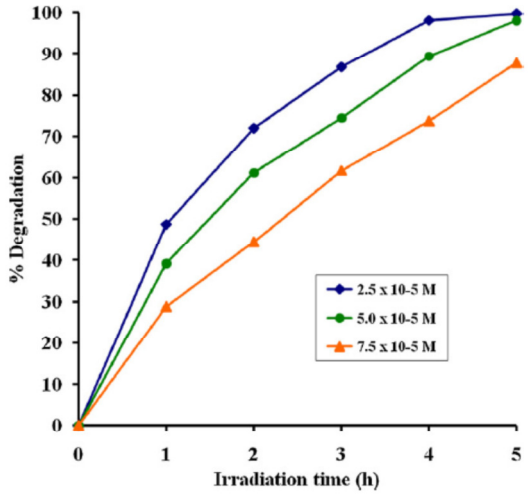

Fig. 10. Effects of the initial concentration on the photodegradation efficiency of IC dye by 5 wt% FT sheet.

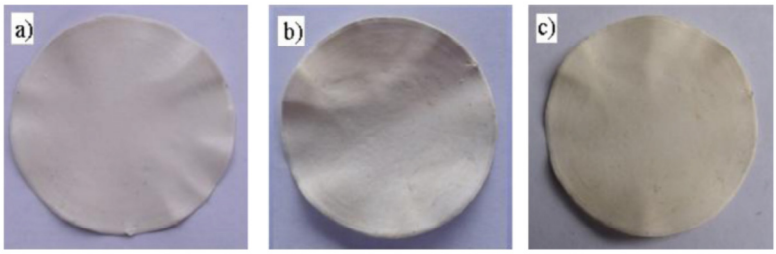

Fig. 11. Photographs of the 5 wt% FT sheet: (a) new sheet, (b) after the 5th use, and (c) after the 10th use.

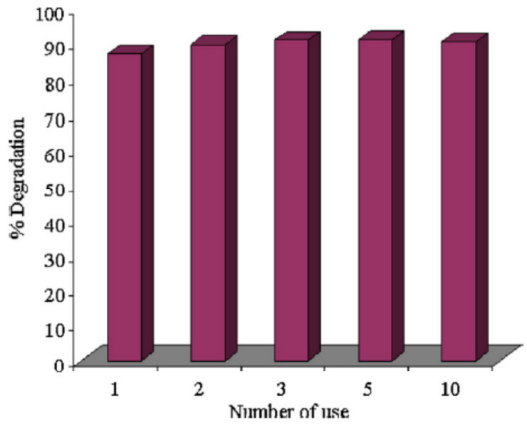

Fig. 12. The efficiencies of IC dye degradation by 5 wt% FT sheet after repeated uses under UV light irradiation for 3 h.

4. Conclusions

A novel, simple, and low cost method for the preparation of thin paper-like FT sheet is presented. The sheet still retains the photocatalytic property of TiO_2 particles by photodegrading IC dye solution under UV light illumination. From the SEM results, the 5 wt% FT sheet contained very dense and appropriately covered by titanium dioxide particles on the sheet surface rendering high surface roughness from which the highest photocatalytic efficiency was originated. Dependencies of photocatalytic degradation of IC dye on the pH and initial concentration of dye solution were also investigated. The kinetics of the photocatalytic degradation was of the first-order reaction. Although the sheets embedded with TiO_2 usually show less activity than the loose powder of the same catalyst [26], it has one clear advantage over the loose powder that it can be easily recovered after having been used and can be reused many times. The recyclability of the TiO_2 sheet should be attractive to the water treatment industry as it helps keep the operation cost low. The relatively low cost of the materials (photocatalyst powder and rubber latex) is a one time investment and will last over a long period of uses.

Acknowledgements

This research is supported by the Thailand Research Fund through the Royal Golden Jubilee Ph.D. Program (Grant No. PHD/0003/2550), the Center for Innovation in Chemistry (PERCH-CIC), Commission on Higher Education, Ministry of Education, and the Graduate School of Prince of Songkla University. Sample of Degussa P25 used throughout this work was donated by Degussa AG, Frankfurt, Germany, through its agency in Bangkok, Thailand.

References

[1] Y. Ao, J. Xu, D. Fu, X. Shen, C. Yuan, Low temperature preparation of anatase TiO_2-coated activated carbon, Appl. Surf. Sci. 254 (2008) 4001–4006.
[2] K.R. Wu, T.P. Cho, Photocatalytic properties of visible light enabling layered titanium dioxide/tin indium oxide films, Appl. Catal. B: Environ. 80 (2008) 313–320.
[3] M. Qamar, M.A. Gondal, Z.H. Yamani, Removal of Rhodamine 6G induced by laser, and catalyzed by Pt/WO_3 nanocomposite, Catal. Commun. 11 (2010) 768–772.
[4] K. Nagaveni, G. Sivalingam, M.S. Heged, Solar photocatalytic degradation of dyes: high activity of combustion synthesized nano TiO_2, Appl. Catal. B: Environ. 48 (2004) 83–93.
[5] K.M. Parida, N. Sahu, N.R. Biswal, B. Naik, A.C. Pradhan, Preparation, characterization, and photocatalytic activity of sulfate-modified titania for degradation of methyl orange under visible light, J. Colloid Interface Sci. 318 (2008) 231–237.
[6] J. Kirchnerova, M.-L. Herrera Cohen, C. Guy, D. Klvana, Photocatalytic oxidation of *n*-butanol under fluorescent visible light lamp over commercial TiO_2 (Hombicat UV100 and Degussa P25), Appl. Catal. A: Gen. 282 (2005) 321–332.
[7] H.E. Byrne, W.L. Kostedt I.V., J.M. Stokke, D.W. Mazyck, Characterization of HF-catalyzed silica gels doped with Degussa P25 titanium dioxide, J. Non-Cryst. Solids 355 (2009) 525–530.
[8] X. Qin, L. Jing, G. Tian, Y. Qu, Y. Feng, Enhanced photocatalytic activity for degrading Rhodamine B solution of commercial Degussa P25 TiO_2 and its mechanisms, J. Hazard. Mater. 172 (2009) 1168–1174.
[9] B. Ohtani, O.O. Prieto-Mahaney, D. Li, R. Abe, What is Degussa (Evonic) P25? Crystalline composition analysis, reconstruction from isolated pure particles and photocatalytic activity test, J. Photochem. Photobiol. A: Chem. 216 (2010) 179–182.
[10] R. Yuan, R. Guan, W. Shen, J. Zheng, Photocatalytic degradation of methylene blue by a combustion of TiO_2 and activated carbon fibers, J. Colloid Interface Sci. 282 (2005) 87–91.
[11] M.H. Habibi, N. Talebian, J.H. Choi, The effect of annealing on photocatalytic properties of nanostructured titanium dioxide thin films, Dyes Pigments 73 (2007) 103–110.
[12] J. Shi, J. Zheng, P. Wu, X. Ji, Immobilization of TiO_2 films on activated carbon fiber and their photocatalytic degradation properties for dye compounds with different molecular size, Catal. Commun. 9 (2008) 1846–1850.
[13] H. Guo, M. Kemell, M. Heikkila, M. Leskela, Novel metal-modified TiO_2 thin film photocatalyst on porous steel fiber support, Appl. Catal. B: Environ. 95 (2010) 358–364.
[14] T. Wang, H. Wang, P. Xu, X. Zhao, Y. Liu, S. Chao, The effect of properties of semiconductor oxide thin films on photocatalytic decomposition of dyeing waste water, Thin Solid Films 334 (1998) 103–108.
[15] C.H. Kwon, H. Shin, J.H. Kim, W.S. Choi, K.H. Yoon, Degradation of methylene blue via photocatalysis of titanium dioxide, Mater. Chem. Phys. 86 (2004) 78–82.
[16] I. Losito, A. Amorisco, F. Palmisano, P.G. Zambonin, X-ray photoelectron spectroscopy characterization of composite TiO_2-poly(vinylidenefluoride) synthesized for applications in pesticide photocatalytic degradation, Appl. Surf. Sci. 240 (2005) 180–188.
[17] S.B. Sankapal, M.Ch. Steiner, A. Ennaoui, Synthesis and characterization of anatase-TiO_2 thin films, Appl. Surf. Sci. 239 (2005) 165–170.
[18] H. Yang, Y.S. Han, J.H. Choy, TiO_2 thin-films on polymer substrates and their photocatalytic activity, Thin Solid Films 495 (2006) 266–271.
[19] P. Sao Marcos, J. Marto, T. Trindade, J.A. Labrincha, Screen-printing of TiO_2 photocatalytic layers on glazed ceramic tiles, J. Photochem. Photobiol. A: Chem. 197 (2008) 125–131.
[20] M.P. Seabra, E. Rego, A. Ribeiro, J.A. Labrincha, Photodegradation of Orange II solutions by TiO_2 active layers jet sprayed on aluminium sheets, Chem. Eng. J. 171 (2011) 175–180.

[21] Z. Ding, X. Hu, P.L. Yue, G.Q. Lu, P.F. Greenfield, Synthesis of anatase TiO_2 supported on porous solids by chemical vapor deposition, Catal. Today 68 (2001) 173–182.
[22] W. Weng, M. Ma, P. Du, G. Zhao, G. Shen, J. Wang, G. Han, Superhydrophilic Fe doped titanium dioxide thin films prepared by a spay pyrolysis deposition, Surf. Coat. Technol. 198 (2005) 340–344.
[23] S.E. Partsinis, Flame synthesis of nanosize particles: precise control of particle size, J. Aerosol Sci. 27 (1996) s153–s154.
[24] S. Sen, S. Mahanty, S. Roy, O. Heintz, S. Bourgeois, D. Chaumont, Investigation on sol–gel synthesized Ag-doped TiO_2 cermets thin film, Thin Solid Films 474 (2005) 245–249.
[25] C. Yogi, K. Kojima, N. Wada, H. Tokumoto, T. Takai, T. Mizoguchi, H. Tamiaki, Photocatalytic degradation of methylene blue by TiO_2 film and Au particles–TiO_2 composite film, Thin Solid Films 519 (2008) 5881–5884.
[26] C. Sriwong, S. Wongnawa, O. Patarapaiboolchai, Photocatalytic activity of rubber sheet impregnated with TiO_2 particles and its recyclability, Catal. Commun. 9 (2008) 213–218.
[27] C. Sriwong, S. Wongnawa, O. Patarapaiboolchai, Degradation of indigo carmine by rubber sheet impregnated with TiO_2 particles, ScienceAsia 36 (2010) 52–58.
[28] A.M. Mittal, J.M. Mittal, L. Kurup, Batch and bulk removal of hazardous dye, indigo carmine from wastewater through adsorption, J. Hazard. Mater. 137 (2006) 162–591.
[29] I. Othman, R.M. Mohamed, I.A. Ibrahim, M.M. Mohamed, Synthesis and modification of ZSM-5 manganese and lanthanum and their effects on decolorization of indigo carmine dye, Appl. Catal. A: Gen. 299 (2006) 95–102.
[30] I. Othman, R.M. Mohamed, I.A. Ibrahim, M.M. Mohamed, Study of photocatalytic oxidation of indigo carmine dye on Mn-supported TiO_2, J. Photochem. Photobiol. A: Chem. 189 (2007) 80–85.
[31] N. Barka, A. Assabbane, A. Nounah, Y.A. Ichou, Photocatalytic degradation of indigo carmine in aqueous solution by TiO_2 coated non-woven fibres, J. Hazard. Mater. 152 (2008) 1054–1059.
[32] M. Vautier, C. Guillard, J.-M. Herrmann, Photocatalytic degradation of dyes in water: case study of indigo and indigo carmine, J. Catal. 201 (2001) 46–59.
[33] A. Houas, H. Lachheb, M. Ksibi, E. Elaloui, C. Guillard, J.-M. Herrmann, The effect of annealing on photocatalytic properties of nanostructured titanium dioxide thin films, Appl. Catal. B: Environ. 31 (2001) 145–157.
[34] A.B. Prevot, C. Baiocchi, M.C. Brussino, E. Pramauro, P. Savarino, V. Augugliaro, G. Marc, L. Palmisano, Photocatalytic degradation of acid blue 80 in aqueous solutions containing TiO_2 suspensions, Environ. Sci. Technol. 35 (2001) 971–976.
[35] A.O. Ibhadon, G.M. Greenway, Y. Yue, P. Falaras, D. Tsoukleris, The photocatalytic activity of TiO_2 foam and surface modified binary oxide titania nanoparticles, J. Photochem. Photobiol. A: Chem. 197 (2008) 321–328.
[36] F. Kiriakidou, D.I. Kondarides, X.E. Verykios, The effect of operational parameters and TiO_2-doping on the photocatalytic degradation of azo-dyes, Catal. Today 54 (1999) 119–130.
[37] C.G. Silva, W. Wong, J.L. Faria, Photocatalytic and photochemical of mono-, di- and tri-azo dyes in aqueous solution under UV irradiation, J. Photochem. Photobiol. A: Chem. 181 (2006) 314–324.
[38] A.P. Toor, A. Verma, C.K. Jotshi, P.K. Bajpai, V. Singh, Photocatalytic degradation of direct 12 yellow dye using UV/TiO_2 in a shallow pond slurry reactor, Dyes Pigments 68 (2006) 53–60.
[39] S. Senthilkumaar, K. Porkodi, Heterogeneous photocatalytic decomposition of crystal violet in UV-illuminated sol–gel derived nanocrystalline TiO_2 suspension, J. Colloid Interface Sci. 288 (2005) 184–189.
[40] J. Sun, L. Qiao, S. Sun, G. Wang, Photocatalytic degradation of Orange G on nitrogen-doped TiO_2 catalysts under visible light and sunlight irradiation, J. Hazard. Mater. 155 (2008) 312–319.
[41] I.K. Konstantinou, T.A. Albanis, TiO_2-assisted photocatalytic degradation of azo dyes in aqueous solution: kinetic and mechanistic investigation. A review, Appl. Catal. B: Environ. 49 (2004) 1–14.

VITAE

Name Mr. Chaval Sriwong

Student ID 5010230024

Education Attainment

Degree	Name of Institution	Year of Graduation
B. Sc. (Chemistry)	Prince of Songkla University	2004
M. Sc. (Inorganic Chemistry)	Prince of Songkla University	2007

Scholarship Awards during Enrolment

1. The Royal Golden Jubilee Ph.D. Program (RGJ) Grant No. PHD/0003/2550 of the Thailand Research Fund (TRF)
2. The Center for Innovation in Chemistry (PERCH-CIC), Commission on Higher Education, Ministry of Education
3. The Thesis Research Fund through the Graduate School, Prince of Songkla University
4. Teaching assistance (TA; General Chemistry Laboratory I & II, 2011-2012)

List of Publications and Presentations

Publications

1. **Chaval Sriwong**, Sumpun Wongnawa, and Orasa Pattarapibolchai, "Photocatalytic activity of rubber sheet impregnated with TiO_2 particles and its recyclability" *Catalysis Communications*, 9 (2008) **213-218**.
2. **Chaval Sriwong**, Sumpun Wongnawa, and Orasa Pattarapibolchai, "Degradation of indigo carmine by rubber sheet impregnated with TiO_2 particles" *ScienceAsia*, 36 (2010) **52-58**.
3. Cheewita Suwanchawalit, **Chaval Sriwong**, and Sumpun Wongnawa, "Recyclable rubber sheets impregnated with potassium oxalate doped TiO_2 and their uses in decolorization of dye-polluted waters" *International Journal of Environmental Research*, 4 (2010) **615-628**.

4. **Chaval Sriwong,** Sumpun wongnawa, and Orasa Pattarapibolchai, "Rubber sheet strewn with TiO_2 particles: photocatalytic activity and recyclability" *Journal of Environmental Science,* 24 (2012) **464-472**.
5. **Chaval Sriwong,** Sumpun Wongnawa, and Orasa Pattarapibolchai, "Recyclable thin TiO_2-embedded rubber sheet and dye degradation" *Chemical Engineering Journal*, 191 (2012) **210-217**.

Presentations

Oral presentations

1. **Chaval Sriwong,** Sumpun Wongnawa, and Orasa Pattarapibolchai, "*Degradation of methylene blue by immobilized titanium dioxide*" PERCH-CIC Congress V. Jomtein Palm Beach Hotel & Resort, Pattaya, Chonburi, Thailand. 6-9 May 2007.
2. **Chaval Sriwong**, Sumpun Wongnawa, and Orasa Pattarapibolchai, "*Photocatalytic degradation of two selected dyes using UV-light in the presence of immobilized titanium dioxide*" The 2nd USM Penang International Postgraduate Convention. Universiti Sains Malaysia, Penang, Malaysia. 18-20 June 2008.
3. **Chaval Sriwong**, Avinash J. Patil, Sumpun Wongnawa, and Stephen Mann, "*A stable aqueous dispersion of graphene nanosheets by chemical method and its flexible conducting sheet*" RGJ-PhD Congress XII. Jomtein Palm Beach Hotel & Resort, Pattaya, Chonburi, Thailand. 1-3 April 2011.
4. **Chaval Sriwong**, Sumpun Wongnawa, and Orasa Pattarapibolchai, "*Photocatalytic activity of TiO_2 immobilized sheets prepared by different methods*" The International Congress for Innovation in Chemistry (PERCH-CIC Congress VII). Jomtein Palm Beach Hotel & Resort, Pattaya, Chonburi, Thailand. 4-7 May 2011.

Poster presentations

1. **Chaval Sriwong**, Sumpun Wongnawa, and Orasa Pattarapibolchai, "*Degradation of methylene blue by immobilized titanium dioxide*" Proceeding of the 32nd Congress on Science and Technology of Thailand (STT32). Queen Sirikit National Convention Center, Bangkok, Thailand. 10-12 October 2006.

2. **Chaval Sriwong**, Sumpun Wongnawa, and Orasa Pattarapibolchai, "*Photocatalytic activity of TiO_2 immobilized in latex sheets*" The International Congress for Innovation in Chemistry (PERCH-CIC Congress VI). Jomtein Palm Beach Hotel & Resort, Pattaya, Chonburi, Thailand. 3-6 May 2009.